34th CANADIAN MATERIALS SCIENCE CONFERENCE 2023

June 27 – 30

University of Manitoba

Note: This schedule is a draft and may undergo changes later.

27-Jun			
Agenda	**Short course I: Synchrotron Applications in Materials Research**	**Agenda**	**Short Course II: In-situ Nanoindentation**
		9:00am-10:30am	Lecture
		10:30am-11:00 am	coffee break
		11:00am-12:30pm	Hand-on demo I
12:00pm-12:45pm	Lunch	12:30pm-1:30pm	lunch
12:45pm-1:45pm	Lecture I		
1:45pm-2:45pm	Lecture II	1:30pm-3:00pm	Hand-on demo II
2:45pm-3:00pm	coffee break	3:00pm-3:30pm	coffee break
3:00pm-4:00pm	Lecture III	3:30pm-5:00pm	Hand-on demo III
4:00pm-5:00pm	Lecture IV		
		Hand-on Demos will be in the building of Manitoba Institute for Materials.	
5:00pm-7:00pm	**Welcome Reception**		

AAM: Additive and advanced manufacturing			BMSM: Biomaterials and soft materials			
MTC: Materials theory, computation and data			PMC: Physical metallurgy and characterization			
Session ID	Time		28-Jun			
			E2-110	E2-130	E2-125	E2-160
	8:00am-9:00am		Registrations and Breakfast			
	9:00am-9:10am		Conference Welcome (By CMSC chair, E3-270)			
	9:10am-10am		**Gianluigi Botton, McMaster University** DKC McDonald Lecture (E3-270, introduced by CMSC chair)			
		AM	AAM1	BMSM1	MTC1	PMC1
A1	10:10am-10:30am	Talk 1	**Jingjie (Peter) Wei (Invited)**	**Wen Zhong (invited)**	**Jun Song (invited)**	**Akindele Odeshi (Invited)**
A2	10:30am-10:50am	Talk 2	Joseph Agyapong	Mohammad Muzammil Kuddushi	Mahdi Mohsini	Diego Mateos
A3	10:50am-11:10am	Talk 3	Ekundayo Binuyo	Yuqing Liu	Jaarli Suviranta	Timothy Odiaka
A4	11:10am-11:30am	Talk 4	Shazaib Ahsan	Jungkyu Lee	Ziqi Cui	
	11:30am-11:50am	Coffee break				
A5	11:50am-12:10pm	Talk5	Lulu Guo	Ebrahim Karamian	**Ron Miller (invited)**	**Bhaveshkumar Kamaliya (Invited)**
A6	12:10pm-12:30pm	Talk6	Mohammad Rezayat	Chenyu Qiao	Gurnek Tak	Moein Iman Fourmani
A7	12:30pm-12:50pm	Talk7	Rasool Mokhtari Homami	Xingying Zhang	Zuoyong Zhang	Muhammad Umer
A8	12:50pm -1:10pm	Talk8	Ravinder Singh	Muhammad Rizwan		Tamara Kazoun
	1:10am-2:20pm	Lunch	Poster setup/Invited industry talk			
		PM	AAM2	BMSM2	MTC2	PMC2
P1	2:20pm - 2:40pm	Talk1	**Toan Truong (Invited)**	**Yongfeng Ai (invited)**	**Chad Sinclair (invited)**	**Jamie Hogan (Invited)**
P2	2:40pm - 3:00pm	Talk2	Ajay Talbot	Mojtaba Abbasi	Sidharth Sarmah	Oluwasegun Adesola
P3	3:00pm - 3:20pm	Talk3	Sangeev Selvaratnam	Kaige Xu	Alex Mamaev	Zhina Razaghi
P4	3:20pm - 3:40pm	Talk4	Solomon Hanson Duntu	Yawei Zhao	Ruitian Chen	Imtiaz Ahmed
	3:40pm - 4:00pm	Coffee break				
P5	4:00-4:20pm	Talk5	Amardeep Singh Kang	Liane Middleton	**Md Mijanur Rahman (invited)**	Christine Vo
P6	4:20pm - 4:40pm	Talk6	Rabea Al-Kershi	Ziqian Zhao	Xinyuan Song	Reza Khatib Zedeh Davani
P7	4:40pm - 5:00pm	Talk7	Bo Cui	Chelsea Wu	Haijun Zhang	Hamed Shirazi
P8	5:00-5:20pm	Talk8		Muhammad Amirul Islam		Hiroyuki Tanaka
	5:20-6:20pm	Poster session	Poster session 1			

Please note that each symposium has its own unique schedule. To find the specific talk time for each symposium, kindly refer to the detailed schedule provided below.

GS: Green and sustainability			FMS: Functional materials and structures			
MTC: Materials theory, computation and data			PMC: Physical metallurgy and characterization			
Session ID	Time		29-Jun			
			E2-110	E2-130	E2-125	E2-160
	8:00am-9:00am		Registrations and Breakfast			
	9:00am-9:50am		**Chad Sinclair, The University of British Columbia** Metal Physics Lecture (E3-270, introduced by CMSC chair)			
		AM	GS1	FMS1	MTC3	PMC3
A1	10:10am-10:30am	Talk 1	**Drew Higgins (Invited)**	**Hamid Jafari (Invited)**	**Hao Sun (invited)**	
A2	10:30am-10:50am	Talk 2	Feizhou He	Babak Mokhtarnia	Karim Zongo	
A3	10:50am-11:10am	Talk 3	Graeme Francolini	Ron Miller	Abu Anand	
A4	11:10am-11:30am	Talk 4	Mariam Odetallah		Yuxuan Wang	
	11:30am-11:50am	Coffee break				
A5	11:50am-12:10pm	Talk5	**Ge Li (invited)**	Seyed Hossein Mussavi Rizi	Semere Araya	
A6	12:10pm-12:30pm	Talk6	Anh Mai	Christina Balanduk	Mohamed Hendy	
A7	12:30pm-12:50pm	Talk7	Melissa Isabel Ayala Sánchez	Anita Amir Labonno	Javad Shirani	
A8	12:50pm -1:10pm	Talk8	Melani Guadalupe Ayala Sánchez			
	1:10am-2:20pm	Lunch	Student award announcement			
		PM	GS2	FMS2	MTC4	PMC4
P1	2:20pm - 2:40pm	Talk1	**Sami Khan (invited)**	Sumin Han	Ying Zhao	**Ben Britton (Invited)**
P2	2:40pm - 3:00pm	Talk2	Goitom Gebreyohannes Berhe	Gamaliel Azariah	Pedro Guerra Demingos	Yushun Liu
P3	3:00pm - 3:20pm	Talk3	Sandeep Kaur Gill	Shashwata Moitra	Ying Yang	Tonye Jack
P4	3:20pm - 3:40pm	Talk4	Idil Mutlu Tuncer			Nima Nikpoor Badr
	3:40pm - 4:00pm	Coffee break				
P5	4:00-4:20pm	Talk5	**Scott Kroeker (invited)**	Jehangir Khan		Johnson Aina
P6	4:20pm - 4:40pm	Talk6	Gökhan Başman	Sameed Khan		Intekhab Alam
P7	4:40pm - 5:00pm	Talk7	Xue Yao			Modupeola Dada
P8	5:00-5:20pm	Talk8	Ying Zhao			
	5:00-6:00pm					
	6:15pm-8:30pm		Banquet Dinner			

Please note that each symposium has its own unique schedule. To find the specific talk time for each symposium, kindly refer to the detailed schedule provided below.

GS: Green and sustainability			FMS: Functional materials and structures			
Session ID	Time		30-Jun			
			E2-110	E2-130		
	8:00am-9:00am		Registrations and Breakfast			
	9:00am-9:50am		**Edward (Ted) Roberts, University of Calgary** Metal Chemistry Lecture (E3-270, introduced by CMSC chair)			
		AM	GS3	FMS3		
A1	10:10am-10:30am	Talk 1	**Wiqar Hussain Shah (invited)**	Ramin Hamzehei		
A2	10:30am-10:50am	Talk 2	Mohammad Palimi	Lala Agamirov-Nost		
A3	10:50am-11:10am	Talk 3	Masoud Taherijam	Yu Xiao		
A4	11:10am-11:30am	Talk 4	Saiedeh Sadat Marashi			
	11:30am-11:50am	Coffee break				
A5	11:50am-12:10pm	Talk5	Goroh Itoh	Mirette Fawzy		
A6	12:10pm-12:30pm	Talk6	Ali Goksu	Doha Mohammed		
A7	12:30pm-12:50pm	Talk7	Hassan Alshahrani	Niranjanmurthi Lingappan		
A8	12:50pm -1:10pm	Talk8				
	1:10am-2:20pm	Lunch				
		PM	Royal Canadian mint tour (TBD)			
	2:30pm					

Please note that each symposium has its own unique schedule. To find the specific talk time for each symposium, kindly refer to the detailed schedule provided below.

Symposium:

Additive and advanced manufacturing (AAM)

Wednesday, June 28th 2023

Room: E2-110, Engineering & Information Technology Complex

Chair: *Gbenga Asala, Solomon Boakye-Yiadom*

Talks:

10:10am - 10:40am, June 28th (invited) (*abstract*)

AAM1: Investigation of Microstructure and Deformation Mechanism in Cold Sprayed CuNi, CuSn, and CuNiSiCr Alloys
Jingjie (Peter) Wei, Yu Zou, University of Toronto

10:40am - 11:00am, June 28th (*abstract*)

AAM2: Assessing the Mechanical Response of an Additively Manufactured CoCrFeMnNi High Entropy Alloy Using DIHPB Tests and Electron Microscopy
Joseph Agyapong, Solomon Boakye-Yiadom, Alexander Czekanski, York University

11:00am - 11:20am, June 28th (*abstract*)

AAM3: Dynamic Impact and Ballistic Behaviour of Additively Manufactured AlCrFeCoNi High Entropy Alloy
Ekundayo Binuyo, G. Asala, O.T. Ola, O.A Ojo, A.G Odeshi, University of Saskatchewan, University of Manitoba, Red River College Polytechnic

11:20am - 11:40am, June 28th (*abstract*)

AAM4: Quality Prediction and Energy Consumption Optimization in Selective Laser Melting
Shazaib Ahsan, MD Rokibujjaman Sabuj, and Xihui Liang, University of Manitoba

12:00pm - 12:20pm, June 28th (*abstract*)

AAM5: Effect of Heat Treatment on Mechanical Compression Properties of Wire Arc Additive Manufactured C250 Maraging Steel
Lulu Guo, Lina Zhang, Joel Andersson, Olanrewaju Ojo, University of Manitoba, University West

12:20pm - 12:40pm, June 28th (*abstract*)

AAM6: Effects of Laser Surface Texturing on the 301LN stainless steel
Mohammad Rezayat, Antonio Mateo, Polythecnic University of Catalunya

12:40pm - 1:00pm, June 28th (*abstract*)

AAM7: Simulation of Laser Powder Bed Fusion Process for Nickel Alloy Inconel 718 Using Representative Volume
Rasool Mokhtari Homami, Olanrewaju Ojo, University of Manitoba

1:00pm - 1:20pm, June 28th (*abstract*)

AAM8: Improved Corrosion Resistance of WE43/TiC Reinforced Surface Composites
Ravinder Singh, Amardeep Singh Kang, Shivali Singla, Lovely Professional University, Baba Hira Singh Bhattal Institute of Engineering and Technology

2:20pm - 2:50pm, June 28th (invited) (*abstract*)

AAM9: Texture and Damage Evolution in Additively Manufactured 18%Ni-M350 Maraging Steel under Dynamic Impact Loading: Effects of Heat Treatment and Process Parameters
Toan Truong, G. Asala, O.T. Ola, O.A. Ojo, A.G. Odeshi, University of Saskatchewan, Red River College Polytechnic, University of Manitoba

2:50pm - 3:10pm, June 28th (*abstract*)

AAM10: A Fundamental Analysis on Laser Remelting of High-Entropy Alloys: towards Enhanced Printability
Ajay Talbot, Xiao Shang, Wandong Wang, Yu Zou, University of Toronto

3:10pm - 3:30pm, June 28th (*abstract*)

AAM11: Subtractive vs Additive Manufacturing of a Custom Scanning Tunnelling Microscope Head
Sangeev Selvaratnam, University of Manitoba

3:30pm - 3:50pm, June 28th (*abstract*)

AAM12: Microstructural and Wear Characterization of Additive Manufactured Ceramics via Lithography-based Ceramic Manufacturing (LCM) Technique
Solomon Hanson Duntu, Diego Mateos, Solomon Boakye-Yiadom, York University

4:10pm - 4:30pm, June 28th (*abstract*)

AAM13: Electrochemical Corrosion Behavior of We43/SiC Reinforced Surface Composites
Amardeep Singh Kang, Ravinder Pal Singh, Shivali Singla, Lovely Professional University, Baba Hira Singh Bhattal Institute of Engineering and Technology

4:30pm - 4:50pm, June 28th (*abstract*)

AAM14: Modification of Diffraction, Microscopic and Spectroscopic Characterizations of Ni-Zn Ferrimagnetic Nanoparticles Via Cerium Element as Advanced Engineering Materials
Rabea Al-Kershi, A. M. Alsheri, R. M. Attiyah, King Khalid University

4:50pm - 5:10pm, June 28th (*abstract*)

AAM15: Fabricating 316L Stainless Steel Unsupported Rods by Controlling the Flow of Molten Pool via Wire Arc Additive Manufacturing
Chenchen Jing, Bo Cui, Changmeng Liu , Xihui Liang, Beijing Institute of Technology, University of Manitoba

Posters (5:20pm-6:20pm, June 28th):

AAM16: Laser Powder Bed Fusion of Alumina-Based Ceramic Matrix Composite (*abstract*)
Mohammad Azami, Zahra Kazemi, Concordia University, University of Toronto

AAM17: On the Development of a New Pre-Weld Heat Treatment Procedure for Preventing Gas Tungsten Arc Weld Heat-Affected Zone Cracking in a Newly Developed Co-Based Superalloy (*abstract*)
H.R Abedi, O.A. Ojo, University of Manitoba

Symposium:

Biomaterials and soft materials (BMSM)

Wednesday, June 28th 2023

Room: E2-130, Engineering & Information Technology Complex

Chair: *Malcolm Xing, Yuqing Liu, Xingying Zhang, Kaige Xu*

Talks:

10:10am - 10:40am, June 28th (invited) (*abstract*)

BMSM1: Hydrogels for wearable biosensors
Wen Zhong, University of Manitoba

10:40am - 11:00am, June 28th (*abstract*)

BMSM2: A Biocompatible Self-healable Hydrogel Film with High Mechanical Strength and Antibacterial Properties
Mohammad Muzammil Kuddushi, Xiaoyi Deng, Xuehua Zhang, University of Alberta

11:00am - 11:20am, June 28th (*abstract*)

BMSM3: A Strong Hemostatic Adhesive of Self-Assembled Amphiphilic Granular Hydrogel from Andrias Davidianus Skin Secretion with Underwater Instant Adhesion Capacity
Yuqing Liu, University of Manitoba

11:20am - 11:40am, June 28th (*abstract*)

BMSM4: Kirigami-Inspired Shape Memory Polymer Structures: Effects of Structural Design on Mechanical Performance under Cyclic Loading
Jungkyu Lee, Bruker Nano Surfaces

12:00pm - 12:20pm, June 28th (*abstract*)

BMSM5: Bioactivity Improvement of AZ31 Substrates via PCL-Chitosan - Bioglass Composite Nanofibers Electrospun Coating

Ebrahim Karamian, M. Haddadia, H. Bakhsheshirada, M. Kasiri-Asgarania and H. Gheisaria, Najafabad Branch, Islamic Azad University

12:20pm - 12:40pm, June 28th (*abstract*)

BMSM6: Multifunctional Wet Adhesive Film Enabled by a Single-Component Poly(ionic liquid)

Chenyu Qiao, Binmin Wang, Hong Wang, Hongbo Zeng, University of Alberta, Nankai University

12:40pm - 1:00pm, June 28th (*abstract*)

BMSM7: Mussel Inspired Graphene Aerogel for Skeletal Muscle Atrophy Regeneration

Xingying Zhang, Malcolm Xing, University of Manitoba

1:00pm - 1:20pm, June 28th (*abstract*)

BMSM8: Metal Organic Frameworks as Promising Sensing Tools for Electrochemical Detection of Persistent Heavy Metal Ions from Water Matrices: A Concise Review

Muhammad Rizwan, University of Lahore

2:20pm - 2:50pm, June 28th (invited) (*abstract*)

BMSM9: Understanding gelation mechanisms of starches varying in molecular structures for industrial applications

Yikai Ren and Yongfeng Ai, University of Saskatchewan

2:50pm - 3:10pm, June 28th (*abstract*)

BMSM10: Investigating the Dissolution Properties of Bioactive Silver-loaded Borophosphate Glasses for Wound Healing

Scott Kroeker, Mojtaba Abbasi, University of Manitoba

3:10pm - 3:30pm, June 28th (*abstract*)

BMSM11: Viscosity and Degradation Controlled Injectable Hydrogel for Esophageal Endoscopic Submucosal Dissection

Kaige Xu, Malcom Xing, University of Manitoba

3:30pm - 3:50pm, June 28th (*abstract*)

BMSM12: Self-powered Plant-wearable Hydrogel Sensors for Smart Farming

Yawei Zhao, Helen Hsu, Wen Zhong, Malcolm Xing, University of Manitoba

3:50pm - 4:10pm, June 28th (*abstract*)

BMSM13: Material Property Changes in Face Mask Silicone after 100 Sterilization Cycles by Autoclave, Hydrogen Peroxide, or Bleach Treatments

Liane Middleton, Tian Zhao, Stephanie Toigo, Richard Leask, Dan Deckelbaum, Sidney Omelon, McGill University, Research Institute of the McGill University Health Center, Montreal General Hospital, McGill University Health Center

4:30pm - 4:50pm, June 28th (*abstract*)

BMSM14: Engineered Protein-based Materials Boosting Anti-fouling in Complex Biological Fluids

Ziqian Zhao, Mingfei Pan, Chenyu Qiao, Li Xiang, Xiong Liu, Wenshuai Yang, Xing-Zhen Chen, Hongbo Zeng, University of Alberta

4:50pm - 5:10pm, June 28th (*abstract*)

BMSM15: Injectable and Ultra-compressible Shape-memory Mushroom: Highly Aligned Microtubules for Ultra-fast Blood Absorption and Hemostasis

Xiaozhuo (Chelsea) Wu, Malcolm Xing, University of Manitoba

5:10pm - 5:30pm, June 28th (*abstract*)

BMSM16: Supramolecular Hydrogels from Functionalized Dipeptides for Drug Delivery

Muhammad Amirul Islam, Darren Makeiff, Mickie Wiebe, Aria Khalili, Ashley Wagner, JaeYoung Cho, Marianna Kulka, National Research Council Canada (NRC), Nanotechnology Research Centre

Posters (5:20pm-6:20pm, June 28th):

BMSM17: The Effects and Potential Opportunities of Phosphorus Recovery by Elemental Sulphur Addition to Municipal Biosolids and Its Anaerobic Microbial Reduction to Sulphide (*abstract*)
Samantha Gangapersad, Tian Zhao, Sidney Omelon, McGill University

---

Symposium:

Materials theory, computation and data(MTC)

Wednesday-Thursday, June 28th – 29th 2023

Room: E2-125, Engineering & Information Technology Complex

Chair: *Chuang Deng, Hao Sun, Jun Song, Xinyuan Song, Zuoyong Zhang*

Talks:

10:10am - 10:40am, June 28th (invited) (*abstract*)

MTC1: Unfaulting of Dislocation Loops in Metals: Atomistic Simulations and Continuum Modeling
Jun Song, Cheng Chen, McGill University, Northwestern Polytechnical University

10:40am - 11:00am, June 28th (*abstract*)

MTC2: Modeling the Formation of Basal Vacancy Loops via the Collapse of Pre-existing Prismatic Vacancy Loops
Mahdi Mohsini, Peyman Saidi, Mark Daymond, Queen's University

11:00am - 11:20am, June 28th (*abstract*)

MTC3: Defect Microstructures in 3D Rapid Solidification
Jaarli Suviranta, McGill University

11:20am - 11:40am, June 28th (*abstract*)

MTC4: Vacancy Patterns in Nitride Precipitates and Implication to Hydrogen Embrittlement of High Strength Steels
Ziqi Cui, McGill University

12:00pm - 12:30pm, June 28th (invited) (*abstract*)

MTC5: Atomic Simulations of Spall and Penetration Resistance of polymers and nanolaminates
Ron Miller, Nuwan Dewapriya, Carleton University, University of Delaware

12:30pm - 12:50pm, June 28th (*abstract*)

MTC6: Deformation Behavior and Microstructural Evolution of Al 7050 and Al 7075 Under High Strain Rate Compression
Gurnek Tak, York University

12:50pm - 1:10pm, June 28th (*abstract*)

MTC7: Solid Solution Softening in Single Crystalline Metal Nanowires Studied by Atomistic Simulations
Zuoyong Zhang, Chuang Deng, University of Manitoba

2:20pm - 2:50pm, June 28th (invited) (*abstract*)

MTC8: Exploring the Slow Dynamics of Interfaces and Glasses via Markov State Models
Chad Sinclair, Siavash Soltani, Joerg Rottler, The University of British Columbia

2:50pm - 3:10pm, June 28th (*abstract*)

MTC9: Continuum Modeling of Stress Coupled Hydrogen Diffusion and Hydrogen-induced Cracking in High Strength Steels
Sidharth Sarmah, Jun Song, McGill University

3:10pm - 3:30pm, June 28th (*abstract*)

MTC10: An Atomistic Perspective of Discontinuous Precipitation Reactions
Alex Mamaev, Nikolas Provatas, McGill University

3:30pm - 3:50pm, June 28th (*abstract*)

MTC11: A Survey of Energies of Pure Metals and Multi-component Alloys
Ruitian Chen, Yu Zou, University of Toronto

4:10pm - 4:40pm, June 28th (invited) (*abstract*)

MTC12: Applications and Recent Developments of the Kinetic Activation-relaxation Technique
Md Mijanur Rahman, McGill University

4:40pm - 5:00pm, June 28th (*abstract*)

MTC13: Computing the Intrinsic Grain Boundary Mobility Tensor from Interface Random Walk method

Xinyuan Song, Chuang Deng, University of Manitoba

5:00pm - 5:20pm, June 28th (*abstract*)

MTC14: Numerical Study of Influence of Oxide on Metal Powder Deposition and Bonding Behaviors During Cold Spray using Peridynamic Simulations

Haijun Zhang, Jun Song, Baihua Ren, McGill University

10:10am - 10:40am, June 29th (invited) (*abstract*)

MTC15: A Robust Moment Tensor Potential for Molten Salt, Solid Salt, and Chlorine Gas

Hao Sun, Queen's University

10:40am - 11:00am, June 29th (*abstract*)

MTC16: Unified Inter-atomic Potential for Silica, Silicon and Oxygen

Karim Zongo, Laurent Karim Béland, Claudiane Ouellet-Plamondon, Ecole de technologie superieure, Queen's university

11:00am - 11:20am, June 29th (*abstract*)

MTC17: Origin of Gamma Surface Asymmetries in Body-centered Cubic Refractory High Entropy Alloys

Abu Anand, Chandra Veer Singh, University of Toronto

11:20am - 11:40am, June 29th (*abstract*)

MTC18: A Calculation Method to Estimate Thermal Conductivity of High Entropy Ceramic for Thermal Barrier Coatings

Yuxuan Wang, Jun Song, McGill University

12:00pm - 12:20pm, June 29th (*abstract*)

MTC19: Deep Learning-based Design of Multi-Layered Chiral Metasurface

Semere Araya, Yonsei Universiy

12:20pm - 12:40pm, June 29th (*abstract*)

MTC20: Alchemical Perturbation Density Functional Theory Coupled with Machine Learning for Accelerated Screening of High-Entropy Alloys Catalysts

Mohamed Hendy, Okan Orhan, Homin Shin, Ali Malek, Mauricio Ponga, The University of British Columbia, National Research Council Canada (NRC)/Government of Canada

12:40pm - 1:00pm, June 29th (*abstract*)

MTC21: Artificial Intelligence Driven Design of Dingle-atom Dlloy Catalysts via Electronic Structure Features

Javad Shirani, Hanh D. M. Pham , Shuaishuai Yuan ,Alain B. Tchagang , Julio J. Valdés and Kirk H Bevan, McGill University

2:20pm - 2:40pm, June 29th (*abstract*)

MTC22: Activation of Electrocatalytic CO2 Methanation on Defective 1T' Phase TMDCs

Ying Zhao, Jun Song, McGill University

2:40pm - 3:00pm, June 29th (*abstract*)

MTC23: Tuning the Properties of 2D Iron Ores through Surface Passivation: an Ab-initio Investigation of Magnetene, Ilmenene and Pyrite

Pedro Guerra Demingos, Chandra Veer Singh, University of Toronto

3:00pm - 3:20pm, June 29th (*abstract*)

MTC24: Creating BIC via Long-distance Coherently Coupled Cavity Magnonics

Ying Yang, Yihui Zhang, Jiguang Yao, Yang Xiao, Jun Li, Can-Ming Hu, University of Manitoba

Posters (5:20pm-6:20pm, June 28th):

MTC25: An Improved Frequency Domain Stress Evaluation Method for Fatigue Life Determination of Welded Structures Subjected to Random Loadings (*abstract*)

Uchenna Kalu, Xihui Liang, University of Manitoba

MTC26: Characterizing Uncertain Elastic Properties of Materials 3D‑Printed by the Fused Filament Fabrication Method (*abstract*)
Zahra Kazemi, Craig A Steeves, University of Toronto

MTC27: I-substituted Halide-rich Lithium Argyrodites Solid electrolytes with improved stability for All Solid State Batteries (*abstract*)
Adwitiya Rao, University of Toronto

Symposium:

Physical metallurgy and characterization (PMC)

Wednesday-Thursday, June 28th – 29th 2023

Room: E2-160, Engineering & Information Technology Complex

Chair: *Guozhen Zhu, Akindele Odeshi, Jamie Hogan, Yushun Liu*

Talks:

10:10am - 10:40am, June 28th (invited) (*abstract*)

PMC1: Shear Strain Localization and Adiabatic Shear Failure under Dynamic Shock Loading
Akindele Odeshi, University of Saskatchewan

10:40am - 11:00am, June 28th (*abstract*)

PMC2: Adiabatic Shear Banding and Dynamic Tensile Fracture of Armour Steel
Diego Mateos, Solomon Hanson Duntu, Solomon Boakye-Yiadom, York University

11:00am - 11:20am, June 28th (*abstract*)

PMC3: Dynamic Impact Response of Additively Manufactured M350 Maraging Steel-High Entropy Alloy Hybrid Plate
Timothy Odiaka, G. Asala, O.T. Ola, O.A. Ojo, I.N.A. Oguocha, A.G. Odeshi, University of Saskatchewan, Red River College Polytechnic, University of Manitoba

11:40am - 12:10pm, June 28th (invited) (*abstract*)

PMC4: Nanoscale Manipulations by Unusual Focused Ion Beam (FIB) – Material Interactions
Bhaveshkumar Kamaliya, Morvarid Ghorbani, Angela Cleri, Adrian Kitai, Jon-Paul Maria, Jing Fu, Rakesh Mote, Nabil Bassim, McMaster University, Pennsylvania State University, Monash University, Indian Institute of Technology Bombay, Canadian Centre for Electron Microscopy

12:10pm - 12:30pm, June 28th (*abstract*)

PMC5: Evaluation of Twinning Formation in Mg-Gd Alloy during Nanoindentation
Moein Iman Fourmani, Guo-zhen Zhu, Yushun Liu, University of Manitoba

12:30pm - 12:50pm, June 28th (*abstract*)

PMC6: Micro-computed Tomography (µ-CT) Assessment of TIG Welded AA 6061- T651
Muhammad Umer, Dr. Ahmed Alade Tiamiyu, University of Calgary

12:50pm - 1:10pm, June 28th (*abstract*)

PMC7: Quantification of TiN Precipitates and CaS Inclusions in a Microalloyed Steel using EMPA Mapping
Tamara Kazoun, University of Alberta

2:20pm - 2:50pm, June 28th (invited) (*abstract*)

PMC8: Designing Next-Generation Additively Manufactured Ceramic-Metal Structures
Jamie Hogan, James David Hogan, Zahra Zaiemyekeh, Saman Sayahlatifi, Haoyang Li, University of Alberta

2:50pm - 3:10pm, June 28th (*abstract*)

PMC9: Dry Sliding Wear Properties of Cold Sprayed Fe-based Bulk Metallic Glass Coating on Aluminum Alloy
Oluwasegun Adesola, I. N. A. Oguocha, O. Ojo, G. Asala, and O. T. Ola, University of Saskatchewan, University of Manitoba, Red River College Polytech

3:10pm - 3:30pm, June 28th (*abstract*)

PMC10: Controlling TiO2 Nanowire Growth Direction, Morphology, and Shape by Manipulating the Surface Characteristics of the Seed

Zhina Razaghi, Guozhen Zhu, University of Manitoba

3:30pm - 3:50pm, June 28th (*abstract*)

PMC11: Effect of Particle Size, Shape and Void Fraction on Fixed Bed Electrical Resistivity of Commercial Graphite Flakes

Imtiaz Ahmed, Marc Duchesne, Natural Resources Canada

4:10pm - 4:30pm, June 28th (*abstract*)

PMC12: Effect of Mechanical Loading Conditions on Near-neutral pH Stress Corrosion Cracking (NNpHSCC) Initiation and Early-stage Growth in Bent Pipeline

Christine Vo, University of Alberta

4:30pm - 4:50pm, June 28th (*abstract*)

PMC13: Influence of Nb Addition on the Microstructure Evolution and Hydrogen Defects Susceptibility and Corrosion Resistance of X70 Pipeline Steel

Reza Khatib Zedeh Davani, University of Saskatchewan

4:50pm - 5:10pm, June 28th (*abstract*)

PMC14: Crack Growth Behavior of Circumferential Near-Neutral pH Corrosion Fatigue in a Bent Pipeline

Hamed Shirazi, Weixing Chen, Reg Eadie, Unicersity of Alberta

5:10pm - 5:30pm, June 28th (*abstract*)

PMC15: Effect of Girth Weld and Bending Residual Stresses On Initiation and Early Growth of Circumferential Near-Neutral pH Stress Corrosion Cracking in Thin Pipeline Steel

Hiroyuki Tanaka, University of Alberta

2:20pm - 2:50pm, June 29th (invited) (*abstract*)

PMC16: Advancing Electron Backscatter Diffraction for Quantitative Corelative Characterization of Microstructures

Ben Britton, The University of British Columbia

2:50pm - 3:10pm, June 29th (*abstract*)

PMC17: Real-time Tracking of Slip Planes in Many Grains using Hollow-cone Dark-field Imaging

Yushun Liu, Guozhen Zhu, University of Manitoba

3:10pm - 3:30pm, June 29th (*abstract*)

PMC18: Microstructural Analysis of the Hydrogen Assisted Failure of Nb-containing and Deficient Pipeline Steels

Tonye Jack, Jerzy Szpunar, University of Saskatchewan

3:30pm - 3:50pm, June 29th (*abstract*)

PMC19: Characterization of the Interface Areas of Zirconium Hydride Precipitates

Nima Nikpoor Badr, Fei Long, Mathew Topping, Zhongwen Yao, Mark Daymond, Queen's University

4:10pm - 4:30pm, June 29th (*abstract*)

PMC20: Improved Weldability of a Difficult-to-Weld Aerospace Superalloy

Johnson Aina, Olanrewaju Ojo, Mahesh Chaturvedi, University of Manitoba

4:30pm - 4:50pm, June 29th (*abstract*)

PMC21: Revisiting the Phase Stability Rules in the Design of High-Entropy Alloys: A Case Study of Quaternary Alloys Produced by Mechanical Alloying

Intekhab Alam, Ahmed Alade Tiamiyu, University of Calgary

4:50pm - 5:10pm, June 29th (*abstract*)

PMC22: Investigating the Microstructural, Mechanical, Tribological, and Electrochemical Properties of AlCuFeNiSix and AlCuFeNiTix High Entropy Alloys via Arc Melting for Energy Storage Applications.
Modupeola Dada, Popoola Patricia, Tshwane University of Technology

Posters (5:20pm-6:20pm, June 28th):

PMC23: Calculation of Variable Atomic Diffusivity in a Cu-Ni alloy System (*abstract*)
Samuel Afolabi, Amir Safaei, Olanrewaju A. Ojo, University of Manitoba

PMC24: Tracking of Cathode Degradation in LiNi0.5Mn1.5O4 Lithium-Ion Batteries through Intermittent Post-Mortem Material Characterizations (*abstract*)
Kelsey Duncan, Farhang Nesvaderani, O'Rian Reid, Lida Hadidi, Byron D. Gates, Simon Fraser University, NanoOne Materials Corp.

PMC25: Investigating the Effect of Rapid Induction Heating on Phase Transformation in Martensitic Stainless Steel 15-5 PH (*abstract*)
Mahsa Fatemi Mehrabani, Mehrdad Aghaei Khafri, K.N. Toosi University of Technology

PMC26: Study of Aluminization and Its Effects on High Temperature Oxidation of Austenitic Stainless Steel AISI 304 (*abstract*)
Sonya Redjala, Said Azem, Mouloud Mammeri University

PMC27: Steel decarbonization using iron ultra-fine grains recovered from tailings in a new HDDRI process (*abstract*)
Fernando Berlinck, SmartDry Liquefaction

PMC28: Tribological Properties of Cold Sprayed Fe-based Metallic Glass Coating on ZE41A-T5 Magnesium Alloy (*abstract*)
Oluwasegun Adesola, Charles Obiechefu, Ikechukwuka N. A. Oguocha, Olanrewaju Ojo, Gbenga Asala, and O. T. Ola, University of Saskatchewan, University of Manitoba, Red River College Polytech.

Symposium:

Green and sustainability (GS)

Thursday - Friday, June 29th – 30th 2023

Room: E2-110, Engineering & Information Technology Complex

Chair: Jing Liu, Farzaneh Sadri, Christian Kuss

Talks:

10:10am - 10:40am, June 29th (invited) (*abstract*)

GS1: In situ Transmission Electron Microscopy to Understand Electrochemical Processes
Drew Higgins, McMaster University

10:40am - 11:00am, June 29th (*abstract*)

GS2: Synchrotron Applications in Energy Materials and Catalysts
Feizhou He, Canadian Light Source

11:00am - 11:20am, June 29th (*abstract*)

GS3: Developing an Elevated Temperature Pourbaix Diagram of Zirconium and Zircaloy-4
Graeme Francolini, University of Ontario Institute of Technology

11:20am - 11:40am, June 29th (*abstract*)

GS4: Investigating the Effect of Electrode Microstructure on Battery Performance Using IL-TEM
Mariam Odetallah, Christian Kuss, University of Manitoba

12:00pm - 12:30pm, June 29th (invited) (*abstract*)

GS5: Regulate Anode Behaviors in Lithium Metal Batteries
Ge Li, University of Alberta

12:30pm - 12:50pm, June 29th (*abstract*)

GS6: Water-Processable Composite as a Conductive Binder for Graphite Anode in Lithium-ion Batteries
Anh Mai, Christian Kuss, University of Manitoba

12:50pm - 1:10pm, June 29th (*abstract*)

GS7: Effect of Sb Doping and Polyvinylpyrrolidone on the Mesoporous TiO2 Photoanodes for Sb2Se3 Sensitized Solar Cells
Melissa Isabel Ayala Sánchez, CINVESTAV Unidad Saltillo

1:10pm - 1:30pm, June 29th (*abstract*)

GS8: Synthesis of Ternary Compounds of SnxSbySz Metal Chalcogenides by Chemical Bath Deposition for Their Application in Solar Cells
Melani Guadalupe Ayala Sánchez, Centro de Investigación y de Estudios Avanzados del IPN (Cinvestav Saltillo)

2:20pm - 2:50pm, June 29th (invited) (*abstract*)

GS9: Deploying Interfacial Engineering to Maximize Efficiency in a Biomass Combuster
Sami Khan, Simon Fraser University

2:50pm - 3:10pm, June 29th (*abstract*)

GS10: Bioleaching of Silca-Sulfide Gold Ore Deposits, Tigray-Ethiopia
Goitom Gebreyohannes Berhe, Desta Berhe Sbhatu, Samuel Estifanoc Gebre, Kiros Hagos Abay, Genet Gebryohannes Mihretu, Gebrekidan Mebrahtu Tesfamariam, Sumuel Alemayo, Mulugeta Sisay Cheru, Afewerk Gebre, Mekelle University, College of Natural and Computational Sciences

3:10pm - 3:30pm, June 29th (*abstract*)

GS11: Use of Carbonized Rice Bran for Adsorption of Lead (ii) Ions in Aqueous Solution
Sandeep Kaur Gill, Rajiv Arora, Bohar Singh, G. N. Constructions, Shaheed Bhagat Singh State University

3:30pm - 3:50pm, June 29th (*abstract*)

GS12: Assessing the Feasibility of a 2-Step Method for Leaching Synthetic Scheelite in H2SO4 and H2O2 Solution
Idil Mutlu Tuncer, Jing Liu, University of Alberta

4:10pm - 4:40pm, June 29th (invited) (*abstract*)

GS13: Built to Last: How NMR Spectroscopy is Improving Materials for Nuclear Waste Disposal
Scott Kroeker, University of Manitoba

4:40pm - 5:00pm, June 29th (*abstract*)

GS14: The Investigation of Usability of High Carbon Ferrochrome Slag as a Slag Conditioner at Iron&Steel Industry
Gökhan Başman, Tuğçe ERGÜL, Hande Ardıçoğlu, Tuğçe Özcan, Eti krom INC.

5:00pm - 5:20pm, June 29th (*abstract*)

GS15: Work Function-tailored Nitrogenase-like Fe Double-atom Catalysts on Transition Metal Dichalcogenides for Nitrogen Fixation
Xue Yao, Zhiwen Chen, Chandra Veer Singh, University of Toronto

5:20pm - 5:40pm, June 29th (*abstract*)

GS16: Basal Plane Activation via Grain Boundaries in Monolayer MoS2 for Carbon Dioxide Reduction
Ying Zhao, Jun Song, McGill University

10:10am - 10:40am, June 30th (invited) (*abstract*)

GS17: Nano-materials for Waste Heat Conversion into Electrical Energy Thermoelectric generator
Wiqar Hussain Shah, International Islamic University

10:40am - 11:00am, June 30th (*abstract*)

GS18: Green Corrosion Inhibitors for Drilling Operation: New Derivatives of Fatty Acid-based Inhibitors in Drilling Fluids for 1018 Carbon Steel in CO2-saturated KCl Environments
Mohammad Palimi, Y. Tang, V. Alvarez, E. Kuru, D.Y. Li, University of Alberta

11:00am - 11:20am, June 30th (*abstract*)

GS19: Investigating the Localized Deformation Induced by Hydride Precipitation in Zirconium
Masoud Taherijam, Saiedeh Marashi, Hamidreza Abdolvand, Western University

11:20am - 11:40am, June 30th (*abstract*)

GS20: Crack Nucleation and Propagation in Dual Phase HCP-BCC Zirconium
Saiedeh Sadat Marashi, Hamidreza Abdolvand, Western University

12:00pm - 12:20pm, June 30th (*abstract*)

GS21: Aluminum Hydride Formed on Aluminum Base Substrates by Hydrogen Plasma Irradiation
Goroh Itoh, Tomoharu Ouchi, Naoyuki Sato, Shigeru Kuramoto and Junya Kobayashi, Ibaraki University

12:20pm - 12:40pm, June 30th (*abstract*)

GS22: PON1 Enzyme Mutation and Organ Pesticide Usage
Ali Göksu, Tuana Glass Mould, University of Manitoba

12:40pm - 1:00pm, June 30th (*abstract*)

GS23: The Effect of Adding Green Pea Pod Lignin and Industrial Hemp Fiber to Polyester Resin
Hassan Alshahrani, Najran University

Posters (5:20pm-6:20pm, June 28th):

GS24: Strain Rate Induced Mechanical Changes in NASICON Solid Electrolyte Materials (*abstract*)
Zachary Carroll, Yu Zou, University of Toronto

GS25: Vitrification of Zeolites and Geopolymers for Long-term Immobilization of Cesium and Strontium (*abstract*)
Thulasi Elumalai, University of Manitoba

GS26: The Effects of Polypyrrole:Carboxymethyl Cellulose Composite Morphology on Capacitance and Conductivity: An Alternative Battery Binder Material (*abstract*)
Gamaliel Azariah, Christian Kuss, University of Manitoba

GS27: A Novel Approach to Mineral Carbonation from Ultramafic Tailings (*abstract*)
Sara Gardideh, Mansoor Barati, University of Toronto

GS28: The Role of Atomic-scale Defects in Single-Atom Catalysis (*abstract*)
Shiva Mohajernia, University of Alberta

GS29: Visible Light Driven Nd2O3/Mo(S,O)3-x·0.34H2O Heterojunction for Enhanced Photocatalytic Degradation of Organic pollutants (*abstract*)
Sleshi Fentie Tadesse, Dong-Hau Kuo, Worku Lakew Kebede, Girma Sisay Wolde, Ming Chi University of Technology, National Taiwan University of Science and Technology

Symposium:

Functional materials and structures (FMS)

Thursday - Friday, June 29th – 30th 2023

Room: E2-130, Engineering & Information Technology Complex

Chair: Nan Wu

Talks:

10:10am - 10:40am, June 29th (invited) (*abstract*)

FMS1: Development of an Adaptive Periodic Magnetorheological based Metamaterial to Attenuate Wide-Band Low-Frequency Noise and Vibration
Hamid Jafari, Ramin Sedaghati, Concordia University

10:40am - 11:00am, June 29th (*abstract*)

FMS2: Loading Variable Effects on Fatigue Behavior of Wood Flour HDPE Composites
Babak Mokhtarnia, Mohammad Layeghi, University of Tehran

11:00am - 11:20am, June 29th (*abstract*)

FMS3: Synthesis, Characterization and Molecular Simulation of Polymers Enhanced with Halloysite Nanotubes
Ron Miller, Rafaela Aguiar, Oren Petel, Carleton University, University of Toronto

11:40am - 12:00pm, June 29th (*abstract*)

FMS4: Optimizing Extrusion and Fabrication of Phosphate Glass-Based Microstructured Optical Fibers for Biomedical Applications
Seyed Hossein Mussavi Rizi, Davide Luca Janner, Nadia Boetti, Diego Pugliese, Politecnico di Torino

12:00pm - 12:20pm, June 29th (*abstract*)

FMS5: A Scanning Fabry-Perot Cavity for the Study of THz Frequency Magnon Polaritons
Christina Balanduk, University of Manitoba

12:20pm - 12:40pm, June 29th (*abstract*)

FMS6: N-halamine-based Antimicrobial Fabric Finish for Frontline Workers – Application Techniques and Performance Evaluation
Anita Amir Labonno, René Arredondo, Paulina de la Mata, Jane Batcheller, James Harynuk, Patricia I. Dolez, University of Alberta

2:20pm - 2:40pm, June 29th (*abstract*)

FMS7: Mechanistic Study of Pathogen Inactivation on Salt-coated Filters
Sumin Han, University of Alberta

2:40pm - 3:00pm, June 29th (*abstract*)

FMS8: Polypyrrole:Caboxymethyl Cellulose as Electrode Binder Material: Comparative Study Between Nanoscale Morphologies
Gamaliel Azariah, University of Manitoba

3:00pm - 3:20pm, June 29th (*abstract*)

FMS9: Fluorinated Omniphobic Coatings for Low-Surface-Tension Liquids
Shashwata Moitra, Constantine M Megaridis, University of Illinois at Chicago

3:40pm - 4:00pm, June 29th (*abstract*)

FMS10: 4-Alkoxycinnamic Acid Derived Calamitic Liquid Crystals (LCs) as Potential Low Molecular Mass LC Alignment Materials
Jehangir Khan, Paris Lodron University of Salzburg

4:00pm - 4:20pm, June 29th (*abstract*)

FMS11: TTB-based Ba2K2Gd3Fe5O15 Electroceramic with Sodium (Na) as a Dopant for Capacitors: Electrical and Magnetic Properties
Sameed Khan, Fayaz Hussain, NED University of Engineering and Technology

10:10am - 10:30am, June 30th (*abstract*)

FMS12: Curved-based Auxetic Metamaterials for Energy Absorption, Vibration Isolation, and Electricity Generation Applications
Ramin Hamzehei, Nan Wu, University of Manitoba

10:30am - 10:50am, June 30th (*abstract*)

FMS13: Innovative Piezo Materials /Technologies
Lala Agamirov-Nost, Single Crystals Innovative Sensors Inc.

10:50am - 11:10am, June 30th (*abstract*)

FMS14: Analysis of Nonlinear Piezoelectric Energy Generator under Friction-induced Vibration
Yu Xiao, Nan Wu, University of Manitoba

11:30am - 11:50am, June 30th (*abstract*)

FMS15: Aptasensors Based on 2D Asymmetric Geometry MoS2 Diodes for Label-Free and Ultrasensitive Detection of Cytokine Biomarkers
Mirette Fawzy, Thushani De Silva, Michael M. Adachi, Karen L. Kavanagh, Simon Fraser University

11:50am - 12:10pm, June 30th (*abstract*)

FMS16: Optimized Lithography-Free Fabrication of Sub-100 nm Nb2O5 Nanotube Films as Negative Supercapacitor Electrodes: Tuned Oxygen Vacancies and Cationic Intercalation
Doha Mohammed, Kholoud E. Salem, Nageh K. Allam, Cairo University, The American University in Cairo

12:10pm - 12:30pm, June 30th (*abstract*)

FMS17: Nickel-doped Cobalt Oxyhydroxide Nanowires Coupled Polyaniline Functionalized Carbon Cloths as Multifunctional Electrocatalysts for Hydrogen/Oxygen Evolution Reactions at All pH Levels
Niranjanmurthi Lingappan, Wonoh Lee, Chonnam National University

Keynote speech: D.K.C. MacDonald Memorial Lecturer

From Electrons to Photons and From Plasmons to Phonons. What can we Learn from State-of-the-Art Characterization Techniques?

Gianluigi Botton

McMaster University

Abstract:

Electron microscopes are very power tools to study the structure of materials at unprecedented spatial and energy resolution. These improvements are the results of the numerous efforts and foresight of the pioneers in electron optics, instrument developers and risk takers that have led to commercial aberration correctors, monochromators and new detectors. These new tools have increased the performance and information content that can be obtained from electron microscopes. While physicists, chemists and materials scientists benefit tremendously from these improvements, we need to be mindful of the fact that there are many other tools that provide complementary information and that there are limitations to all techniques. In this presentation, I will show some recent examples of electron microscopy work related to the quantum materials, battery materials and detection of plasmonic modes in complex noble metal structures and phonon excitations in crystals. Then I will focus on the complementary photon-based techniques that are available in synchrotrons. With energies ranging from sub-meV to 100keV, there is a wealth of information that can be extracted from imaging, spectroscopy and scattering methods, from bonding environments of single atom catalysts, electronic structure of buried interfaces, and Fermi surfaces, to imaging of cochlear implants, spectroscopy in *in-operando* conditions and trace contaminants in the eyes of zebra fish larvae and whales. These examples highlight the benefits of considering multiple techniques when one needs to understand the structure and composition of a very broad range of materials.

→ *Return to the schedule*

A Scientific Approach to Sustainable Development: What Can Metal Physics Offer?

Chad Sinclair

The University of British Columbia

Abstract:

Material production is responsible for nearly one third of all greenhouse gas emissions. The primary production of aluminum, alone, has a particularly significant environmental impact, contributing 1% of global energy demand and 2-3% of global greenhouse gas emissions. As the demand for commodity metals continues to rise, it is imperative that we, as a community, find ways to reduce the impact of metals on energy consumption and the environment. Basic science, including metal physics, has the potential to play a crucial role in achieving this goal. In my talk, I will explore the challenges associated 1) decarbonized steel production and 2) increased recycling of aluminum alloys. In both cases I will emphasize how a better understanding of the role of trace elements can simultaneously benefit properties and sustainable development.

→ *Return to the schedule*

Keynote speech: Metal Chemistry Lecturer

Metal Chemistry in Electrocoagulation and Redox Flow Battery Technologies

Edward (Ted) Roberts

University of Calgary

Abstract:

Sacrificial iron or aluminum electrodes are used in electrocoagulation water treatment processes. The process involves simultaneous metal dissolution and hydrogen evolution, leading to formation of metal hydroxide coagulants. Electrode fouling / passivation leads to operational challenges, and polarity reversal is typically used to mitigate these detrimental processes. Recent studies on the impact of solution chemistry and operating conditions on the fouling and electrode processes will be presented[1,2]. Visualization of the pH boundary layer and gas-solid-liquid interactions in the electrode boundary layer (see Figure 1) have provided new insights into the electrocoagulation process.

In redox flow batteries (RFBs), redox active metal species dissolved in liquid electrolytes are used to store energy. Metal solutions are pumped through the battery during charge and discharge. RFBs are being developed and commercialized for energy storage on electricity networks, to integrate intermittent renewable energy and to improve network performance. Widely used metals used in RFB systems include zinc, vanadium, iron and chromium. Performance of RFBs depends upon the metal chemistry, including the redox potential, solubility, electrochemical activity, and speciation. The effect of metal impurities in the electrolyte and approaches being used to develop new RFB systems with improved performance and lower cost will be discussed.

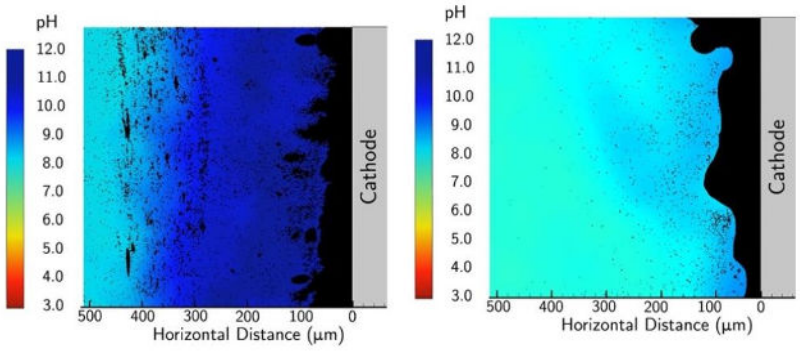

Figure Operando visualization of pH distribution and phases close to an aluminum cathode during electrocoagulation, obtained by laser scanning fluorescence microscopy. In synthetic process water (a), with a low buffering capacity, the high pH at the electrode mitigates aluminum hydroxide fouling, while for field samples with high buffering capacity, the pH at the electrode is lower, leading to precipitation close to the electrode surface and associated fouling.

References:

[1] Fuladpanjeh-Hojaghan, Elsutohy, Trifkovic, Roberts(2019) In-Operando Mapping of pH Distribution in Electrochemical Processes. *Chem.* **131**, 16971 –16975.
[2] Chow, Ingelsson, Roberts, Pham (2021) How does periodic polarity reversal affect the faradaic efficiency and electrode fouling during iron electrocoagulation? *Water Research* **203,** 117497.

→ *Return to the schedule*

Investigation of Microstructure and Deformation Mechanism in Cold Sprayed CuNi, CuSn, and CuNiSiCr Alloys

Jingjie (Peter) Wei, Yu Zou

University of Toronto

Abstract:

The microstructure and mechanical properties of cold sprayed Cu-10wt%Ni, Cu-10wt%Sn and Cu-7wt%Ni-2wt%Si-0.9wt%Cr are examined and compared to conclude the deformation mechanism. All coating samples show a dense structure with high deposition efficiency, indicating that the parameters and conditions of the cold spray process were well selected. The cross-sections of both coatings and feedstock powders were analyzed using SEM and EBSD. Heterogenous microstructure with highly refined grains at particle interfaces is observed. The high strain rate deformation of the particles at impact locations may have led to the local refinement of grains by dynamic recrystallization. Comparison of microhardness on cross-sections of feedstock powder and coatings show significant enhancement in microhardness after cold spray. Nanoindentation maps show local nanohardness distributions that correlate to the heterogeneous microstructure observed. Increasing the processing temperature from 800℃ to 950℃ led to higher average kinetic energy and thermal softening of the CuNi powders upon impact, resulting in a denser coating with slight decreases in mechanical hardness.

→ *Return to the schedule*

Assessing the Mechanical Response of an Additively Manufactured CoCrFeMnNi High Entropy Alloy Using DIHPB Tests and Electron Microscopy

Joseph Agyapong, Solomon Boakye-Yiadom, Alexander Czekanski

York University

Abstract:

This abstract covers an investigation into the mechanical behavior and microstructure evolution of CoCrFeMnNi high entropy alloy (HEA) using Direct Impact Hopkinson Pressure Bar (DIHPB) tests at ambient temperatures. The HEA is produced via selective laser melting (SLM) and possesses distinctive microstructures and mechanical qualities that make it a potential material for a variety of applications, particularly those involving dynamic conditions. Additionally, electron microscopy is used to investigate the mechanical response of the CoCrFeMnNi HEA and its deformation mechanisms, focusing on the defect structures created during deformation, such as adiabatic shear bands. The results provide insights into the mechanical behavior of the SLM built CoCrFeMnNi HEA and highlight the significance of electron microscopy for comprehending the fundamental principles driving its dynamic deformation. The findings are anticipated to help to the development of HEAs with increased mechanical characteristics that are appropriate for applications involving high stresses. Additionally, it demonstrates the potential of SLM-printed HEAs as highly advanced materials and gives valuable insight for their future application in a variety of engineering areas. The findings will be presented and discussed, providing vital insights for the development of advanced materials for usage in dynamic environments and the conference.

→ *Return to the schedule*

Dynamic Impact and Ballistic Behaviour of Additively Manufactured AlCrFeCoNi High Entropy Alloy

Ekundayo Binuyo, G. Asala, O.T. Ola, O.A Ojo, A.G Odeshi

University of Saskatchewan, University of Manitoba, Red River College Polytechnic

Abstract:

The dynamic impact and ballistic behaviour of AlCrFeCoNi1.4 high entropy alloy (HEA) produced using directed energy deposition (DED) additive manufacturing (AM) technology were investigated in this work. The influence of processing parameters, loading directions and post-deposition heat treatment on the damage evolution of the AM alloy were evaluated. A Split Hopkinson pressure bar (SHPB) system was used to characterize the dynamic impact behaviour of the deposits, and a 0.50 FSP calibre weapon was used for the ballistic penetration test. The alloy was subjected to post-deposition heat treatment at 700°C for 1.5 hr, followed by air-cooling, which increased the hardness of the deposit by about 20%. Experimental results from the ballistic penetration test showed that the absorbed energy of the projectile along the build direction is greater than that in the direction orthogonal to it. In addition, the dynamic stress-strain curves obtained from the impact tests displayed higher impact strength when tested along the build direction. The additive-manufactured HEA produced with low (energy area density) EAD displays a significantly greater impact strength compared to those produced with high EAD. Although the HEA subjected to post-deposition heat treatment exhibited a higher impact strength, it suffers from low ductility compared to the as-built alloy. Furthermore, the effects of plastic deformation on the microstructure of AM AlCrFeCoNi HEA under dynamic impact loading are evaluated.

→ *Return to the schedule*

Quality Prediction and Energy Consumption Optimization in Selective Laser Melting

Shazaib Ahsan, MD Rokibujjaman Sabuj, Xihui Liang

University of Manitoba

Abstract:

The production of high-quality parts using additive manufacturing is of utmost importance. Selective LASER Melting (SLM) is a popular additive manufacturing technique to produce high-quality components. Tuning the SLM process parameters such as LASER power and scan speed can assure high-quality components. Although the existing studies have shown promising results, they rely on limited inputs and outputs and often ignore energy consumption's impact. To address this gap, this study proposes a Multiple-Inputs-Multiple-Outputs (MIMO) artificial neural network. The network uses four input parameters (LASER power, scan speed, overlap rate, and hatch distance) to predict four critical product quality measures as outputs namely, relative density, hardness, tensile strength, and porosity. To obtain a more comprehensive and generalized model suitable for use in real-life industrial applications, training data from various sources are combined. Additionally, the study also proposed a genetic algorithm-based energy optimization method that balances product quality and energy consumption. The result from this study shows a remarkable reduction in energy consumption of 26%, without compromising the product quality which is desirable for industrial applications.

→ *Return to the schedule*

Effect of Heat Treatment on Mechanical Compression Properties of Wire Arc Additive Manufactured C250 Maraging Steel

Lulu Guo, Lina Zhang, Joel Andersson, Olanrewaju Ojo

University of Manitoba, University West

Abstract:

The mechanical compression properties of C250 maraging steel fabricated by wire arc additive manufacturing (WAAM), in the as-deposited and post-fabrication heat treated conditions are investigated under quasi-static testing condition. The microstructure of the material is studied by analytical transmission electron microscopy and a comparison is made between the WAAM-ed and conventionally produced wrought materials. The results reveal that the WAAM-ed material, in the as-deposited condition, exhibits a lower yield and ultimate compressive strengths compared to the commercial heat-treated wrought alloy, due to the absence of strengthening precipitates and the presence of a retained austenite phase. However, post-fabrication thermal treatment significantly improves the compressive strengths of the as-processed material to levels comparable to those of the conventionally produced wrought material. This is attributed to the formation of nano-sized Ni3Mo strengthening precipitates, reduction in the amount of austenite phase, as well as refinement of prior austenite grains during the thermal treatment.

→ *Return to the schedule*

Effects of Laser Surface Texturing on the 301LN stainless steel

Mohammad Rezayat, Antonio Mateo

Polythecnic University of Catalunya

Abstract:

In this project, nanosecond pulsed laser is used to create a linear pattern on the surface of 301LN stainless steel. The aim is to find the optimal parameters in order to achieve the desired metallurgical and mechanical properties. In this regard, after laser surface processing, the surface of the samples was examined by SEM and confocal microscopes. Tensile and fatigue tests were also performed on standard samples so that the changes in mechanical properties after surface laser treatment and before that are analyzed and investigated. The results show that after the surface laser treatment, the mechanical properties have been improved to an optimal extent.

→ *Return to the schedule*

Simulation of Laser Powder Bed Fusion Process for Nickel Alloy Inconel 718 Using Representative Volume

Rasool Mokhtari Homami, Olanrewaju Ojo

University of Manitoba

Abstract:

Residual stress is a major issue that inhibits the Laser Powder Bed Fusion (LPBF) process from being widely used in the industry. In this study, a coupled thermo-mechanical simulation is performed to simulate the LPBF process using the plugin tool AM Modeler and the representative volume (RV) approach. This study focuses on evaluating the effects of laser speed, laser power, and pre-heating temperature on resultant residual stress, which influences components' fatigue life and shape distortions. The developed finite element method (FEM) model reduces the computational time without sacrificing accuracy. The results match well with the literature and show the effectiveness of AM Modeler and the RV approach. The in-process nodal temperature and stress show that the newly deposited layer affects part quality and components' fatigue life up to seven layers beneath it. Furthermore, the FEM findings demonstrate that pre-heating of the build platform to the temperature of 225 °C significantly reduces the residual stress. Also, the influence of laser speed on the reduction of residual stress is greater than the effect of laser power. Additionally, the FEM findings show higher tensile stress at the surface and compressive stress close to the substrate.

→ *Return to the schedule*

Improved Corrosion Resistance of WE43/TiC Reinforced Surface Composites

Ravinder Singh, Amardeep Singh Kang, Shivali Singla

Lovely Professional University, Baba Hira Singh Bhattal Institute of Engineering and Technology

Abstract:

The use of friction stir processing (FSP) of magnesium alloys is anticipated to enhance their resistance to corrosion. In this study, WE43 magnesium alloy was reinforced with nano-TiC particles by using various tool pin geometries (triangular, taper cylindrical, and square), at different tool rotation speeds (800 and 1700 rpm) and transverse speeds (30 and 60 mm/min) and subsequently examined for their corrosion resistance. The findings revealed that FSP led to a significant improvement in the corrosion resistance of both processed WE43 alloy and its composite. Furthermore, the square tool pin geometry was found to provide the highest corrosion resistance compared to the other pin profiles. The WE43/TiC composite demonstrated 33% more corrosion resistance than the FSPed WE43 alloy. Moreover, the WE43/TiC composite that was FSPed with the square tool pin profile, a low tool rotation speed of 800 rpm, and a higher transverse speed of 60 mm/min showed the greatest corrosion resistance. This increase in corrosion resistance was linked to the substrate's grain size.

→ *Return to the schedule*

Texture and Damage Evolution in Additively Manufactured 18%Ni-M350 Maraging Steel under Dynamic Impact Loading: Effects of Heat Treatment and Process Parameters

Toan Truong, G. Asala, O.T. Ola, O.A. Ojo, A.G. Odeshi

University of Saskatchewan, Red River College Polytechnic, University of Manitoba

Abstract:

The mechanical and microstructural response of 18%Ni M350 maraging steel produced by additive manufacturing (AM) using the direct energy deposition (DED) laser process under impact loading was investigated. The materials were manufactured using low and high energy area density (EAD) to identify the influence of AM processing parameters on the impact strength, microstructural, and texture evolution during deformation. In addition to the as-built (AB) state, maraging steel samples subjected to aging heat treatment (HT) were also investigated. Electron backscatter diffraction (EBSD) was used to characterize texture evolution under the impact loading. The test results reveal that the low-EAD as-built materials exhibit the greatest impact strength consistently for the applied strain rates that ranged from 200 to 3300 s^{-1}. This finding is attributed to the high local misorientation that is closely correlated with the high number of geometrically necessary dislocations (GND) generated as a result of the rapid cooling process. In particular, the geometry of the molten pool has a significant effect on the cooling rate. The activation of a new slip system $\{112\}\langle 11\bar{1}\rangle$ is observed after deformation at high strain rates in the as-built material. A higher degree of new slip activation in low-EAD samples suggests a higher susceptibility to the formation of an adiabatic shear band (ASB). The improvement in impact strength of the steel materials after being heat-treated can be attributed to the dominance of precipitate-dislocation interactions as the primary strengthening mechanism.

→ *Return to the schedule*

A Fundamental Analysis on Laser Remelting of High-Entropy Alloys: towards Enhanced Printability

Ajay Talbot, Xiao Shang, Wandong Wang, Yu Zou

University of Toronto

Abstract:

Additive manufacturing (AM) techniques have gained popularity in fabricating novel high entropy alloys (HEAs); however, these high-energy processes often result in defects such as porosity, microcracking, and elemental micro-segregation. This study investigates the effects of laser remelting on HEAs to reduce these defects. Two HEAs, CoCrFeNiMn and NbMoTaW, were fabricated via arc melting and subsequently laser remelted with a directed energy deposition (DED) system at various laser power and scanning speeds. The laser remelted samples exhibited fully dense and refined microstructures compared to the as-cast samples. EDS analysis revealed that micro-segregation of low melting point elements occurs at energy densities below 20J/mm2 and above 50J/mm2 due to inadequate time for elemental mixing and slower cooling rates, respectively. In addition to experimental investigations, both mechanisms are confirmed through finite element analysis. The present work identifies the competing mechanisms that lead to micro-segregation within AM HEAs with respect to laser processing parameters and provides optimized laser remelting strategies to guide researchers and industry professionals towards producing more robust and high-performance AM materials.

→ *Return to the schedule*

Subtractive vs Additive Manufacturing of a Custom Scanning Tunnelling Microscope Head

Sangeev Selvaratnam

University of Manitoba

Abstract:

The primary goal of this project is to design and fabricate highly stable Scanning Tunnelling Microscope (STM) heads that will be used in the Ultrafast Microscopy and Magnetism Laboratory to measure sub-picosecond magnetodynamics with atomic resolution. To achieve this goal, the STM head must have high vibrational stability, low thermal drift, optical access to allow coupling to THz light, and custom coarse motion piezo motors to facilitate the positioning of the tip. The project has spanned multiple full design and prototyping cycles for the heads that are based on the Pan head design [1]. The main design goals were to minimize the mass and maximize rigidity and the resonant frequencies of the head.

Two versions of the STM head components were made using Autodesk Inventor and simulated with NASTRAN, one with the subtractive manufacturing constraints taken into consideration and the other with the aid of generative design for additive manufacturing.

Once the designs were finalized, multiple prototypes were 3D printed with plastic for further testing before they were machined, and 3D printed using a five-axis CNC mill and a laser sintering 3D printer respectively. Currently, the STM chambers are fully assembled and are being tested on their Ultra-high Vacuum (UHV) compatibility and the heads are being assembled for their first coarse walking test.

The successful completion of this project will provide two custom STM heads that will allow us to study the capabilities of additive manufacturing compared to traditional machining methods as well as the UHV compatibility, rigidity, and thermal drift of additive manufacturing with unprecedented detail.

[1] S. H. Pan, E. W. Hudson, and J. C. Davis. “3He refrigerator based very low temperature scanning tunnelling microscope”. In: Rev. Sci. Instrum. 70 (1999), pp. 1459–1463.

→ *Return to the schedule*

Microstructural and Wear Characterization of Additive Manufactured Ceramics via Lithography-based Ceramic Manufacturing (LCM) Technique

Solomon Hanson Duntu, Diego Mateos, Solomon Boakye-Yiadom

York University

Abstract:

Additive manufacturing (AM) or three-dimensional (3D) printing has revolutionized the manufacturing industries in recent times. In addition to high throughput and cost minimization, the AM process offers high geometric freedom for intricate structures. Despite the enormous impact of AM in the metal and polymer industries, the deployment of 3D printing in ceramic structures has not received much exposure due to challenges including processing route with AM and discrepancy in properties relative to a conventionally produced ceramic parts. In the current work, an approach has been made to manufacture high dense ceramic structures using a lithography-based technique. This lithography-based ceramic manufacturing (LCM) process utilizes polymerization principle, where selective curing of a photosensitive slurry of dispersed ceramic powder within a polymer matrix is achieved using a photolithographic process to produce ceramic green parts layer-by-layer, followed by debinding and final sintering to achieve dense parts. Alumina, Yttria Stabilized Zirconia (YSZ) and Zirconia Toughened Alumina (ZTA) ceramic structures were produced using the novel LCM process. The evolving microstructure of the AM-built ceramics were studied to assess the effect of printing parameters such as layer thickness and build direction during the LCM process. Wear property characterizations were also performed on the ceramic AM parts to analyze their tribological integrity as biomaterials.

→ *Return to the schedule*

Electrochemical Corrosion Behavior of We43/SiC Reinforced Surface Composites

Amardeep Singh Kang, Ravinder Pal Singh, Shivali Singla

Lovely Professional University, Baba Hira Singh Bhattal Institute of Engineering and Technology

Abstract:

Friction stir processing (FSP) of magnesium alloys is expected to improve their corrosion resistance. In this work, WE43 magnesium alloy was FSPed with nanodimensional SiC particles with different tool pin geometries (taper cylindrical, triangular, and square), transverse speeds (30 and 60 mm/min) and tool rotation speeds (800 and 1700 rpm) and later tested for their corrosion resistance. Results confirmed that the FSP substantially improved the corrosion resistance of both processed WE43 alloy and its SiC-reinforced composite. Also, both WE43 alloy and its SiC-reinforced composite substrates processed with square tool pin geometry exhibited maximum corrosion resistance over other pin profiles. WE43/SiC composite showed 41% more corrosion resistance compared to FSPed WE43 alloy. Furthermore, WE43/SiC composite FSPed with square tool pin profile at low tool rotation speed of 800 rpm and higher transverse speed of 60 mm/min exhibited the best corrosion resistance. This enhanced corrosion resistance was substantiated as a function of grain size of substrates.

→ *Return to the schedule*

Modification of Diffraction, Microscopic and Spectroscopic Characterizations of Ni-Zn Ferrimagnetic Nanoparticles Via Cerium Element as Advanced Engineering Materials

Rabea Al-Kershi, A. M. Alsheri, R. M. Attiyah

King Khalid University

Abstract:

This work is interested in the fabrication of Cerium rare-earth element doped nickel-zinc compounds ferrimagnetic nanoparticles (Ni 0.55 Zn 0.45 Fe 2-x CexO4; x=0, 0.022, 0.044, and 0.066) via coprecipitation technique and Modification of their Diffraction, Microscopic and Spectroscopic Characterizations as Advanced Engineering Materials. The structures and morphologies of the synthesized compounds were characterized by XRD, FTIR, SEM and Raman techniques. XRD patterns displayed that the specimens exhibited a monophasic spinel structure without other impurities for cerium concentration (x) ⩽ 0.066 at 1200 oC. Both average crystallite size and lattice parameters became smaller with the increasing Ce ions substitution content. SEM images indicate that grains of the prepared compounds are smaller, more perfect, homogeneous and have less agglomeration than that of the undoped Ni-Zn ferrite. The maximum intensities of first-order Raman spectroscopic peaks (Eg, F2g(2), A1g(2) and A1g(1)) of NiZn-Ce ferrite nanoparticles were observed at about (330, 475, 650, and 695) cm-1 respectively which confirm the formation of cubic spinel structure. The concentration of cerium ions (x) can be used to engineer the optical band gap for specific potential applications, where the values of direct and indirect optical band gaps are shown in a wide range from insulators to semiconductor materials.

→ *Return to the schedule*

Fabricating 316L Stainless Steel Unsupported Rods by Controlling the Flow of Molten Pool via Wire Arc Additive Manufacturing

Chenchen Jing, Bo Cui, Changmeng Liu , Xihui Liang

Beijing Institute of Technology, University of Manitoba

Abstract:

The Wire Arc Additive Manufacturing (WAAM) technique is ideal for fabricating large lattice structures. However, producing inclined rods using additive manufacturing, a fundamental component of such structures, without a support structure is challenging. The limited inclination angles of rods and lower deposition efficiency constrain the application. To address these issues, the hot wire pulse arc additive manufacturing technique is proposed for manufacturing rods in lattice structures. By utilizing a pulse arc to control the flow of the molten pool, the range of inclination angles that can be manufactured was expanded, allowing for the successful production of unsupported rods with negative angles. Additionally, the use of hot wires reduces the heat input, improving the deposition efficiency of the rods. In this work, a comprehensive analysis of the heat input, macrostructure, microstructure and mechanical properties of rods with different diameters, inclination angles, and efficiency was conducted. It is found that the diameter of the rod negatively correlates with arc heat input per volume, and the tensile strength initially increases and then decreases with diameter. Furthermore, negative inclination angle rods require additional heat input for the molten pool to flow, resulting in slightly inferior mechanical properties when compared to rods with positive inclination angles. Increasing the torch travel speed and wire feeding speed appropriately significantly enhances deposition efficiency, reduces arc heat input, refines grains, and improves mechanical properties. Finally, a screw rod, an arc-curved rod, and a body-centred cubic (BCC) lattice structure were successfully fabricated, demonstrating the practicality and effectiveness of our method.

→ *Return to the schedule*

Laser Powder Bed Fusion of Alumina-based Ceramic Matrix Composite

Mohammad Azami, Zahra Kazemi

Concordia University, University of Toronto

Abstract:

This study focuses on the development of an alumina-based composite bonded with Fe-Ni-Cu alloy using laser powder bed fusion (LPBF) additive manufacturing technology. The LPBF process parameters were optimized to ensure high-quality printed samples. The as-printed structures underwent a sintering cycle under an inert atmosphere to promote bonding between the ceramic and metallic phases. The sintering process increased the average Vickers hardness of the green samples from 1475 Hv to 1960 Hv, resulting in improved mechanical properties. Despite the presence of pores generated during LPBF that could not be entirely eliminated after sintering, the sintered samples exhibited enhanced mechanical properties. To reduce internal porosities and microcracks, the sintered specimens were immersed in a polymeric solution. Results from mercury porosimetry showed a decrease in porosities from 36% to 27% after sintering and polymer immersion. Furthermore, immersing the specimens in the polymeric solution significantly improved the compression strength of the specimens, increasing it from 56 to 120 MPa. The microstructural examinations demonstrated a uniform distribution of steel particles in the alumina matrix using LPBF.

→ *Return to the schedule*

On the Development of a New Pre-Weld Heat Treatment Procedure for Preventing Gas Tungsten Arc Weld Heat-Affected Zone Cracking in a Newly Developed Co-Based Superalloy

H.R Abedi, O.A. Ojo

University of Manitoba

Abstract:

CoWAlloy1 is a new gamma prime (γ') precipitation-strengthened cobalt (Co)-based superalloy that is developed to replace conventional nickel (Ni)-based superalloys for high-temperature applications. Unfortunately, joining precipitation-hardened superalloys such as CoWAlloy1 is severely limited due to their high susceptibility to the heat-affected zone (HAZ) cracking during welding. A careful examination of the microstructure shows that a primary cause of HAZ cracking in this alloy is intergranular liquation due to the subsolidus liquation reaction of the MC-type carbides and γ' precipitates, which are identified by transmission electron microscopy (TEM) to be present in the material before welding. Total crack length (TCL) analysis on pre-weld heat-treated samples reveals that hardness of the pre-weld alloy does not impact the cracking susceptibility of the HAZ during welding. Time-of-flight secondary ion mass spectrometry (ToF-SIMS) analysis confirms the dependency of the cracking susceptibility of the HAZ on the grain boundary segregation of boron (B). In addition, it is observed that a reduction in grain size contributes to the resistance of CoWAlloy1 to HAZ cracking. Accordingly, a new pre-weld heat treatment that couples reduction in grain boundary segregation of B with small grain size, is found to effectively inhibit HAZ cracking during welding.

→ *Return to the schedule*

Hydrogels for wearable biosensors

Wen Zhong

University of Manitoba

Abstract:

Hydrogels are highly hydrated, porous and soft materials that resemble animal tissues, therefore, have attracted extensive interests in the development of wearable biosensors. Both natural (e.g., polysaccharides, proteins) and synthetic polymers have been utilized in the development of hydrogels for a variety of biosensors, including E-skin for health monitoring and management, E-nose that detects hazardous gases (like ammonia gas), and growth sensors that monitor plant growth. These hydrogels can also be developed into triboelectric generators, which convert environmental mechanical energy into electricity and endow self-powered biosensors.

→ *Return to the schedule*

A Biocompatible Self-healable Hydrogel Film with High Mechanical Strength and Antibacterial Properties

Mohammad Muzammil Kuddushi, Xiaoyi Deng, Xuehua Zhang

University of Alberta

Abstract:

Natural bio-materials widely investigated and used in the biomedical field. In this research work, thin hydrogel films composed by biopolymer mixture in different proportions (40:40:20 v/v) were prepared and characterized. The films were evaluated regarding the light transmission behavior, contact angle measurements, and chemical, thermal and mechanical properties. The water absorption and swelling behavior of these films were greatly improved by the increase hydrophilic polymer proportion in fabrication process. These thin transparent hydrogel films, shows the excellent self-healing and stretchability by multiple hydrogel bonding networks, were also investigated in-vitro biocompatibility and antibacterial properties. Results showed that excellent cell viability and effectively kill the positive and negative bacteria.

→ *Return to the schedule*

A Strong Hemostatic Adhesive of Self-Assembled Amphiphilic Granular Hydrogel from Andrias Davidianus Skin Secretion with Underwater Instant Adhesion Capacity

Yuqing Liu, Malcolm Xing

University of Manitoba

Abstract:

The widespread use of biological adhesives for tissue repair and hemostasis is limited by their weak adhesion in a wet environment of blood or body fluid. In the wet environment, biological adhesives face the huge challenges of surface water layer on tissue substrates and water swelling influence. The surface water layer on wet tissue substrates hinders formation of strong adhesion bridging adhesives and tissue substrates, and water swelling affects negatively on the adhesion capacity of biological adhesives as well. The biological adhesives with strong underwater adhesion capacity have great potential as the candidates of hemostatic adhesives. Herein, we report the wet adhesion mechanism of a dry granular natural bioadhesive from Andrias davidianus skin secretion (ADS). Once contacting water, amphiphilic ADS granules absorb surface water and self-assemble to form a hydrophobic hydrogel strongly bonding to wet substrates in seconds, which has good water resistance as well. ADS showed higher shear adhesion than current commercial tissue adhesives and an impressive 72-h underwater adhesion strength of 47kPa on porcine skin tissue. The assembled hydrogel in water maintained dissipation energy of 8 kJ/m3, comparable to the work density of muscles, exhibiting its robustness. Unlike catechol adhesion mechanism, ADS wet adhesion mechanism is attributed to water absorption by granules, and the unique equilibrium of protein hydrophobicity, hydrogen bonding, and ionic complexation. The in vivo adhesion study demonstrated its excellent wet adhesion and hemostasis performance in a rat hepatic and cardiac hemorrhage model.

→ *Return to the schedule*

Kirigami-Inspired Shape Memory Polymer Structures: Effects of Structural Design on Mechanical Performance under Cyclic Loading

Jungkyu Lee

Bruker Nano Surfaces

Abstract:

Shape memory polymer structures can be produced through compressive buckling of 2D precursors, enabling them to undergo substantial elastic strains. These microscale structures possess a shape memory effect that makes them ideal for various applications such as functional scaffolding for tissue engineering, energy storage, metamaterials, biomedical devices, and more. Optimizing the lifetime of these structures requires several factors, including the geometry of the structure, the presence of defects, and their performance under cyclic loading.

To evaluate these factors, structures made of epoxy monomers were fabricated and tested under cyclic compression using a nanomechanical test instrument at both room and elevated temperatures. The experimental results demonstrated significant variations in load bearing capacity and resilience under compression, depending on the structural shape.

In addition, complementary finite element modeling was conducted to examine the internal stress distributions of the structures, which were in agreement with the experimental observations.

These findings emphasize the significant influence of structural design on the mechanical performance of kirigami structures. Therefore, it is essential to consider the design parameters carefully when developing these structures for various applications.

→ *Return to the schedule*

Bioactivity Improvement of AZ31 Substrates via PCL-Chitosan - Bioglass Composite Nanofibers Electrospun Coating

Ebrahim Karamian, M. Haddadia, H. Bakhsheshirada, M. Kasiri-Asgarania and H. Gheisaria

Najafabad Branch, Islamic Azad University

Abstract:

Many natural and synthetic polymers have been investigated with respect to their use in tissue engineering and biomedical application. Among them, poly (ε-caprolactone) (PCL) and chitosan are widely used as biopolymers because of their desirable properties. To improve bioactivity of AZ31 Magnesium alloys in SBF (Simulated Body Fluid), a two layers PCL-Chitosan-Bioglass composite coating was developed on the surface of AZ31 substrates. To do this, the first layer was deposited via deep coating process, and PCL-Chitosan-Bioglass nanofiber was coated on the surface of metallic substrates. The morphology of the coating with various amounts of bio glass was observed by Scanning Electron Microscopy. SEM observation showed that the average diameter of PCL-Chitosan was less than 100 nm. ASTM D3359 standard was also carried out to evaluate the adhesion of the coating to the substrates. Increasing the bioglass in the coating improved the adhesion of the coating to its substrates. Roughness measurement was utilized to evaluate the surface roughness and surface area of the coated substrates. With an increase in the percentage of 58S bioglass nano powder up to 3 %wt., the surface roughness of the coating increased. In fact, it could be concluded that PCL-Chitosan-Bioglass Nano fibers coating can be applied on the surface of AZ31 to improve its bioactivity behavior for biomedical applications.

→ *Return to the schedule*

Multifunctional Wet Adhesive Film Enabled by a Single-Component Poly(ionic liquid)

Chenyu Qiao, Binmin Wang, Hong Wang, Hongbo Zeng

University of Alberta, Nankai University

Abstract:

In the past decade, wet adhesive materials have received increasing attention from global researchers due to their promising application in different areas, including biosensing and surface modification. Although tremendous effort has been devoted to exploiting synthetic wet adhesives, developing low-cost, robust, and multifunctional wet adhesive materials remains a challenge. In this work, a supramolecular wet adhesive that is composed of a single-component poly(ionic liquid) (PIL) and enables fast and robust underwater adhesion is reported. The PIL adhesive film possesses excellent stretchability and flexibility, which enables its anchoring on target substrates regardless of deformation and water scouring. The wet adhesion capability of the PIL adhesive film was systematically investigated by direct force measurements at nanoscale, and the PIL could achieve a strong adhesion (up to 56.7 mN/m) on diverse substrates (both hydrophilic and hydrophobic substrates) in aqueous media, within ~30 s after being applied. The related interfacial interaction mechanisms were also investigated using nanomechanical technologies. We found that the PIL adhesive film achieves robust and strong wet adhesion by synergistically employing different non-covalent interactions, such as hydrogen bonding, cation−π, electrostatic, and van der Waals interactions. Surprisingly, this PIL adhesive film exhibited impressive underwater sound absorption capacity. The absorption coefficient of a 0.7 mm-thick PIL film to 4-30 kHz sound waves could be as high as 0.92. This work reports a multifunctional PIL wet adhesive that has promising applications in many areas and provides deep insights into interfacial interaction mechanisms underlying the wet adhesion capability of PILs.

→ *Return to the schedule*

Mussel Inspired Graphene Aerogel for Skeletal Muscle Atrophy Regeneration

Xingying Zhang, Malcolm Xing

University of Manitoba

Abstract:

Cell-free materials that can transmit both mechanical and electrical stimulations provide a promising strategy for myo-injury repair. Skeletal muscle is sensitive to electrical stimulation (ES), and accordingly, materials are required to transmit the electrical signal while maintaining their elasticity to build the cellular communication network in denervated muscle for retarding muscle atrophy. In this study, tannic acid functionalized with methacrylate group (TA-MA), dopamine, and hydrothermal reduction were employed in multi-step base reduction to fabricate a polydopamine (PDA)/reduced graphite oxide (rGO) aerogel. This mussel-inspired PDA/rGO aerogel possessed good conductivity, electromechanical stability, and appropriate Young's modulus, which were favorable for the growth and differentiation of C2C12 myoblasts. After the cells-free PDA/rGO aerogel-transplanted denervated muscle was loaded with cyclic ES for three weeks, the mean muscle fiber size increased by 90% and the maximum contraction force of denervated muscle elevated by 50%, accompanied with a slight inflammation infiltration in muscle. In conclusion, PDA/rGO aerogel is a safe and effective implant for retarding the disuse muscle atrophy.

→ *Return to the schedule*

Metal Organic Frameworks as Promising Sensing Tools for Electrochemical Detection of Persistent Heavy Metal Ions from Water Matrices: A Concise Review

Muhammad Rizwan

University of Lahore

Abstract:

Water bodies are being polluted rapidly by disposal of toxic chemicals with their huge entrance into drinking water supply chain. Among these pollutants, heavy metal ions (HMIs) are the most challenging one due to their non-biodegradability, toxicity, and ability to biologically hoard in ecological systems, thus posing a foremost danger to human health. This can be addressed by robust, sensitive, selective, and reliable sensing of metal ions which can be achieved by Metal organic frameworks (MOF) based electrochemical sensors. In the present era, MOFs have caught greater interest in a variety of applications including sensing of hazardous pollutants such as heavy metal ions. So, in this review article, types, synthesis and working mechanism of MOF based sensors is explained to give general overview with updated literature. First time, detailed study is done for sensing of metal ions such as chromium, mercury, zinc, copper, manganese, palladium, lead, iron, cadmium and lanthanide by MOFs based electrochemical sensors. The use of MOFs as electrochemical sensors has attractive success story along with some challenges of the area. Considering these challenges, we attempted to highlight the milestone sensing devices for HMIs. Finally, challenges and future prospects have been discussed to promote the development of MOFs-based sensors in future.

→ *Return to the schedule*

Understanding gelation mechanisms of starches varying in molecular structures for industrial applications

Yikai Ren and Yongfeng Ai

University of Saskatchewan

Abstract:

As a biorenewable, biodegradable, and affordable polysaccharide, starch is a versatile gelling agent that has broad industrial applications. This presentation will focus on recent research to elucidate the gelation mechanisms of starches with different granular and molecular structures and under different processing conditions. For normal starches (< 45% amylose), swollen starch granules/remnants with good integrity after heating are essential for them to develop firm and viscoelastic hydrogels; for high-amylose starch (> 50% amylose), re-association and alignment of dispersed amylose molecules supports strong hydrogel formation. Because of the different gelling mechanisms, the strength of normal starch hydrogels tends to decrease with higher heating temperatures, whereas that of high-amylose starch hydrogels shows an increasing trend. The gelling behaviors of the different starches at various heating temperatures will also be linked to the microscopic structures of their respective gels using scanning electron microscopy (SEM) and synchrotron-based X-ray computed tomography (SXCT). Good examples of using starchbased biogels of different physical forms in various foods, bioplastics, pharmaceutical products, and biomedical materials will also be highlighted.

→ *Return to the schedule*

Investigating the Dissolution Properties of Bioactive Silver-loaded Borophosphate Glasses for Wound Healing

Scott Kroeker, Mojtaba Abbasi

University of Manitoba

Abstract:

Soft-tissue wound healing can be accelerated by the application of vacuum therapy or dressings made of collagen. A major challenge facing conventional wound treatments is that they are not capable of restoring the full anatomy of the native host's skin in the injured site. Moreover, antibiotics are currently the main means to prevent microbial infection, raising the possibility of antibiotic resistance. Bioactive borophosphate glasses doped with silver may provide a simpler, controllable and more effective approach to overcome these challenges. Silver has shown promising effectiveness in soft-tissue regeneration applications, allowing for precise targeting of the injury location since the bioactive glass matrix dissolves on a timescale favourable for wound healing. Candidate glasses have been proposed but there is little fundamental understanding to guide materials design. A series of melt-quenched borophosphate glasses with nominal compositions of (Ag2O)x(Na2O)35-x (P2O5)25(B2O3)40 ($0.5 \leqslant x \leqslant 3.0$) was prepared. 11B and 31P MAS NMR spectroscopy were used to investigate the glass structure. The results reveal that the dissolution rate is governed by the relative number of network linkages in the glass, i.e., P–O–[4]B (four-coordinated boron), [4]B–O–[3]B (three-coordinate boron) and P–O–P. Elemental release profiles in aqueous medium are interpreted to provide insight into the correlation between glass structure and dissolution behaviour. Even low Ag2O contents alter the dissolution behaviour of the glass, necessitating care in balancing dissolution rate and therapeutic efficacy.

→ *Return to the schedule*

Viscosity and Degradation Controlled Injectable Hydrogel for Esophageal Endoscopic Submucosal Dissection

Kaige Xu, Malcom Xing

University of Manitoba

Abstract:

Endoscopic submucosal dissection is a common procedure to treat early and precancerous gastrointestinal lesions. Via submucosal injection, a liquid cushion is created to lift and separate the lesion and malignant part from the muscular layer where the formed indispensable space is convenient for endoscopic incision. Saline is a most common submucosal injection liquid, but the formed liquid pad lasts only a short time, and thus repeated injections are needed, which increases the potential risk of adverse events. Hydrogels with high osmotic pressure and high viscosity are used as an alternative; however, there are some drawbacks such as tissue damage, excessive injection resistance, and high cost. In this article, we report a nature-derived hydrogel of gelatin-oxidized alginate (G-OALG) that is manufactured via in-situ Schiff's base reaction. According to the rheological analysis and compare to commercial endoscopic mucosal resection solution (0.25% hyaluronic acid), a designed G-OALG hydrogel of desired concentration and composition shows higher performances in controllable gelation and injectability, higher viscosity and more stable structures. The G-OALG gel also reveals lower propulsion resistance than 0.25% hyaluronic acid in the injection force assessment under standard endoscopic instruments, which eases the surgical operation. In addition, the G-OALG hydrogel exhibits good in vivo degradability and biocompatibility. By comparing the results acquired via endoscopic submucosal dissection to normal saline, the G-OALG shows great histocompatibility and excellent endoscopic injectability; and enables create a longer-lasting submucosal cushion. All the features have been confirmed in the living both pig and rat models. The G-OALG could be a promising submucosal injection agent for esophageal endoscopic submucosal dissection.

→ *Return to the schedule*

Self-powered Plant-wearable Hydrogel Sensors for Smart Farming

Yawei Zhao, Helen Hsu, Wen Zhong, Malcolm Xing

University of Manitoba

Abstract:

The current demand for high-yielding agricultural production has led to a concomitant increase in energy consumption and synthetic fertilizer usage, which has contributed to the proliferation of greenhouse gas emissions and water/soil contamination. Fortunately, smart farming has emerged as a potential solution to mitigate these issues by allowing for precise site-specific management and monitoring of crops. In this study, we present a smart-farming system composed of a novel multifunctional double-network hydrogel that can function as a triboelectric nanogenerator (TENG), supercapacitor, plant growth sensor, and ammonia sensor. The double-network hydrogel is fabricated using a combination of polyacrylic acid and conductive reduced graphene oxide, which is subsequently coated with polyaniline (PAA-RGO-PANI). The hydrogel exhibits remarkable mechanical properties, including a stretchability of 650% and mechanical strength of 1050 kPa, rendering it an ideal candidate for plant growth sensors. TENGs made using this hydrogel demonstrate clean energy harvesting potential with a power density of 424 mW/m^2 from sound waves, wind, and mechanical pressure. Additionally, our supercapacitor can maintain stability at 2330 mF/cm2 after 5000 charge–discharge cycles. Our self-powered smart farming system offers significant potential for resource conservation and plant management in modern agriculture.

→ *Return to the schedule*

Material Property Changes in Face Mask Silicone after 100 Sterilization Cycles by Autoclave, Hydrogen Peroxide, or Bleach Treatments

Liane Middleton, Tian Zhao, Stephanie Toigo, Richard Leask, Dan Deckelbaum, Sidney Omelon

McGill University, Research Institute of the McGill University Health Center, Montreal General Hospital, McGill University Health Center

Abstract:

Silicone is durable and pliable; it can create a seal with skin. Silicone gaskets seal unique full-face snorkel masks that are under investigation as potential re-purposed medical masks, with a replaceable filter at the inlet and outlet ports. Silicone sealing performance after 100 sterilization cycles was tested for gaskets cut from these masks. The sterilization methods were autoclaving, 6% hydrogen peroxide or 0.5% bleach immersion for 5 minutes, followed by a tap water rinse and air dry. Mechanical properties (tensile testing and Shore-A hardness testing) and crosslink density (swelling test) were measured after blocks of each of 25 sterilization cycles.

Hydrogen peroxide sterilization increased the Youngs modulus, Shore A hardness and cross-link density. Hydrogen peroxide cross-links silicone; it was hypothesized that hydrogen peroxide sterilization may continue silicone cross-linking. Bleach treatment reduced the Youngs modulus and Shore A hardness, and increased the cross link density. The bleach effect is not yet understood. Autoclave sterilization increased, then decreased the Youngs modulus to almost its original value, and did not significantly change the crosslink density. Both chemical sterilization methods may decrease silicone skin-sealing properties after 100 sterilization cycles.

→ *Return to the schedule*

Engineered Protein-based Materials Boosting Anti-fouling in Complex Biological Fluids

Ziqian Zhao, Mingfei Pan, Chenyu Qiao, Li Xiang, Xiong Liu, Wenshuai Yang, Xing-Zhen Chen, Hongbo Zeng

University of Alberta

Abstract:

Implantable medical devices (IMDs), such as implantable sensors for chronic disease diagnosis, knee replacements, and artificial blood vessels, save countless lives for organ restoration and have a huge global market valued at USD 120.5 Billion in 2021. More than 5% of citizens in developed countries currently need IMDs for essential clinic use. However, IMDs often suffer from dysfunction and infections due to irreversible biofouling. Constructing antifouling coatings on devices is considered as the most straightforward and effective approach to addressing biofouling issues. Inspired by the self-defensive 'vine-thorn' structure of climbing thorny plants, we have developed a zwitterion-conjugated protein engineered via grafting sulfobetaine methacrylate (SBMA) segments on native bovine serum albumin (BSA) protein molecules through click chemistry for surface coating and antifouling applications in complex biological fluids. Unlike traditional synthetic polymers of which the coating operation requires arduous surface pretreatments, the engineered protein BSA@SBMA can achieve facile and surface-independent coating on various substrates through a simple dipping/spraying method. Molecular force measurements by surface forces apparatus (SFA) and dynamic adsorption tests demonstrate that the substrate-foulant attraction is significantly suppressed due to strong interfacial hydration and steric interactions of the bionic structure of BSA@SBMA, enabling the coating surface to exhibit superior resistance to biofouling for a broad spectrum of species including proteins, metabolites, cells, and biofluids under various biological conditions. This work provides an innovative paradigm of using native proteins to generate protein-based coatings with extraordinary antifouling capability and desired surface properties for various medical and non-medical applications, such as molecule detection, point-of-care diagnostics, environmental toxin sensing, and microfluidic systems.

→ *Return to the schedule*

Injectable and Ultra-compressible Shape-memory Mushroom: Highly Aligned Microtubules for Ultra-fast Blood Absorption and Hemostasis

Xiaozhuo (Chelsea) Wu, Malcolm Xing

University of Manitoba

Abstract:

Noncompressible bleeding is associated with a significant source of traumatic fatality. Due to its inaccessibility to the pressure dressing, patients admitted with internal bleeding mainly rely on blood transfusion, coming with a high cost and immunological side effects. Injectable materials have emerged as a strategy; however, they have limitations on either large mechanical compressibility or blood clotting speed and blood absorbing capacity.

Here, we report that the mushroom's (Agaricus bisporus) stalk has aligned microtubular passages, which shows exceptionally fast capillary effects to draw liquid. After decellularization, the foam has primary component of chitin and maintains the highly parallel microtubules, which endorse exceptionally compressible (90% strain) and injectable to the deep wound, swiftly absorb the blood, elicit clotting by activating blood cells and platelets to promote blood clot formation. The foams' negatively charged surface and fast absorption channels can activate the intrinsic coagulation pathway and non-clotting factor dependent pathway to promote immediate fibrin growth. The hydrophilicity improves the adhesion of the platelets and blood cells, forming firm clotting. The channelled and high compressible foams show great hemostatic performances in vitro blood and in vivo livers and hearts.

→ *Return to the schedule*

Supramolecular Hydrogels from Functionalized Dipeptides for Drug Delivery

Muhammad Amirul Islam, Darren Makeiff, Mickie Wiebe, Aria Khalili, Ashley Wagner, JaeYoung Cho, Marianna Kulka

National Research Council Canada (NRC), Nanotechnology Research Centre

Abstract:

Supramolecular hydrogels from low molecular weight gelators (LMWGs) are a fascinating class of functional nanomaterials for applications spanning environmental remediation, tissue engineering, 3D printing and drug delivery amongst numerous others. Peptide-based LMWGs feature tunable self-assembly properties via chemical functionalization of the side chain, Nterminus and/or C-terminus capping groups. Here, new functionalized dipeptide gelators are presented, including their pH and solvent triggered self-assembly behavior in aqueous media. The driving forces for the self-assembly process were probed using various spectroscopic techniques (NMR, FTIR, UV-Vis, and CD), while the hydrogel properties were examined using microscopy and rheology. Robust hydrogels were formed at low gelator concentrations (i.e., <0.1 wt %), which were composed of fibrillar networks with tunable rheological properties. Finally, the release of the drug berberine chloride from hydrogel matrices are also discussed. This study provides further insight into the self-assembly of functionalized dipeptide-based LMWGs and their development towards biological applications.

→ *Return to the schedule*

The Effects and Potential Opportunities of Phosphorus Recovery by Elemental Sulphur Addition to Municipal Biosolids and Its Anaerobic Microbial Reduction to Sulphide

Samantha Gangapersad, Tian Zhao, Sidney Omelon

McGill University

Abstract:

We investigated the recovery of insoluble phosphorus from biosolids produced at municipal wastewater treatment plant in Ottawa, Canada: the Robert O. Pickard Environmental Center (ROPEC). ROPEC biosolids contain low solubility iron and aluminium phosphates and are applied to farmland. We hypothesized that iron phosphate could be dissolved by the reduction of elemental sulphur by endogenous biosolids microbes. Sulphide would precipitate insoluble iron sulphides and consequently dissolve iron phosphate.
Optimization of the molar ratio of elemental sulphur (S) to biosolids total phosphorus (TP) (0, 0.5, or 1), incubation temperature (22 °C, 32 °C, or 42 °C) and time (24 – 168 h) to maximise orthophosphate liberation was examined with Design of Experiments. The orthophosphate concentration increased with time for 32°C and 42°C incubations, but less significantly at 22°C. Only samples treated at 32°C and 42°C showed evidence of iron phosphate dissolution by x-ray diffraction. Maximum orthophosphate release occurred after 168 h with 0.5 M S/TP at 32°C. Biosolids incubation with 0.5 M S/TP showed a mean orthophosphate increase of 0.93 mg P/g dry biosolids (3.0% of TP in dry biosolids) when compared with control experiments. Further research is required to increase the orthophosphate release using this process.

→ *Return to the schedule*

Unfaulting of Dislocation Loops in Metals: Atomistic Simulations and Continuum Modeling

Jun Song, Cheng Chen

McGill University, Northwestern Polytechnical University

Abstract:

Dislocation loops are important secondary defects produced in metals subjected to irradiation and large deformation, playing a critical role in subsequent microstructure and damage evolution in the material. Here, the unfaulting of single and multi-layer dislocation loops in different metallic systems have been investigated through comprehensive atomistic simulations combining continuum modeling. A versatile approach properly accounting for atom insertion/removal and displacement field was developed, able to correctly construct single and multi-layer loop structures of arbitrary geometries. The unfaulting mechanisms and corresponding dislocation reaction intermediates in different unfaulting scenarios were clarified. Critical conditions necessary for unfaulting have been identified, and analytical models on base of continuum mechanics have been developed to accurately predict these conditions. Various loop morphologies observed in experiments have been accurately reproduced, with the underlying dislocation reactions fully clarified. The present work provides important mechanistic insights to address key knowledge deficits regarding dislocation loop unfaulting, essential for better understanding of deformation and irradiation-induced damages in structural metals. The new modeling techniques and predictive tools offered are expected to be of great merits to not only the study of unfaulting of dislocation loops, but also future investigation of other complex dislocation or defect ensembles.

→ *Return to the schedule*

Modeling the Formation of Basal Vacancy Loops via the Collapse of Pre-existing Prismatic Vacancy Loops

Mahdi Mohsini, Peyman Saidi, Mark Daymond

Queen's University

Abstract:

Microstructural degradation can be induced in materials during neutron irradiation. Zirconium and its alloys are of significant materials used in thermal reactors due to its particular crystal structure (HCP). However, differences in the diffusivity of radiation products in <a> and <c> directions result in phenomena such as irradiation-induced growth and creep. Vacancies, self-interstitial atoms and clusters are categorized as primary cascade products which can be either annihilated by one another or gather in the form of dislocation loops in the inter-cascade interactions. While it has been experimentally shown that prismatic dislocation loops can appear in the form of vacancies and interstitials from the very beginning of irradiation, they grow in size as the dose increases up to 3 dpa. The appearance of c-component loops is the main reason for breakaway irradiation growth, and it is reported that their nucleation is related to the concentration of interstitial-type dislocation loops in the microstructure. C-component loop formation is correlated with a-type dislocation loop saturation in prismatic planes and – potentially - their subsequent collapse after several dpa. The goal of this research is to model the mechanism of the nucleation of c-component loops based on rate theory and explain the relationship between the collapse of preexisting a-type loops and the incubation time of c-loops formation after several dpa in basal planes.

→ *Return to the schedule*

Defect Microstructures in 3D Rapid Solidification

Jaarli Suviranta

McGill University

Abstract:

Rapid solidification in the high temperature gradient and solidification front velocity regime is a subject of continued interest for applications in e.g. 3D printing. Earlier works in 2D modeling have demonstrated grain bifurcation, continuous rotation, and emission of voids from triple junctions during rapid solidification of pure metals and binary alloys, as a phenomenon specific to this dynamic regime. Generalization of this work to 3D simulations probes the different behaviors of defects in two and three dimensions and the increased degrees of freedom for strain relaxation. Preliminary results show continuous rotation of solidifying cells at high solidification rates.

→ *Return to the schedule*

Vacancy Patterns in Nitride Precipitates and Implication to Hydrogen Embrittlement of High Strength Steels

Ziqi Cui

McGill University

Abstract:

Nitride precipitates are commonly observed in high strength steels and can strengthen the material and trap hydrogen, reducing hydrogen embrittlement (HE) susceptibility. Previous studies have shown that non-stoichiometric precipitates can form in high strength steels and that vacancies within these precipitates may serve as deep hydrogen traps. However, the role of non-stoichiometric nitrides in HE has not been thoroughly studied, particularly with regards to vacancy configurations and diffusion mechanisms. In this work, we employed first-principles calculations, coupled with Cluster Expansion (CE) theory, to predict the ground state structures of titanium nitrides and vanadium nitrides with varying vacancy concentrations, and to analyze the resulting vacancy configurations. On base of these results, hydrogen diffusion pathways and associated barriers were also examined. Our analysis shows that the vacancy configurations would exhibit certain patterns, and these patterns have profound impact on both hydrogen trapping and kinetics. Our findings provide valuable insight into the effect of non-stoichiometric nitrides on HE and can inform the design of future HE-resistant steels.

→ *Return to the schedule*

Atomic Simulations of Spall and Penetration Resistance of polymers and nanolaminates

Ron Mille, Nuwan Dewapriya

Carleton University, University of Delaware

Abstract:

We conducted density functional theory (DFT) and molecular dynamics (MD) studies that reveal insight into the shock and high strain rate behaviour of polymers and nanolaminates. First, we examined the fidelity of a non-reactive MD force field by comparing its predictions with available experimental data and DFT calculations. That study helped us establish the upper limits of the shock pressure that can be accurately modeled using the non-reactive potentials. Subsequently, we used MD simulations of spall to test common assumptions used in analysing experimental spall results. We then showed that nanolaminates exhibit novel properties in small-scale ballistic tests. Finally, we explore the possibility of using DFT calculations to predict shock behaviour in polymers.

→ *Return to the schedule*

Deformation Behavior and Microstructural Evolution of Al 7050 and Al 7075 Under High Strain Rate Compression

Gurnek Tak

York University

Abstract:

Al 7xxx series alloys are used heavily in aerospace and aircraft structures to increase performance and safety during high strain rate incidents such as bird strikes and collisions. These alloys are rarely compared directly in high strain rate testing and the microstructural properties and evolution of the adiabatic shear bands with increasing strain rates are also not compared in studies. This paper compares and analyses the stress strain curves, deformation, and microstructural evolution of Al 7075-T6 and Al 7050-T651 cylindrical specimen with increasing compressive high-strain rates and impact momentum until failure of the material is reached using a Direct Hopkinson Pressure Bar. Results indicate that both materials fractured at a similar strain rate around 6500 s-1, however, Al 7050-T651 fractured at a significantly lower impact momentum than Al 7075-T6. Al 7050-T651 proved to be much softer as it deformed drastically with larger grain sizes and evidence of deformed bands more than Al 7075-T6 which demonstrated the higher hardness and more distinct transformed bands at higher strain rates. The location of these adiabatic shear bands were confirmed by a Vickers Hardness Test on and outside of the shear band region. Al 7075-T6 also demonstrated a brittle and sharper fracture due to its material composition and less initial stress relief compared to a T651 manufacturing process.

→ *Return to the schedule*

Solid Solution Softening in Single Crystalline Metal Nanowires Studied by Atomistic Simulations

Zuoyong Zhang, Chuang Deng

University of Manitoba

Abstract:

Solid solution strengthening is a classical pathway to design metals with higher strength in conventional physical metallurgy. However, solute atoms can also reduce the strength of some metals, known as the solid solution softening effect. In this work, atomistic simulations based on both molecular dynamics and Monte Carlo simulations were employed to systematically investigate the softening phenomenon in single crystalline metal nanowires of different alloy systems. It shows that for single crystalline metal nanowires whose yielding is dominated by surface dislocation nucleation, softening is more commonly observed than strengthening when solute atoms are introduced. This is in stark contrast to the solid solution strengthening that has been widely observed in bulk metals. The underlying softening mechanisms can be attributed to the reduction of unstable stacking fault energy, increase in atomic size misfit, or solute clustering, all of which can make the surface dislocation nucleation easier than in their pure counterpart. It is further revealed that while the nanowire diameter, orientation, surface segregation, and chemical short-range ordering all strongly influence the yield strength, they nevertheless do not change the overall softening trend in the alloyed nanowires. It is expected that the revealed softening mechanisms based on the current study are general to metallic structures whose yielding is controlled by dislocation nucleation.

→ *Return to the schedule*

Exploring the Slow Dynamics of Interfaces and Glasses via Markov State Models

Chad Sinclair, Siavash Soltani, Joerg Rottler

The University of British Columbia

Abstract:

A persistent challenge for molecular simulations is to assess slow processes efficiently from short trajectories. Important examples of slow phenomena in materials are the motion of interfaces in alloy crystals or the structural relaxation in glass forming liquids. Markov State Models (MSM) are an attractive tool to unveil the slowest processes of a complex atomistic system in a low dimensional space of feature variables. This talk describes the predictions and insights gained from such MSMs constructed using machine learning techniques. For grain boundaries, the model learns a hierarchy of timescales associated with transformations between geometrically distinct motifs. When applied to a binary glass former, our model finds a transition timescale between states that is larger than the conventional structural alpha-relaxation time. In both systems, the MSMs are able to access kinetics at temperatures where brute force calculations become computationally expensive or impossible.

→ *Return to the schedule*

Continuum Modeling of Stress Coupled Hydrogen Diffusion and Hydrogen-induced Cracking in High Strength Steels

Sidharth Sarmah, Jun Song

McGill University

Abstract:

The present work is focused on studying hydrogen-mediated fracture in high-strength steels which is a serious concern in various industries related to fasteners, aerospace, automobile, etc. A stress-coupled diffusion finite element model is presented to investigate the distribution of hydrogen under both internal and external hydrogen embrittlement conditions. It considers the influence of hydrostatic stress and plastic strain influencing dislocation trap sites along with carbides, and grain boundaries which alter hydrogen flux. The diffusion of hydrogen is assumed to occur implicitly through the lattice since the jumps between fewer isolated traps are unlikely. The study investigates the small-scale yielding of a boundary layer problem to simulate the diffusion kinetics near the blunting crack tip under a mode I stress intensity factor KI. Of particular interest relating to hydrogen embrittlement is the critical concentration of hydrogen which stimulates pre-mature and even brittle fracture in metals. To investigate the occurrence of fracture the diffusion model is integrated with a cohesive zone model that uses a stiffness-separation law, tailored to accounting for different responses to local hydrogen concentration. The aim of this work is to establish a continuum framework to elucidate the role of stress-coupled hydrogen diffusion in instigating mechanical failure in high strength steels.

→ *Return to the schedule*

An Atomistic Perspective of Discontinuous Precipitation Reactions

Alex Mamaev, Nikolas Provatas

McGill University

Abstract:

The discontinuous precipitation reaction is a solid-state phase transformation driven by grain boundary motion. The characteristic morphology of discontinuous precipitates, most often the spacing in the case of lamellar precipitates, can lead to dramatically different structural properties in materials that exhibit this reaction. Predictions of precipitate morphologies during formation and steady-state growth require careful consideration of compositional, and importantly, deformation driven components of free energy changes. In this talk, a brief review the relevant theory of discontinuous precipitation from a thermodynamic perspective is presented. The phase-field crystal model which is conveniently positioned to investigate this reaction is briefly described and numerical results in 2D are presented. The parametric dependence of modes of precipitate growth and formation on the model parameters are then discussed.

→ *Return to the schedule*

A Survey of Energies of Pure Metals and Multi-component Alloys

Ruitian Chen, Yu Zou

University of Toronto

Abstract:

In materials science, the properties and behavior of materials are related to their energies at various levels. In 2005, Dr. Spaepen published an article discussing various energies associated with materials science, using crystalline face-centred-cubic copper as an example. These energies included thermal, structural, and chemical properties, the formation of vacancies, dislocations and interfaces, and the effects of external loads, strain, magnetic fields, and supersaturation. In this study, we extend these energies to series of other metals and alloys. we conduct a thorough analysis of both face-centred-cubic (FCC) and body-centred-cubic (BCC) metals, as well as equiatomic multicomponent alloys. By collecting data and calculating, we are able to construct comprehensive energy tables that offer a detailed view of the energy changes across these different materials. Specifically, we can observe the transition from metals to high-entropy alloys and examine the differences and connections among these energies. Further, we discuss the underlying reasons for these trends and offer perspectives on their implications for structural transformations of materials. Overall, this study deepens our understanding of the role of energies in determining material behavior and provides valuable insights into the fundamental properties of materials and their applications.

→ *Return to the schedule*

Applications and Recent Developments of the Kinetic Activation-relaxation Technique

Md Mijanur Rahman

McGill University

Abstract:

The microscopic mechanisms associated with the evolution of metallic materials remain a major challenge, as both experimental and numerical approaches fail to provide a detailed atomic picture of their time evolution. The kinetic activation-relaxation technique (kART) [1], an unbiased off-lattice kinetic Monte Carlo method with on-the-fly catalog building to overcome these limitations. kART allows us to construct an extensive description of the energy landscape surrounding various defects and obtain detailed information regarding the different activation mechanisms and diffusion pathways. Here, we apply this method to investigate the pressure effect on carbon diffusion in the grain boundary (GB) of alpha iron [2]. We find that the effect of pressure can strongly change the C stability and diffusivity in the GB in a way that closely depends on the local environment and the type of deformation. We also study the structural evolution of vacancy clusters with two to eight vacancies in alpha iron. Our results show complex scattering mechanisms even for defects as simple as small vacancy clusters. We note that the stabilization of vacancy clusters is achieved by kinetics (larger vacancy clusters have a higher thermal lifetime), and by energetics (larger vacancy clusters have a lower energy). These larger clusters are less likely to interact with each other, as the diffusion coefficient decreases dramatically with increasing size. These results showcase kART strength to describe local kinetics. Yet, kinetic Monte Carlo simulations become inefficient in systems where the energy landscape consists of basins with numerous states connected by very low energy barriers compared to those needed to leave these basins. As the system evolves state by state, it is much more likely to perform repeated events (so-called flickers) inside the trapping energy basin than to escape the basin. Such flickers do not progress the simulation and provide little insight beyond the first identification of those states. To address this issue, I'll also present a newly proposed local basin approach to handling low-barrier events in the kART. This algorithm detects, on the fly, groups of flickering states and consolidates them into local basins, which we treat with the basin-auto-constructing Mean Rate Method (bac-MRM), a master equation-like approach based on the mean-rate method, opening up the application of kART to a whole new family of complex activated problems.

→ *Return to the schedule*

Computing the Intrinsic Grain Boundary Mobility Tensor from Interface Random Walk method

Xinyuan Song, Chuang Deng

University of Manitoba

Abstract:

A recent study has revealed that expressing grain boundary (GB) mobility as a tensor, rather than a single value, may offer a more comprehensive explanation for GB migration phenomena, including GB shear coupling effect and GB sliding. In this research, we examined GB mobility in various directions and discovered that they all adhere to the same physical rule. We then introduced the concept of shear coupling strength to extract the intrinsic GB mobility tensor at the zero-driving force limit from interface random walk simulation. Our testing confirmed that the intrinsic GB mobility tensor is symmetrical, demonstrating the Onsager reciprocal relations in GB mobility. Additionally, the impact of temperature and external driving force on the GB mobility tensor and its symmetry is systematically investigated.

→ *Return to the schedule*

Numerical Study of Influence of Oxide on Metal Powder Deposition and Bonding Behaviors During Cold Spray using Peridynamic Simulations

Haijun Zhang, Jun Song, Baihua Ren

McGill University

Abstract:

Cold spray, a process where micro-sized powder particles are accelerated to impact with and adhere to a substrate to form a coating, has emerged in recent years as a promising technology for various applications (e.g., coating fabrication, structural repair, additive manufacturing). Typically for cold spray of metal powders under ambient conditions, it has been demonstrated by many studies that bonding or adherence of powder particles to the substrate is critically dependent on rupture of the native oxide film on the metal particle to enable close metallic contacts. However, the exact process of oxide rupture and how it participates in the establishment of bonding remain unclear. Motivated by this, we have conducted numerical simulations based on the mesh-free peridynamics (PD) method. A three-dimensional model was developed to simulate copper particles impacting copper and aluminum substrates, considering oxide layer(s) on the particle and/or the substrate. The detailed process underlying oxide rupture and contact formation as a function of material properties (e.g., strain to failure, Young's modulus, yield strength), process parameters (e.g., impact velocity, pre-heating temperature, spray angle), along with oxide thickness and fracture energy, are investigated. The results of the PD simulation approach are found to reproduce experimentally established patterns in the oxide content effect and provide new insights into the mechanisms of oxide rupture and formation of bonding during cold-spray.

→ *Return to the schedule*

A Robust Moment Tensor Potential for Molten Salt, Solid Salt, and Chlorine Gas

Hao Sun

Queen's University

Abstract:

Nuclear reactors and solar power technologies use molten salts to transfer/store heat that can be subsequently converted into other energy forms. Safe and efficient heat transfer/storage requires excellent thermophysical and transport properties (e.g., heat capacity, thermal conductivity, viscosity, diffusivity, etc.), as well as compatibility with primary structural materials. Thus, choosing appropriate salt systems for different applications requires a deep understanding of the molecular structures, chemistry, and dynamics of various molten salts. However, evaluating molten salt properties remains challenging. Experimental measurements by neutron diffraction are expensive under high temperatures and difficult to control impurity. Theoretical analysis via Ab initio molecular dynamics (AIMD) simulations are incredibly costly for properties (e.g., melting temperature, heat capacity, thermal conductivity) that require average over long time and large dimensions. Classical atomistic simulations can be many orders of magnitude faster than AIMD, but the accuracy is limited by the expressive power of the interatomic potential functional form. Hence, investigating molten salt properties is subjected to an accuracy-versus-cost trade-off.

Recently, machine-learning-based interatomic potentials emerge as a promising solution to overcome this trade-off, affording accuracy close to AIMD with computational costs comparable to classical atomistic simulations. In this work, we chose sodium, chlorine gas, and NaCl to demonstrate the feasibility of a moment tensor potential (MTP) framework in training high-quality interatomic potentials. The obtained MTP potential effectively captures pair distribution functions, atomic forces, equation of states, thermal conductivities, and self-diffusion coefficients for all these three structures. Our research suggests a paradigm shift from empirical/semiempirical/ab initio approaches to machine learning schemes in molten salt simulation.

→ *Return to the schedule*

Unified Inter-atomic Potential for Silica, Silicon and Oxygen

Karim Zongo, Laurent Karim Béland, Claudiane Ouellet-Plamondon

Ecole de technologie superieure, Queen's university

Abstract:

On account of the spatio-temporal limitations of electronic density functional theory (DFT) modeling methods, classical molecular dynamics simulation remains the only practical tool for large scale atomistic materials modeling. However, the accuracy of classical modeling is mostly dictated by the employed force fields. Historically, simulation based on force fields used semi-classical potentials that suffer from limited transferability. Moreover, much computational effort may be required to apply semi-classical models incorporating charge-equilibration (QEq) models for simulation involving atomic charge transfer. Here we employed a machine learning approach to bridge the gap between density functional theory and the semi-classical approach. We propose a unified machine learning inter-atomic potential based on the moment tensor potential model for Si/O/SiO2. This potential is trained against a DFT database containing diverse crystal structures, point defects, extended defects, and disordered structures. We demonstrate that this moment tensor potential can properly describe silicon, oxygen, and silica polymorphs.

→ *Return to the schedule*

Origin of Gamma Surface Asymmetries in Body-centered Cubic Refractory High Entropy Alloys

Abu Anand, Chandra Veer Singh

University of Toronto

Abstract:

In this study, we develop an understanding of the effect of high stacking fault elements in the γ -surfaces and twinnability of NbMoTaW refractory High Entropy Alloy (HEA) using first-principles density functional theory calculations. γ -surfaces developed low energy pathways leading to asymmetries by controlling the concentration of high stacking fault energy elements in the HEA. This effect was correlated to the strength of specific solid-state pair interactions using the projected crystal orbital Hamilton population analysis, and they were found to be weak except for W-Mo and W-Ta. Since the interactions involving Tungsten are stronger than the other interactions, stacking fault and twin formation is less likely to happen near tungsten rich portions of the alloy. This suggests the formation of tungsten deficient twins in NbMoTaW which will further improve the ductility of the system. Vibrational analysis on the alloy system has indicated that tungsten and tantalum contribute to the acoustic phonon frequencies of the HEA. Fundamental insights from this study will help in engineering high entropy alloys with high strength and ductility.

→ *Return to the schedule*

A Calculation Method to Estimate Thermal Conductivity of High Entropy Ceramic for Thermal Barrier Coatings

Yuxuan Wang, Jun Song

McGill University

Abstract:

High entropy ceramics are very promising candidates as the next generation thermal barrier coating. Unique disorder structure makes high entropy materials own ultra-low thermal conductivity and good high temperature stability. However, unlike traditional crystal ceramic materials, the thermal resistance of high entropy ceramic mainly comes from phonon-disorder scattering instead of phonon-phonon interaction. Therefore, based on phonon unfolding method, we constructed a calculation method to predict thermal conductivity for high entropy ceramics and applied it on rocksalt oxides structure. The main idea of the prediction is to regard the reciprocal value of phonon spectra linewidth as the indicator of phonon lifetime. The results show that the prediction indicator match the data in experimental measurement, which prove the feasibility of our calculation method.

→ *Return to the schedule*

Deep Learning-based Design of Multi-Layered Chiral Metasurface

Semere Araya

Yonsei University

Abstract:

Metasurfaces have gained significant attention due to their ability to manipulate electromagnetic waves, which has led to various applications in biosensing, nano-imaging, and communication. Designing metasurfaces with desired electromagnetic properties can be a challenging task due to the complex geometries and materials involved. In this article, we propose a deep learning-based approach for designing multi-layered crescent chiral metasurfaces. The design contains a multi-layer crescent chiral metasurface using a numerical approach and the respective circular dichroism result. We utilize generative adversarial networks (GANs) to generate realistic and diverse designs of the crescent chiral metasurfaces that exhibit desired chiroptical behaviors. The proposed method provides a fast and efficient way to design chiral metasurfaces with desired functionalities, which can significantly reduce the design cycle time and improve the overall performance of metasurface-based devices. These deep neural network methodology is an appropriate technique for designing metasurfaces that interact with complex wave phenomena, and can be used for designing metasurfaces that work with dual-polarized waves.

→ *Return to the schedule*

Alchemical Perturbation Density Functional Theory Coupled with Machine Learning for Accelerated Screening of High-Entropy Alloys Catalysts

Mohamed Hendy, Okan Orhan, Homin Shin, Ali Malek, Mauricio Ponga

The University of British Columbia, National Research Council Canada (NRC)/Government of Canada

Abstract:

High-entropy alloys (HEAs) have attracted significant interest in recent years due to their exceptional properties over conventional alloys. Recently, HEAs have shown remarkable catalytic performance for the complex carbon dioxide reduction reaction (CO2RR). First-principle calculation methods such as density functional theory (DFT) are typically used to explore active and stable electrocatalysts. However, the ability to use explore HEAs for catalytic application using conventional DFT is hindered by the vast configuration space due to the large number of possible arrangements of surface sites. This requires a huge number of DTF calculations, which can be infeasible. To tackle this issue, robust approaches to efficiently screen the configurational space of catalytic HEA materials need to be developed and employed. An efficient method to navigate the configuration space of HEA alchemical perturbation density functional theory (APDFT). A key advantage of APDFT is that a single Density functional theory (DFT) calculation of the adsorbate's binding energy (BE) can be used to predict many hypothetical catalysts surface structures' BE at a negligible additional computational cost. This characteristic makes computational alchemy an appealing technique to explore the configurational space of catalytic HEAs at significantly less time compared to conventional DFT calculations. Coupled with APDFT, machine learning models can be developed based on fewer computationally expensive DFT calculations, accelerating the screening of HEAs for catalysis applications. Our proposed framework is to develop a convolutional neural network (CNN) framework using the data from APDFT calculations for training and validation sets. The adopted APDFT method along with a machine learning approach was used to explore the catalytic activity of AuAgPtPdCu HEA surface for CO2RR.

→ *Return to the schedule*

Artificial Intelligence Driven Design of Dingle-atom Dlloy Catalysts via Electronic Structure Features

Javad Shirani, Hanh D. M. Pham , Shuaishuai Yuan ,Alain B. Tchagang , Julio J. Valdés and Kirk H Bevan

McGill University

Abstract:

Single atom alloys (SAAs) have shown great promise as next-geneation catalysts within a wide range of applications, including the electrochemical conversion of {CO}_{2\ }to fuels. In this talk, we explore the degree to which the catalytic properties of SAAs (with a specific focus on kink sites) are determined by the host substrate or the impurity/dopant and the correlation of these properties with electronic structure descriptors. Our density functional theory (DFT) results concerning CO adsorption show that the catalytic properties of SAAs, following the Sabatier principle, can be remarkably transferable across different substrates often displaying an atom-like behaviour independent of the host metal. Subsequently, we explore the degree to which well known electronic structure features (e.g., the d-band center, d-band filling etc.) may predict the catalytic properties of optimal SAAs. Our findings show that despite their preference towards transferability, SAA display complex binding behavior that is not governed by simple linear relationships – in a manner very different from traditional catalytic materials. Though strong predictability is determined to be accessible by machine learning models, this prediction capacity is demonstrated to be limited to a narrow reaction configuration space. In general, the results from this talk indicate that the unique transferability and correlative electronic structure properties of SAAs need to be taken into account when constructing extrapolative trends via artificial intelligence methods in the design next-generation catalysts.

→ *Return to the schedule*

Activation of Electrocatalytic CO2 Methanation on Defective 1T’ Phase TMDCs

Ying Zhao, Jun Song

McGill University

Abstract:

The electrochemical reduction of carbon dioxide (CO2RR) using two-dimensional transition metal dichalcogenides (TMDCs) has emerged as a promising technique for reducing atmospheric carbon dioxide (CO2). However, most recent studies have been focused on semiconducting 2H phase TMDCs, leaving semimetallic 1T' phase VI TMDCs, such as molybdenum ditelluride (MoTe2) and tungsten ditelluride (WTe2), which are stable in ambient conditions, largely unexplored. Our study employs systematic first-principles calculations to investigate the role of intrinsic defects in 1T’ phase TMDCs, specifically MoTe2 and WTe2, for CO2RR. Our findings reveal that certain defects can activate the inert basal plane of MoTe2 and WTe2 for CH4 production, without suffering the competing hydrogen evolution reaction (HER). Our findings demonstrate that defect engineering holds great potential to activate the basal plane of 1T’ TMDCs for CO2RR, and also encourage further research on phase engineering for electrocatalysis.

→ *Return to the schedule*

Tuning the Properties of 2D Iron Ores through Surface Passivation: an Ab-initio Investigation of Magnetene, Ilmenene and Pyrite

Pedro Guerra Demingos, Chandra Veer Singh

University of Toronto

Abstract:

Owing to their unique surface features, non-van der Waals 2D materials have been widely investigated in recent years. Specifically, their high density of surface dangling bonds provide them with great physical and chemical activity. However, these bonds tend to be naturally passivated in most environments, and theoretical work on these materials usually ignores this factor. Therefore, this work is an investigation of the electronic and magnetic properties of monolayer iron ores, which were first exfoliated in 2018. Generated phase diagrams suggest that hydroxyl coverage is thermodynamically most stable in most cases, while also providing a map for surface engineering these systems. This is crucial since both magnetic arrangement and electronic structure are strongly dependent on passivation. For instance, passivation increases the band gap of pyrite from zero to ca. 1.0-2.0 eV, while decreasing the gap of ilmenene and magnetene from the semiconducting to metallic. A key exception is the magnetization of magnetene, which is robust to passivation, making it a promising material for spintronic applications. Interestingly, hydrogen coverage makes ilmenene a multiferroic material, with both ferrimagnetic behavior and charge assymetries. Overall, this work establishes the possibility of fine-tuning the fundamental properties of a new class of non-van der Waals 2D materials for a wide set of applications, ranging from catalysis to electronics.

→ *Return to the schedule*

Creating BIC via Long-distance Coherently Coupled Cavity Magnonics

Ying Yang, Yihui Zhang, Jiguang Yao, Yang Xiao, Jun Li, Can-Ming Hu

University of Manitoba

Abstract:

We couple the dielectric resonator supporting the cavity-BIC and the negative damping to the YIG sphere remotely and indirectly, to access the coherent coupling through the waveguide over 1 meter. In the transmission response, the polariton-BIC is put forward in the long-distance coherent coupling system of the negative-damping cavity mode and the positive-damping magnon mode. Multi-dimensional tunability helps us to realize the transfer and evolution from the cavity-BIC to the polariton-BIC, which illustrates a wishbone shape in the cavity-like eigenmode or a waterdrop shape in the magnon-like eigenmode. A model of indirect coupling involving the negative damping and the back action is proposed and explains our results well. In our work, the magnon-polariton damping is engineered arbitrarily close to 0 or even negative. It's of paramount importance for polaritonic devices that the BICs with localized electromagnetic energy can be transferred and exchanged to different systems in the macroscopic distance with high efficiency due to energy exchange. This high-level remote control gives access to BIC transfer links, help us to build strategies that are related to cloaking, nonlinear optics, sensing and monitoring, as well as optical neural networks.

→ *Return to the schedule*

An Improved Frequency Domain Stress Evaluation Method for Fatigue Life Determination of Welded Structures Subjected to Random Loadings

Uchenna Kalu, Xihui Liang

University of Manitoba

Abstract:

Welded structures are generally more susceptible to fatigue-induced failure than other structural failure modes. Such failures are usually associated with severe economic and in some cases fatal consequences, particularly in structures that are subjected to random fatigue loads. One of the main reasons for the frequent occurrence of premature fatigue failure in welded structures is associated with the discrepancies between the predicted and actual fatigue damage location and lifetime magnitude. These discrepancies emanate from the technique by which the induced stresses at the weld toe and root are extrapolated based on the use of classical nominal, hotspot, and notch stress fatigue life prediction methods in finite element analysis which are inherently associated with some degree of inaccuracies due to sensitivity to Finite Element (FE) model properties and complexities associated with the fatigue life curve selection process.

To significantly improve the accuracy of the predicted fatigue damage and life for welded structures that are subjected to random fatigue loads and typically evaluated using the frequency domain fatigue approach, the Equilibrium Equivalent Structural Stress (EESS) formulations which are based on the decomposition of the weld toe nonlinear stresses have been considered in this research. The EESS method whose equations and applications are currently limited to constant amplitude cyclic loads and quasi-static fatigue life evaluations of welded structures has been modified for suitability with random loads and structural dynamic characteristics effect and then introduced in a new fatigue evaluation frequency domain approach.

The proposed approach has been numerically verified for welded vehicle structural components subjected to road irregular surface-induced vibration accelerations. The simulation fatigue results as well as its numerical efficiency will be compared with the result outcomes from the conventional hotspot stress approach.

→ *Return to the schedule*

Characterizing Uncertain Elastic Properties of Materials 3D‑Printed by the Fused Filament Fabrication Method

Zahra Kazemi, Craig A Steeves

University of Toronto

Abstract:

The layering approach associated with fused filament fabrication (FFF) additive manufacturing technology allows for complex designs generated by topology optimization to be manufactured. However, quality and reliability issues have been observed in additively-manufactured materials. Defects associated with the layer-by-layer process and commonly observed in the fusion regions (the thin regions connecting deposited filaments) introduce considerable variability in the local elastic modulus. Accordingly, additively manufactured components designed by topology optimization will not achieve the desired performance if variations in material properties are not addressed at the design stage. Accurate quantitative measurements of the distribution of the elastic modulus of printed material are essential to achieve robust and reliable optimized designs. This research presents an approach to measuring the randomness in the elastic modulus of materials fabricated by the FFF method. Surface strain fields of samples printed by the FFF method, measured by digital image correlation (DIC), show that the random distributions for the bulk region (the deposited filaments) and fusion layers are different. The goal is to measure the parameters of the random distribution for both the bulk and fusion regions. A machine learning algorithm is developed that can estimate the spatial variations in the elastic modulus.

The model is trained on a dataset of two-dimensional strain fields, generated by finite element analysis of simulated DIC elastic modulus fields, with known random distributions in the corresponding elastic modulus fields. The results indicate that the trained model can approximate randomness in the simulated elastic modulus field from the corresponding strain field. Then, the trained model is employed to measure the parameters of random distribution in the bulk and fusion elastic modulus fields of actual FFF printed samples from their DIC strain fields.

→ *Return to the schedule*

MTC27

I-substituted Halide-rich Lithium Argyrodites Solid electrolytes with improved stability for All Solid State Batteries

Adwitiya Rao

University of Toronto

Abstract:

Halogen substitution has been a widely accepted strategy to boost the ionic conductivity of lithium argyrodites for their application as solid electrolytes in solid-state lithium-ion batteries. Due to the limitation of the total amount of single halogen substitution in a substrate, mixed halide argyrodites containing Cl and Br have been shown to be promising candidates to circumvent this shortcoming. In this work, we conducted a first-principle investigation of the mixed halide argyrodite compositional space, including iodine substitution, which has not been studied previously. Our results provide fundamental insights into the atomistic phenomena responsible for high ionic conductivity (approximately 10 mS/cm) and increased stability of compositions with Br and I substitutions, thus encouraging experimental discovery of novel compounds.

→ *Return to the schedule*

Shear Strain Localization and Adiabatic Shear Failure under Dynamic Shock Loading

Akindele Odeshi

University of Saskatchewan

Abstract:

Failure of metallic alloys at high strain rates is usually traced to shear strain localization along narrow bands called adiabatic shear bands. The occurrence of these bands triggers the fragmentation of metallic components under massive and rapid mechanical loading. At the onset of strain localization, deformed shear bands first form. As the intensity of shear strain localization increases, the deformed bands metamorphose into transformed bands which are more susceptible to cracking than the deformed band or the parent metal. Whereas deformed bands consist of distorted grains, transformed bands consist of fine equiaxed grains which are products of dynamic recovery or dynamic recrystallization. Any microstructural variable which impedes the development of a transformed band in an alloy will make the alloy resistant to failure under dynamic shock loading. These include alloy composition, micro-constituents, and grain size, among others. In this presentation, the effects of these variables on the adiabatic shear failure of some common metallic alloys and composite materials will be reviewed and discussed. High strength low alloy steel, magnesium and aluminum alloys, stainless steels, maraging steels, and functional gradient steels will be covered. Some of the author's research findings on the ballistic impact resistance of hybrid composite plates will also be presented.

→ *Return to the schedule*

Adiabatic Shear Banding and Dynamic Tensile Fracture of Armour Steel

Diego Mateos, Solomon Hanson Duntu, Solomon Boakye-Yiadom

York University

Abstract:

Axisymmetric compression and compression-shear tests are impacted using the direct impact Hopkinson pressure bar (DIHB) at strain rates of ~ 2500 /s. Axisymmetric tension tests have also been conducted using a split-tensile Hopkinson bar (TSHB) at a strain rates of ~ 1500 /s. Specimens are prepared by focused ion beam milling (FIB) and pre-impact transmission electron microscopy (TEM) is conducted to understand the reference microstructure and carbide morphology of the material and taking into account rolling texture. Compression and compression-shear specimens show ductile failure ranging from 11% to 37% compressive elongation by adiabatic shear banding (ASBs), with an increased and predictable susceptibility to form ASBs with increasing shear stress. Grain refinement, bifurcation, transverse cracking, secondary ASBs, secondary band cracking and primary band microcrack coalescence is observed in the ASBs regions. ASBs are also revealed to have on average about a 15% hardness increase in comparison to the regions away from the ASB using Vickers microhardness testing (ASTM E384). Tensile specimens show ductile failure of about 20% tensile elongation: an increase over the quasistatic 10% elongation. Digital image correlation (DIC) provides supporting evidence for the propensity of ASBs in compression-shear specimens as localization increases along the shear plane for specimens with increased shear stress. Synchronized DIC and infrared thermography (IRT) data also offers supporting evidence in tensile tests for the evolution and degree of necking, adiabatic heating, and plastic flow up to 60% major principal strain. Lastly, three specimens with increasing axial strain at a constant impact momentum are taken from the compression-shear specimen ASB regions using FIB and observed under the TEM to reveal the underlying microstructural ASB failure mechanism of the material.

→ *Return to the schedule*

Dynamic Impact Response of Additively Manufactured M350 Maraging Steel-High Entropy Alloy Hybrid Plate

Timothy Odiaka, G. Asala, O.T. Ola, O.A. Ojo, I.N.A. Oguocha, A.G. Odeshi

University of Saskatchewan, Red River College Polytechnic, University of Manitoba

Abstract:

Maraging steels are a choice material in the design of armour plates for defence applications due to their high strength and good impact resistance. However, after heat treatment, they become more prone to cracking when subjected to dynamic impact loading. Hence, the need to establish an optimal balance between their strength and toughness for protective armour applications. In this study, hybrid armour plates with layers of 18% wt. Ni M350 maraging steel (18Ni M350) and AlCoCrFeNi high entropy alloy (AlCoCrFeNi HEA) were manufactured using powder-directed energy deposition (P-DED) additive manufacturing (AM) technology. Post-deposition heat treatment was conducted by austenitizing the build at 850 0C for 0.5 hours and ageing at 535 0C for 0.5 hours. High strain rate (150 to 2220 s-1) dynamic compression test was carried out on the heat-treated and as-built hybrid plates using an instrumented split Hopkinson pressure bar to determine their mechanical response. At the strain rate of 2220 s-1, the peak impact strength of the heat-treated hybrid plate was 2500 MPa while that of the as-built plate was 1990 MPa. However, the elongation of the as-built hybrid plate exceeded that of the heat-treated plate by 11.9 %. The damage evolution within the samples was examined using optical and scanning electron microscopy (SEM). It was found that crack propagation across the 18%-Ni M350 layer of the hybrid plate terminated at the HEA interface at high impact momentum, indicating that the AlCoCrFeNi-HEA layer contributed to the arrest of crack growth within the hybrid plate.

→ *Return to the schedule*

Nanoscale Manipulations by Unusual Focused Ion Beam (FIB) – Material Interactions

Bhaveshkumar Kamaliya, Morvarid Ghorbani, Angela Cleri, Adrian Kitai, Jon-Paul Maria, Jing Fu, Rakesh Mote, Nabil Bassim

McMaster University, Pennsylvania State University, Monash University, Indian Institute of Technology Bombay, Canadian Centre for Electron Microscopy

Abstract:

Direct milling using FIB is deemed as a mask-less and single-step nanofabrication technique; however, it is a time-consuming process due to pixel-by-pixel dwelling, and the effective beam size of FIB restricts minimum feature size. Optimization pathways with ion-induced nanoscale self-organization can be proven to tackle this challenge owing to no such size restrictions on the minimum feature size. Systematic nanoscale control on the topography progression and self-organization of Ge surface during FIB irradiation attained complicated 3D geometries such as polygonal morphologies [1,2]. These periodic nanostructures evolved from the array of circular nanoholes and are jutting out of the surface, bringing the exclusive capability of FIB. Molecular dynamics investigations reveal that the observed self-organization is aided by the nanoscale-control on phase transformation during ion irradiation, which led to a viscous-fingering process with site-specific self-organization. This study fosters the advancement in FIB processes and unique theoretical insights towards manipulating the morphology of individual nanoholes, offering a novel capability of FIB.

Further, using FIB, local defect engineering was carried out on CdO and Silicon SiC to enhance their optoelectrical properties. Site-specific carrier concentration modification in CdO can result in the fabrication of laterally-patterned optical metamaterials with an all-FIB process without requiring a layer-by-layer material deposition to form heterojunction constituents. Tailoring the site-specific defects in SiC P-I-N Junction results in improved photoluminescence properties of the device. These defect engineering attempts provide the pathway towards unconventional optoelectronic devices and photonic properties.

[1]B. Kamaliya, V. Garg, R. Mote, M. Aslam, and J. Fu, Microsc. Microanal. 26, 1684 (2020).

[2]B. Kamaliya, V. Garg, A.C.Y. Liu, Y. (Emily) Chen, M. Aslam, J. Fu, and R.G. Mote, Adv. Mater. 33, 2008668 (2021).

→ *Return to the schedule*

Evaluation of Twinning Formation in Mg-Gd Alloy during Nanoindentation

Moein Iman Fourmani, Guo-zhen Zhu, Yushun Liu

University of Manitoba

Abstract:

Twining is commonly observed during plastic deformation in Mg and its alloys, and it is capable to manipulate both strength and ductility in Mg. In spite of twinning's importance to advanced Mg alloys, how twinning proceeds with the presence of alloying elements, including its nucleation and propagation, in different orientations and loading conditions is still not well understood. In this research, nanoindentation testing was carried out within different orientated grains on the electropolished Mg-2 wt.% Gd coarse-grained alloys. The pop-in appearing in the recorded load-displacement curves, which was likely attributed to twinning, was linked to the observed traces using scanning probe microscopy and high-resolution scanning microscopy. The possibility of twinning in different grains was predicted by the calculated Schmid factor after resolving their orientations by Electron backscattering diffraction technique. Correlating twinning and recorded load-displacement curves are currently under investigation.

→ *Return to the schedule*

Micro-computed Tomography (µ-CT) Assessment of TIG Welded AA 6061- T651

Muhammad Umer, Dr. Ahmed Alade Tiamiyu

University of Calgary

Abstract:

The design of safe and efficient structures is crucial for industrial plants, and welding is considered the most reliable joining process in such sensitive plant designs. However, the strength of the welding joint depends on the metallurgical bonding achieved through either the fusion or diffusion process. Fusion processes such as Tungsten inert gas (TIG) welding are widely used in industries due to their high production rates. However, the involvement of high temperatures in these processes can affect the soundness of the weld and the properties of the neighboring base material—heat-affected zone (HAZ); HAZ is one of the weakest areas in welded components. To overcome the drawbacks of fusion processes, continuous efforts are required to improve existing welding technologies or to develop new processes that can meet quality standards without requiring additional post-processing or investment. This talk will discuss in detail the microstructural evolution and evaluation of a TIG-welded AA 6061-T651, using electron microscopy and micro-computed tomography (µ-CT) techniques, the softening behavior, and its role in the mechanical response of the welded alloy will be discussed.

→ *Return to the schedule*

Quantification of TiN Precipitates and CaS Inclusions in a Microalloyed Steel using EMPA Mapping

Tamara Kazoun

University of Alberta

Abstract:

During solidification, CaS inclusions can act as nucleation sites for titanium nitride (TiN) which may result in large precipitate/inclusion assemblages. Electron microprobe analysis (EMPA) mapping of a titanium rich microalloyed steel was undertaken to quantify the prevalence of TiN nucleation on CaS inclusions. Elemental EMPA maps for Ti, Nb, Mn, Ca and S were generated through the thickness of a microalloyed Grade 100 steel strip. Each elemental map consisted of 285,000 pixels. The grey-scale intensity and location of each element through the strip thickness was obtained using a custom developed code. The grey-scale elemental maps were correlated with EMPA line scan data to quantify the grey-scale values into a wt% value. For a given Ti pixel concentration, co-precipitates of TiN and CaS, including spatial location, were counted. Scanning electron microscopy (SEM) was used to verify the presence and size of TiN-CaS assemblages at a number of specific locations in the steel. The size of the TiN precipitates that nucleated on the CaS inclusions was approximately 4 μm larger than the TiN precipitates not associated with CaS. The total number of TiN-CaS precipitates was < 2.5% of the total number of TiN precipitates.

→ *Return to the schedule*

Designing Next-Generation Additively Manufactured Ceramic-Metal Structures

Jamie Hogan, James David Hogan, Zahra Zaiemyekeh, Saman Sayahlatifi, Haoyang Li

University of Alberta

Abstract:

This research combines the state-of-the-art in multi-scale experimental and computational mechanics approaches to develop weigh-optimized 3D-printed metal-ceramic structures with tailored properties (e.g., stiffness and strength), and microstructures (e.g., grain size distribution and porosity) for different applications, including health (e.g., bone substitutes), defense (e.g., 3D-printed curved body armor) and aerospace (e.g., engine components). In this study, the strain-rate dependent compression strength and failure response of 3D-printed alumina ceramics and ceramic-metal composites were investigated. The material microstructure characterization was carried out using EBSD, SEM, and TEM to provide inputs for multiscale modeling. Ultra-high-speed imaging coupled with digital image correlation was used to monitor strain maps and visualization of crack initiation/propagation of the specimen during the experiments. Computationally, microstructure-property-performance relationships were unveiled through hybrid multi-scale modeling, including nanoscale (e.g., molecular dynamics simulations), microscale (e.g., EBSD-based polycrystalline RVE modeling), and macroscale (e.g., combining FE and DE modeling of test specimen) which were validated by in-house experimental data. Altogether, this work provides a better understanding of the correlation between the microstructure and macro-scale behavior of 3D-printed ceramic-metal structures, which has implications in a range of applications.

→ *Return to the schedule*

Dry Sliding Wear Properties of Cold Sprayed Fe-based Bulk Metallic Glass Coating on Aluminum Alloy

Oluwasegun Adesola, I. N. A. Oguocha, O. Ojo, G. Asala, and O. T. Ola

University of Saskatchewan, University of Manitoba, Red River College Polytech

Abstract:

Aluminum alloys are vital to the aerospace, marine and automobile industries due to their unique properties, such as high specific strength and good atmospheric corrosion resistance. However, aluminum alloys are susceptible to friction-induced wear, making surface engineering imperative for use in several industrial applications. This study investigated the dry sliding friction and wear behavior of cold-sprayed Fe-based bulk metallic glass (BMG) coating on AA5086-H32 plates at room temperature using a ball-on-plate tribometer and a 4 mm diameter Si3N4 counterface. The coating was achieved using a high-pressure cold spray technology by spraying KUAMET6B2-grade powder with a particle size distribution between 8-21 µm on the Al alloy substrate. Five (5) layers of the coating were deposited at a stagnation temperature and pressure of 850 oC and 40 bar, respectively. The average coating thickness was 721 µm, and the porosity was roughly 0.38%. The dry sliding wear test was performed using different loads. Hardness measurements, optical microscopy, surface profilometry, scanning electron microscopy (SEM) and energy dispersive spectroscopy (EDS) were deployed to characterize the hardness, thickness, surface profile, morphology and microstructure of the as-coated and worn surfaces of the substrate and Fe-based BMG coating, while X-ray diffraction was used to clarify the amorphous nature of the powder and the coating. The hardness of the coating was roughly 8 times that of the AA5086-H32 substrate, and their coefficient of friction (COF) decreased with increasing load. The amorphous nature of the coating was unaffected by the wear process. Although the wear rate of both materials increased with increasing load, the wear resistance of the Fe-based BMG coating was approximately 20 times better than that of the substrate. Analysis of the worn surfaces of the coating showed evidence of a dominant abrasive wear mechanism, surface delamination and room-temperature oxidation.

→ *Return to the schedule*

Controlling TiO2 Nanowire Growth Direction, Morphology, and Shape by Manipulating the Surface Characteristics of the Seed

Zhina Razaghi, Guozhen Zhu

University of Manitoba

Abstract:

Nanowires are becoming increasingly important in a variety of industries, especially in energy and sensing applications. Among them, oxide nanowires possess unique characteristics such as high stability, superior electrical and optical properties, and a wide bandgap, making them ideal for these applications. The properties of nanowires are reliant on their crystal structure and morphology, which necessitates precise control to harness their full potential. However, limited success has been achieved in controlling the crystal structure and morphology of oxide nanowires owing to the complexity of their synthesis process and the limited understanding of their growth mechanism. To address this issue, we propose a technique that leverages the recently discovered vapor-adsorbate-solid growth mechanism of TiO2 nanowires to regulate the morphology, shape, and growth direction of oxide nanowires. In this method, vapor species of TiO2 substrates are adsorbed and transferred along the surface of seed nanoparticles to the growth front of nanowires. The results of Transmission Electron Microscopy (TEM), Scanning Electron Microscopy (SEM), and X-ray Adsorption Spectroscopy (XAS) indicate that the structure between the seed (e.g., Au or Au-Ag nanoparticles) and TiOx adsorbates plays a significant role in controlling the shape and growth direction of nanowires. The findings suggest that this technique can establish a means to control the oxide nanowires' morphology and structure while uncovering the growth mechanism's uncertainties.

→ *Return to the schedule*

Effect of Particle Size, Shape and Void Fraction on Fixed Bed Electrical Resistivity of Commercial Graphite Flakes

Imtiaz Ahmed, Marc Duchesne

Natural Resources Canada

Abstract:

Electro thermal purification can be an environmentally friendly way to achieve battery grade graphite and meet future demand thereof. In this work, we investigated the fixed bed electrical resistivity of three different commercial graphite flakes (i.e., jumbo, large and medium) along with standard metal (i.e., stainless steel and copper) spheres. The resistivity was measured using the 4-probe method. Unlike the uniform metal spheres, the graphite flakes have a particle size distribution and non-spherical shape, which complicate the analysis of the resistivity. The void fractions of the beds were estimated from skeleton and bulk density measurements. The fixed bed resistivity was also measured with higher void fractions, as may be expected during electro thermal purification, by introducing nonconductive particles. In general, smaller particles and higher void fractions tend to have a higher resistivity.

→ *Return to the schedule*

Effect of Mechanical Loading Conditions on Near-neutral pH Stress Corrosion Cracking (NNpHSCC) Initiation and Early-stage Growth in Bent Pipeline

Christine Vo

University of Alberta

Abstract:

Near-neutral pH Stress Corrosion Cracking (NNpHSCC) continues causing failures of steel pipelines despite the use of preventative measures such as protective coating and cathodic protection. In bent pipelines, the issue is more profound as stress is concentrated around the bent point and the protective coating layer breaks apart. In this study, axial loads of 50%, 25% and 15% of Specified Minimum Yield Strength (SMYS) were applied to pipes bent to 20 and 40 degree angles under a near-neutral pH condition. Pit and crack distribution, as well as pit and crack depth were analyzed. The larger bending angle suggested a more drastic change in residual stress, resulting in more pits and cracks being initiated on the outer surface of the pipe, but the crack distribution along the length of the pipe appeared to be similar between the two. While the different maximum stresses result in change in number of pits initiated, their effect on depth of pits and cracks appears to be more significant in 20 degree bending angles. The study also suggested that despite having a compressive residual stress near the center of bend, pits and cracks can still be initiated from the breakage of mill scale, exposing the surface of the pipe.

→ *Return to the schedule*

Influence of Nb Addition on the Microstructure Evolution and Hydrogen Defects Susceptibility and Corrosion Resistance of X70 Pipeline Steel

Reza Khatib Zedeh Davani

University of Saskatchewan

Abstract:

The current study is on the effect of Niobium (Nb) content on the microstructure, crystallographic texture, hydrogen defect susceptibility, and corrosion characteristics of X70 pipeline steel. Optical Microscopy (OM) and Scanning Electron Microscopy (SEM) observations as well as, Electron Backscatter Diffraction (EBSD), and X-Ray Diffraction (XRD) analysis were used to evaluate the microstructure and crystallographic texture of X7N1 and X7N2 specimens with Nb content of 0.05%-0.07% and 0.08%-0.1% respectively. The electrochemical hydrogen charging method was used to assess the effect of varying Nb content on the susceptibility to hydrogen blistering (HB) and Hydrogen Induced Cracking (HIC). Moreover, the electrochemical response of the specimens with different Nb content in an acidic media was investigated using potentiodynamic polarization.

The microstructure of the X7N1 specimen comprised of polygonal ferrite as a matrix with a minor fraction of granular bainite and blocks of martensite/austenite as secondary phases. The portion of secondary phases was higher in the X7N2 specimen. The statistical analysis of niobium carbide (NbC) precipitates showed that the X7N1 specimen has larger NbC precipitates with sharp edges compared to the X7N2. The electrochemical hydrogen charging test showed the X7N1 specimen with lower Nb is more susceptible to HB and HIC. Also, the X7N2 specimen has higher resistance to electrochemical corrosion in acidic media.The XRD analysis of texture shows that the X7N1 sample has a relatively higher proportion of the R-cube texture component, which is typically associated with a decrease of hydrogen degradation resistance. In addition, EBSD analysis revealed that X7N1 has a relatively small grain size and a high Kernal Average Misorientation (KAM) value, which is typically correlated with a high dislocation density that acts as reversible trapping sites, and this results in a high susceptibility to hydrogen degradation.

→ *Return to the schedule*

Crack Growth Behavior of Circumferential Near-Neutral pH Corrosion Fatigue in a Bent Pipeline

Hamed Shirazi, Weixing Chen, Reg Eadie

Unicersity of Alberta

Abstract:

For buried pipeline steels, despite using protective coating and cathodic protection, Near-Neutral pH Corrosion Fatigue (NNpH CF) forms a major integrity concern caused by the probability of damage to the coating and the presence of corrosion conditions after that occurrence. The mechanism responsible for around one-third of these service failures is circumferential near-neutral pH corrosion fatigue, in which residual and axial stresses together play a significant role.

In this study, two important sources of axial loading were interacted to determine the growth mechanism of circumferential corrosion fatigue: bending residual stresses which simulated pipeline bending in the field and cyclic loading which represented pipeline internal pressure. In a simulated near-neutral pH soil solution, 10- and 20-degree bending angles samples with artificial notches were cyclically loaded at 35 and 50% of the Specified Minimum Yield Stress (SMYS). Additionally, the final stress distribution in bent samples was determined using the Digital Image Correlation (DIC) method.

The analysis of crack growth in cross-section and fractography images revealed that different factors, such as applied loading, initial notch position, and bending angle/direction, contribute to crack growth by influencing the stress intensity factor (exclusively in the depth direction) and hydrogen diffusion into the notched region. Maximum crack growth was observed under the most severe conditions (20-degree bending, notch at bend centerline and inward direction, 50% SMYS cyclic loading). This hypothesis was confirmed utilizing striation interspacing to determine stress intensity factor range and combined factor.

→ *Return to the schedule*

Effect of Girth Weld and Bending Residual Stresses On Initiation and Early Growth of Circumferential Near-Neutral pH Stress Corrosion Cracking in Thin Pipeline Steel

Hiroyuki Tanaka

University of Alberta

Abstract:

Pipeline failure due to near neutral pH stress corrosion cracking (NNpHSCC) has been concerned in Canada and US. Previous studies focused on axial NNpHSCC that has happened more frequently than circumferential NNPHSCC (C-NNPHSCC). Furthermore, the effect of field bending and presence of girth weld on C-NNPHSCC has not been broadly explored. As such, this study focuses on the significance of residual stress caused by the combination of both girth weld and field bending on initiation and early growth stage of C-NNPHSCC. In order to examine the effect of those factors, corrosion samples with girth weld and no weld were manually bent inwardly and outwardly. The distances between center of bend and center of girth weld were arbitrarily selected. Distribution and depth profiles of corrosion pits and microcracks on those samples revealed that the higher density of microcracks and corrosion pits were observed on the samples with girth weld than those with no girth weld. Furthermore, contrary to a popular belief that the surface with high tensile residual stress yields more localized corrosion sites, direction of bending had little effect on pits and microcracks distribution. Frequency profile of corrosion pits and microcracks showed that the bend angles and the distance between center of bend and girth weld had certain effects on the number of deepest cracks observed. Future study requires the samples with little history of corrosion to rule out the presence of residual pits and thick mill scale.

→ *Return to the schedule*

Advancing Electron Backscatter Diffraction for Quantitative Corelative Characterization of Microstructures

Ben Britton

The University of British Columbia

Abstract:

In this talk, I will present some of our recent efforts to improve the quality and quantitative potential of electron backscatter diffraction (EBSD). This technique enables us to collect and map crystallographic information within the scanning electron microscope (SEM). Our group has been developing this technique extensively, and in this talk I will present a few new developments that include: (1) use of machine learning to improve signal to noise and enable characterisation of fine scale (nm) precipitates in aerospace Ni-based alloys with varimax based principal component analysis (PCA), using EBSD and energy dispersive X-ray spectroscopy (EDS); (2) use of combined EBSD and EDS to systematically map carbides in Ni-based pressure vessel materials and enhance understanding of new manufacturing routes and the potential impact on stress corrosion cracking (SCC); (3) use of indirect and direct electron detectors, with new geometries and algorithms, to enhance the quality of pattern analysis and enable phase classification, even of hard-to-study challenges such as Ni3Al precipitates within the Ni-alloy, as found in Ni-based superalloys.

→ *Return to the schedule*

Real-time Tracking of Slip Planes in Many Grains using Hollow-cone Dark-field Imaging

Yushun Liu, Guozhen Zhu

University of Manitoba

Abstract:

The plastic deformation of polycrystalline metals is largely influenced by dislocation movement, which is closely related to the orientation of slip planes within individual grains. However, current techniques like electron backscatter diffraction (EBSD) lack the temporal resolution to characterize the dynamics during deformation. In this study, we propose a novel approach for real-time tracking of slip planes in many grains using hollow-cone dark-field imaging. Instead of sampling large area of reciprocal space for each pixel in conventional methods, a donut-shaped reciprocal signal is used to simultaneously track the morphology and key crystallographic trains of numerous grains with sufficient temporal and spatial resolution. We demonstrate the effectiveness of this approach using in-situ nanoindentation on nanograined magnesium. Our results suggest that the proposed approach can effectively capture the real-time rotations of slip planes and their evolution trends within dozens of grains. Our approach offers new possibility for addressing orientation-related problems during dynamic process like deformation, leading to better understanding of the mechanical behavior of metals.

→ *Return to the schedule*

Microstructural Analysis of the Hydrogen Assisted Failure of Nb-containing and Deficient Pipeline Steels

Tonye Jack, Jerzy Szpunar

University of Saskatchewan

Abstract:

Although the addition of niobium (Nb) to pipeline steel improves mechanical properties, such as strength and toughness, little is known about its impact on their corrosion, hydrogen embrittlement and stress corrosion cracking performance. This study uses similarly processed Nb-containing and deficient pipeline steels to examine the effect of hydrogen on steel failure from a microstructural perspective. The hot rolled steels in this study were characterized using several material characterization and experimental techniques, such as, electron microscopy, electron backscatter diffraction, X-ray diffraction, computed tomography, thermal desorption spectroscopy, electrochemical and mechanical tests. The steels had a one order of magnitude difference in Nb, and the microstructural examination showed that this considerably altered the microstructure of the steels, resulting in a refined structure for the Nb-containing steel and a non-uniform microstructure in the Nb-deficient steel. These differences in structure were accompanied with distinct differences in lattice misorientation, grain size distribution and crystallographic texture. Hence, clear differences in corrosion and hydrogen related degradation were observed. The results that will be presented confirm an inferior failure resistance and a higher tendency for hydrogen embrittlement, especially in the presence of mechanical loading for the Nb-deficient steel. Interestingly, this behavior was linked to their microstructural characteristics and hydrogen retention capabilities. Ultimately, the findings of this study further reinforce the importance of Nb in pipeline steels, with respect to hydrogen assisted failure.

→ *Return to the schedule*

Characterization of the Interface Areas of Zirconium Hydride Precipitates

Nima Nikpoor Badr, Fei Long, Mathew Topping, Zhongwen Yao, Mark Daymond

Queen's University

Abstract:

In CANDU reactors, zirconium (Zr) fuel rods are susceptible to the formation of brittle Zr-hydride precipitates. In reactor conditions, δ-hydride with FCC structure is the dominant forming phase. In this work, electron energy-loss spectroscopy (EELS) and diffraction were utilized to study the structure of a hydride precipitate in Zircaloy-2.

Both techniques confirmed the δ-FCC nature of the core area of the precipitate. In the interface, however, EELS measured two ribbons with plasmon energy (PE) values of 17.4 and 18.3±0.3 eV (characteristic of the ζ-trigonal and γ-tetragonal hydride phases, respectively). Electron diffraction, however, did not confirm trigonal and tetragonal structures for interfacial ribbons, which ruled out a ζ-- or γ-nature for them.

To discover the origin of the measured PE values, dielectric theory was utilized to simulate the plasmon vibration in the interface between the δ-core and Zr matrix. Simulations revealed that the measured PE values can emerge artificially over a ~5 nm span due to the “interface effect” between the two phases. This span is narrower than the ~20 nm width observed for the interfacial ribbons, which implies alternative mechanisms were operative.

As the first alternative mechanism, the formation of H-rich interfacial ribbons was assessed. This mechanism can be effective only in the tip areas of the precipitate since driving forces that attract H towards interface (such as tensile hydrostatic stresses) exist only in those areas. For flat-side interfaces, however, simulations predict compressive hydrostatic stresses which repel H atoms. As the second alternative mechanism, the delocalization of plasmon vibration was assessed. Calculations revealed that ~10% of the electrons of the electron-probe can interact with areas up to ~10 nm away from the incident point on sample.

It was concluded that combination of the interface effect, delocalization, and H-enrichment explains the origin of measured interfacial PEs.

→ *Return to the schedule*

Improved Weldability of a Difficult-to-Weld Aerospace Superalloy

Johnson Aina, Olanrewaju Ojo, Mahesh Chaturvedi

University of Manitoba

Abstract:

IN738 is a precipitation strengthened nickel-based superalloy used for producing aero-engine components. Welding is important during fabrication and repair of aero-engine parts. The alloy is extremely difficult to weld due to its high susceptibility to grain boundary cracking by liquation reaction in the heat affected zone (HAZ). A new heat treatment is developed with the aim of reducing the susceptibility of the alloy to weld HAZ liquation cracking. Results show that samples subjected to this new pre-weld thermal treatment significantly improve the weldability of the difficult-to-weld alloy by reducing its susceptibility to HAZ liquation post-weld cracking by about 70% better than other existing heat treatments. In addition, the results show that the low extent of cracking by the new pre-weld heat treatment is not compromised during post-weld heat treatment of the superalloy.

→ *Return to the schedule*

Revisiting the Phase Stability Rules in the Design of High-Entropy Alloys: A Case Study of Quaternary Alloys Produced by Mechanical Alloying

Intekhab Alam, Ahmed Alade Tiamiyu

University of Calgary

Abstract:

High-entropy alloys (HEAs) have the potential for many structural applications because of their outstanding mechanical properties. Achieving solid solution (SS) in HEAs is desirable since intermetallic compounds (IMs) can, in most cases, be deleterious. While empirical phase stability rules have been widely used to predict SS or IM phases in HEAs, there are substantial reported cases of their breakdown. To assess the effectiveness of the empirical rules—atomic size difference (δ), mixing enthalpy (ΔHmix), mixing entropy (ΔSmix), entropy to enthalpy ratio (Ω), electronegativity difference ($\triangle\chi$), and valence electron concentration (VEC), a systematic study that isolates the effect of processing pathway was conducted. As a starting point and as a benchmark, an existing equiatomic AlCoCrFe BCC HEA was correctly predicted (following the classical empirical rules) and developed. This was followed by the SS FCC prediction and development of five novel semi-equiatomic AlTiCuZn-based quaternary HEAs (Al0.57TiCuZn, AlTi0.45CuZn, Al0.45TiCuZn, AlTiCu1.76Zn, and AlTiCu2Zn) by mechanical alloying. Among the AlTiCuZn-based HEAs, only AlTi0.45CuZn showed SS, but with FCC+HCP phase contradicting the traditional VEC rule that predicts FCC. Using AlTi0.45CuZn as a guide, conservative SS formation criteria for AlTiCuZn-based HEAs were determined—$\Omega \geqslant 1.6$, $\delta \leqslant 5\%$, and $\Delta Hmix \geqslant -8$ kJ/mol, while retaining conventional ΔSmix and $\triangle\chi$ range. Also, FCC+HCP phase formation is stable at $7.5 \leqslant VEC \leqslant 8.4$. The revised rules were verified by correctly predicting the phases in newly-fabricated non-equiatomic HEAs—AlTi0.37CuZn0.97 and AlTi0.56Cu1.24Zn1.2. This study shows the range of empirical phase stability model values is not fixed, but alloy-dependent due to the differences in bonding nature of HEA-constituting elements.

→ *Return to the schedule*

Investigating the Microstructural, Mechanical, Tribological, and Electrochemical Properties of AlCuFeNiSix and AlCuFeNiTix High Entropy Alloys via Arc Melting for Energy Storage Applications

Modupeola Dada, Popoola Patricia

Tshwane University of Technology

Abstract:

The demand for high-performance materials for energy storage applications has led to the emergence of high entropy alloys (HEAs) as potential candidates. In this study, the microstructural, mechanical, tribological, and electrochemical properties of two HEAs, AlCuFeNiSix and AlCuFeNiTix, were investigated using arc melting. The microstructural analysis of both alloys with a BCC crystal structure revealed a homogeneous distribution of elements. Nanoindentation tests used to evaluate the mechanical properties revealed that the AlCuFeNiTix high entropy alloy composition has a greater strength than the AlCuFeNiSix alloy. The tribological properties of the AlCuFeNiSix high entropy alloys were investigated using a pin-on-disk tribometer, and the results revealed that the AlCuFeNiSix had lower wear rates than the AlCuFeNiTix. The electrochemical properties of the alloys were evaluated using cyclic voltammetry and electrochemical impedance spectroscopy, revealing that both alloys possess good electrochemical stability and can be used as potential electrode materials for energy storage applications. Overall, the results suggest that AlCuFeNiSix and AlCuFeNiTix HEAs can be promising materials for energy storage applications due to their excellent combination of mechanical, tribological, and electrochemical properties.

→ *Return to the schedule*

Calculation of Variable Atomic Diffusivity in a Cu-Ni alloy System

Samuel Afolabi, Amir Safaei, Olanrewaju A. Ojo

University of Manitoba

Abstract:

A recently developed numerical diffusion model that incorporates variable atomic diffusion coefficients and solute conservation is combined with a forward simulation approach to calculate concentration-dependent interdiffusion coefficients in a Cu-Ni alloy system. The approach which combines fully explicit finite difference analysis and the Leapfrog/Dufort-Frankel scheme to extract interdiffusion coefficient is free of the major flaws in conventional methods like Boltzmann-Matano, Sauer-Freise, and Hall methods. The results of the study show that concentration-dependent interdiffusion coefficient can indeed change with time isothermally which is in contrast to what is commonly reported and expected in the literature. A disregard for this crucial concept can have significant implications in the analysis of experimental diffusion data, which can be crucial to proper understanding of microstructural changes produced by diffusion-controlled phase transformations in metallic materials.

→ *Return to the schedule*

Tracking of Cathode Degradation in LiNi0.5Mn1.5O4 Lithium-Ion Batteries through Intermittent Post-Mortem Material Characterizations

Kelsey Duncan, Farhang Nesvaderani, O'Rian Reid, Lida Hadidi, Byron D. Gates

Simon Fraser University, NanoOne Materials Corp.

Abstract:

Understanding the exact causes of failure in lithium-ion battery (LIB) cells is necessary to address electrode material shortcomings and to inform the design of safer, longer lasting, and more robust battery materials. With regards to the cathode materials in LIBs, post-mortem (PM) studies that investigate battery materials after multiple cycles of charging and discharging, are typically limited to assessments of the whole cathode – where the active cathode materials are encased in organic binders and additives, all supported by a metal current collector. On these samples scanning electron microscopy (SEM) based observations are limited to the top layer of materials such that detailed imaging of cathode particle surfaces may be obstructed, missing possible indicators of LIB failure like cracks or pitting textures. When changes to phase or chemical composition are of interest, the mixed media inherent to whole cathodes presents significant hurdles to characterization. To address these challenges, this research has developed a safe and non-destructive method to isolate LiNi0.5Mn1.5O4 cathode particles from 'dead' LIBs. Once isolated, the routine quality control testing performed on freshly synthesized materials can be replicated on these PM samples, providing a means of comparative study to assess degradation in cathode particles specifically. Pairing these findings with standard electrochemical testing that provides information both on whole-device and whole-cathode function, a deeper understanding of how degradation in cathode particles effects LIB failures can be gained.

In this work, LiNi0.5Mn1.5O4 single particles are isolated at PM and characterized by SEM, energy dispersive X-ray spectroscopy, and X-ray diffraction. Performing these assessments on pre-electrochemistry samples, and two sets of PM samples that have been electrochemically cycled to 100 and 500 cycles, respectively, this study aims to track degradation in cathode particles over time.

→ *Return to the schedule*

Investigating the Effect of Rapid Induction Heating on Phase Transformation in Martensitic Stainless Steel 15-5 PH

Mahsa Fatemi Mehrabani, Mehrdad Aghaei Khafri

K.N. Toosi University of Technology

Abstract:

In this study, the effect of rapid induction heating on the phase transformation of precipitation-hardened martensitic steel 5-15 PH was investigated. For this purpose, the samples were applied to induction heating aging at different temperatures and times. The results showed that uniform distribution, spherical shape, and high volume fraction of precipitates obtained with induction aging were more desirable than those obtained with normal aging. To analyze the effect of induction aging on material hardness at various temperatures and times, the Hollomon- Jaffe parameter which considers temperature and time was used. Application of JMAK (precipitation kinetics model) on the induction heating procedure in this alloy demonstrated that the amount of activation energy (Q) in the induction heating method is almost equal to conventional ones while the growth power (n) in the induction method is higher than normal aging. Using the finite element simulation (FEM), the effect of different induction conditions such as frequency, amperage, voltage, and the distance from the induction coil on the temperature distribution and thus the distribution of the precipitates in different parts of the sample was investigated.

→ *Return to the schedule*

Study of Aluminization and Its Effects on High Temperature Oxidation of Austenitic Stainless Steel AISI 304

Sonya Redjala, Said Azem

Mouloud Mammeri University

Abstract:

Stainless steel is known for its resistance to oxidation at temperature by the development of a protective and compact oxide layer Cr2O3 that adheres to the substrate. This thin layer acts as a diffusion barrier that protects the material from the aggressive atmosphere. However, at temperatures exceeding 950°C the Cr2O3 oxide undergoes decomposition into less protective oxides such as CrO and CrO3, which is volatile.

The aim of this work is the improvement of the resistance to oxidation at high temperature of austenitic stainless steel AISI 304. The process called "calorization" consists of adding aluminum to the surface layers by diffusion from a vapor phase containing aluminum atoms. The steel heated in a powder mixture of ammonium chloride, aluminum and alumina where chemical reactions release the aluminum in an atomic state,which diffuses into the steel.

The different layers observed by scanning electron microscopy (SEM) on cross sections of the calorized and oxidized steel. The distribution of elements through the layer formed on the steel substrate was obtained by mapping and EDS-X spectroscopic analyses. The X-ray diffraction revealed the presence of iron and nickel aluminide on the surface layers of the heat-treated steel.

Oxidation kinetics in air at 1000°C has shown that calorized steel is relatively more resistant to oxidation than untreated stainless steel. The presence of aluminum allows the development of an alumina layer, which constitutes a diffusion barrier strongly limiting the phenomenon of oxidation [3]. XRD analyzes carried out on the sample heated and oxidized at 1000°C made it possible to identify stable α alumina in large quantities and transition γ alumina in relatively smaller quantities.

→ *Return to the schedule*

PMC27

Steel decarbonization using iron ultra-fine grains recovered from tailings in a new HDDRI process

Fernando Berlinck

SmartDry Liquefaction

Abstract:

In steel making, the first critical step is the reduction of iron oxides ore to pig/sponge iron. In the classical process, this is done in a open top furnace using coke coal, at high temperatures with large amount of CO2 being produced. Pelleting and sintering processes add energy consumption, costs and CO2 production.

In all chemical reactions, the surface/mass ratio and the pressure in which the chemical reaction takes place are factors that increase efficiency and can diminish energy demands/consumption. The use of iron ultra-fine grains as DUST in a HDDRI (Hydrogen Dust Direct Reduction of Iron) new process where the iron ultra-fine grains recovered from tailing deposits/dams are injected simultaneously with hydrogen into a new furnace model. This new high pressure, lower temperature HDDRI furnace has the potential to reduce H2 consumption, lower OPEX costs and help the ESG performance of the whole steel chain, from mine to steel.

Estimates says that there are over 282 billion tonnes of tailings around the world. Of this, 9% are iron tailing with an average 35% iron content, this translate to 25,38 billion tonnes of iron ultra-fines which is enough to support steel production via HDDRI for the next 10 years at present production level. Iron is also found in other tailing types; Chilean copper tailing have an average 10% iron in it. Copper tailings represent 40% of the total tailing deposits or 112,8 billion tonnes, this means that in Chile there is over 11,28 billion tonnes of iron ultra-fines deposits in copper tailings. The same is true for all tailing around the world, in all tailings there are metals ultra-fines ready for recover at a very low cost.

What was missing was a technology capable of grasping, retaining, recovering all metal ultra-fine grains lost into tailings. We invented such technology using liquefaction effects. Mining tailing has a much lower OPEX cost because the costly steps are done (blasting, chorusing, transporting and milling). Tailing mining requires the digging out of the solids and placing it inside the liquefaction equipment to separate all metals ultra-fine grains from the dirt (lower valuable materials). In liquefaction, we use only water and vibrations, the material leaves the process dry stackable and the process water can be re-use fast since there is no additives in it.

In this poster, we present our results for recovery of iron ultra-fine grains from a tailing material from the Minas Gerais state in Brazil.

→ *Return to the schedule*

Tribological Properties of Cold Sprayed Fe-based Metallic Glass Coating on ZE41A-T5 Magnesium Alloy

Oluwasegun Adesola, Charles Obiechefu, Ikechukwuka N. A. Oguocha, Olanrewaju Ojo, Gbenga Asala, and O. T. Ola

University of Saskatchewan, University of Manitoba, Red River College Polytech.

Abstract:

Surface coatings achieved through plating, thermal spray and cold spray techniques are used to protect engineered products from wear and corrosion. In this study, Fe-based metallic glass powder with a particle size distribution between 8-21 µm was cold-sprayed on ZE41A-T5 magnesium alloy at a pressure of 4 bar using different process temperatures (750 °C, 800 °C, 850 °C, 900 °C, and 950 °C). The dry sliding friction and wear behavior of the Fe-based amorphous coatings under different loads was investigated at room temperature using a ball-on-plate tribometer and a 4 mm diameter Al2O3 counterface. Hardness measurements, X-ray computed tomography, surface profilometry, scanning electron microscopy (SEM) and energy dispersive spectroscopy (EDS) were used to characterize the hardness, porosity, surface profile, morphology and microstructure of the as-coated and worn surfaces of the Fe-based coatings and substrate. In addition, X-ray diffraction was used to clarify the amorphous nature of the powder and the coatings before and after the wear process. The Fe-based BMG coatings displayed superior properties and tribological performance compared to the substrate. Coated samples processed at 850 °C had the highest hardness (665 HV0.3), lowest porosity (0.379%) and lesser cracks compared to those processed at different temperatures. The coefficient of friction (COF) of the coatings decreased with increasing load, while the wear rate increased. The wear resistance of the samples coated at 850 °C was approximately 25 times that of the substrate. Analysis of the worn surfaces of the coating showed evidence of a dominant abrasive wear mechanism and room-temperature oxidation. These results suggest the potential of Fe-based BMGs as coating materials to improve the tribological properties of magnesium alloys.

→ *Return to the schedule*

In situ Transmission Electron Microscopy to Understand Electrochemical Processes

Drew Higgins

McMaster University

Abstract:

Electrochemical CO2 conversion offers a route to use renewable sources of electricity to convert CO2 into valuable carbon-based fuels and chemicals, including carbon monoxide, ethanol and ethylene. For electrochemical CO2 conversion technologies to become viable component of future sustainable energy infrastructures, improved performance materials (catalysts, electrodes, membrane electrode assemblies) are needed to achieve high conversion rates, selectivity and single-pass utilization of CO2. This talk will focus on the development of techniques to characterize the properties of electrochemical CO2 conversion materials under reaction conditions that will guide the design of next generation materials and reactors. The talk will focus primarily on in situ transmission electron microscopy (TEM) and related spectroscopic techniques (energy dispersive X-ray analysis and electron diffraction), along with synchrotron-based methods including scanning transmission soft X-ray microscopy (STXM).

→ *Return to the schedule*

Synchrotron Applications in Energy Materials and Catalysts

Feizhou He

Canadian Light Source

Abstract:

Protecting our one-and-only planet Earth during economic growth is a major challenge for every country in the world. In the recent years we have seen a rapid increase of researches focusing on renewable energies, CO2 reduction, energy storage, and resource extraction. Synchrotrons played an important role in materials researches linked to climate change and sustainability. The researches in topics related to environment aspects and energy materials account for over half of the proposals at the Canadian Light Source. In this talk, I will discuss the advantages of synchrotron techniques, and showcase a few applications in energy materials and catalysts, including in-situ characterization of battery materials during charging and discharging, solar cell degradation in humid environment, converting CO2 into plastics, and examining the catalysts for producing hydrogen, etc.

→ *Return to the schedule*

Developing an Elevated Temperature Pourbaix Diagram of Zirconium and Zircaloy-4

Graeme Francolini

University of Ontario Institute of Technology

Abstract:

Zirconium and zirconium based-alloys are useful in applications that require robustness under extreme conditions, such as in nuclear reactors. This is in part due to their low neutron absorption cross sections, and favorable corrosion properties. Zirconium-based claddings in CANDU reactors are often exposed to aqueous temperatures ranging from 260-310°C, resulting in inevitable corrosion despite their high resistance. The corrosion susceptibility of metals can be investigated through a Pourbaix (potential/pH) diagram, which illustrates the stability domain of various metallic species in aqueous solution. This work focuses on developing an elevated temperature Pourbaix diagram for zirconium and a multi-element (Zr, Cr, and Sn) elevated temperature Pourbaix diagram for Zircaloy-4, at 100°C. Previously, Pourbaix diagrams have been developed for zirconium and other metals at room temperature. However, elevated temperature diagrams have only been constructed using extrapolations of current thermodynamic data through computational methods, or models to estimate thermodynamic properties. The elevated temperature data for these diagrams will be empirically obtained using in-situ pH and oxidation-reduction potential measurements in a batch style pressure vessel. The solubilities of these materials will be obtained at varying pHs, ranging from -1-14 pH. The aqueous zirconium concentrations were obtained using Inductively Coupled Plasma Optical Emission Spectroscopy (ICP-OES), while the aqueous concentrations for Zircaloy-4 were measured using Inductively Coupled Plasma Mass Spectroscopy (ICP-MS). Solubility data will be used to calculate equilibrium constants and the Gibbs energies for the development of their respective Pourbaix diagrams using the FactSage program.

→ *Return to the schedule*

Investigating the Effect of Electrode Microstructure on Battery Performance Using IL-TEM

Mariam Odetallah, Christian Kuss

University of Manitoba

Abstract:

The increasing demand for high energy density energy storage increases research into Lithium-ion batteries (LIB). These batteries consist of two electrodes and an ion-conducting electrolyte. Each electrode is composed of four main components: an active material, a conductive additive, a polymer binder, and a current collector. Si is one of the most promising active material candidates for LIB due to its high specific capacity, and low working potential.

The electrode materials define the battery's cycling ability, energy density, and conductivity. The non-uniform distribution of the electrode's components and microstructure properties produce an inhomogeneous electrode microstructure. This causes local variations in the current density and Li ion concentration. As a result, the battery will suffer from life time shortening, capacity reduction, and active material- matrix disconnection. Especially using Si particles, their high-volume change during cycling leads to severe connection loss in the electrode.

The disconnection process and inhomogeneity effects on the battery performance are of great interest to researchers. Therefore, a variety of characterization and analytical techniques have been developed. Our research combines identical location transmission electron microscopy (IL-TEM), scanning electron microscopy (SEM), and battery cycling to study the microstructure effect before and after cycling. The IL-TEM allows us to visualize and track the structural changes of the battery components. Additionally, it allows the study of the active material- matrix interface. Therefore, we are imaging the Si electrode before and after cycling using IL-TEM and SEM to study microstructural changes and connection loss. Then, we correlate these results with the battery cycling performance, which will be presented here.

→ *Return to the schedule*

Regulate Anode Behaviors in Lithium Metal Batteries

Ge Li

University of Alberta

Abstract:

Lithium metal batteries (LMBs) are considered the most promising energy storage devices for applications such as electrical vehicles. Lithium metal is believed the most favourable anode for future LMBs owing to its extremely high theoretical specific capacity, low density, and lowest electrochemical potential among potential candidates. However, large-scale deployment of lithium metal anode in practical batteries still requires a scientific breakthrough in solving major challenges of dendrite growth and low plating/stripping efficiency of metallic lithium. To address the issues related to lithium anodes in LMBs, several effective strategies are developed to stabilize Li anodes, including liquid electrolyte, surface coating, solid-state electrolyte, and porous current collectors. In this presentation, we will present our recent work on the materials design and development for next-generation LMBs by focusing on the in-depth understanding of the interphase engineering. More specifically, we will discuss: (1) the systematic electrolyte design and (2) the anode construction.

→ *Return to the schedule*

Water-Processable Composite as a Conductive Binder for Graphite Anode in Lithium-ion Batteries

Anh Mai, Christian Kuss

University of Manitoba

Abstract:

In commercial lithium-ion batteries (LIBs), to ensure mechanical integrity of the electrodes and a continuous conductive pathway for both ions and electrons, a polymeric binder is added to bind the electrode particles together. Better performance could result from choosing the right polymers to use as binders and their functional groups. Among them, water-processable composite electrodes are appealing from both ecological and financial standpoints. Recently, it is shown that aqueous sodium carboxymethyl cellulose (CMC-Na) have enhanced electrochemical performance over conventional binders, such as PVDF (polyvinylidene fluoride). Despite its viable properties, CMC is intrinsically insulating and thus can impede electron transport during cycling. The poor electrical conductivity of CMC can be compensated by the addition of polypyrrole (PPy) to form a conducting polymer PPy:CMC composite.

Here, we report the use of PPy:CMC composite as a conducting binder in a graphite anode and evaluate anode degradation in presence of PPy:CMC and conventional binders. Two types of graphite electrodes are prepared, denoted as Graphite:PVDF:C and Graphite:PPy:CMC. The stability of the electrodes is explained through the understanding of binder interactions with the active materials and electrolytes. Electrochemical stability, kinetics and Li transportation properties, and interfacial resistances are analyzed with galvanostatic cycling, cyclic voltammetry, and impedance spectroscopy. Degradation mechanisms and by-products are studied using infrared spectroscopy and EDX. Electrode morphologies and homogeneity are investigated with SEM-EDX. The results demonstrate that the new PPy:CMC binder system could be a promising binder system for high energy density anodes in batteries and beyond.

→ *Return to the schedule*

GS7

Effect of Sb Doping and Polyvinylpyrrolidone on the Mesoporous TiO2 Photoanodes for Sb2Se3 Sensitized Solar Cells

Melissa Isabel Ayala Sánchez

CINVESTAV Unidad Saltillo

Abstract:

Semiconductor-sensitized solar cells (SSSCs) have been proposed as an alternative photovoltaic technology due to the high specific surface of the photoanode (50-100 m^2/g), which is usually constituted by a mesoporous titanium dioxide (mp-TiO2) layer, and the optical absorption of inorganic semiconductor sensitizers, e.g., Sb2Se3, which has been applied due to its advantages such as: high absorption coefficient (>10^5 cm^{-1}), suitable optical bandgap (Eg≈1.3 eV) and p-type photoconductivity of > 10^{-6} Ω^{-1} cm^{-1}. TiO2 has been doped with different transition elements like Sb, to enhance its conductivity.

In the present work, the effect of Sb doping on the morphological, structural, chemical, and optical properties of mp-TiO2 layers was studied. The mp-TiO2:Sb layers were synthesized by the sol-gel technique, using titanium isopropoxide, ethanol, acetic acid, polyvinylpyrrolidone and antimony trichloride, as chemicals. The precursor solutions were deposited by the spin-coating technique at a different speed and calcined for 3 h in air, at 600 °C. Results showed that the morphology and porosity of mp-TiO2:Sb layers depend on the amount of polymer and doping, i.e., the porosity is high for low polymer content while it is low for high Sb doping. Moreover, the XRD analysis indicated the formation of crystalline anatase-TiO2 in all layers. XPS data showed the presence of Ti4+, O2-, and Sb3+, corroborating the doping of TiO2. The optical bandgap obtained by UV-Vis spectroscopy was 3.14 and ~3.47 eV for undoped, and doped layers respectively. Then, the mp-TiO2:Sb layers were evaluated as photoanode in semiconductor-sensitized solar cells (SSSCs) constituted by FTO/bl-TiO2/mp-TiO2:Sb/CdS/Sb2Se3/C. It was found that increasing doping decreases the open-circuit voltage (Voc) but increases the short-circuit current density (Jsc). Preliminary results gave a SSSC with a Voc of 0.280 V, a Jsc of 3.25 mA/cm^2, and a power conversion efficiency of 0.9% under white-LED light of 400 W/m^2.

→ *Return to the schedule*

Synthesis of Ternary Compounds of SnxSbySz Metal Chalcogenides by Chemical Bath Deposition for Their Application in Solar Cells

Melani Guadalupe Ayala Sánchez

Centro de Investigación y de Estudios Avanzados del IPN (Cinvestav Saltillo)

Abstract:

Thin film solar cells (TFSCs) have different advantages over silicon-based technologies, such as light weight, flexibility, and low cost because they require semiconductor material thicknesses less than 1 µm for fabrication. Among the materials studied for TFSC manufacture are Sb and Sn chalcogenides like Sb2S3 and SnS. These chalcogenides present an adequate optical bandgap (Eg, 1.40-2.0 eV), high absorption coefficient (α, 105 cm^{-1}), and are constituted of non-toxic, abundant and inexpensive elements. However, their application as an absorber in TFSCs has resulted in low values of power conversion efficiencies (PCE). One alternative is to synthesize SnxSbySz ternary compounds because it has been reported that they can have better properties than SnS or Sb2S3 materials. Although, it is still unclear what is the best method of synthesis to obtain pure SnxSbySz materials as well as their resulting properties.

In this work is presented the synthesis of SnSb2S4 thin films through chemical bath deposition (CBD) and post-deposition annealing. CdS-coated Corning glass substrates were used to deposit the ternary compound by CBD. The solution was composed of antimony trichloride, tin chloride, tartaric acid, ammonium hydroxide, thioacetamide, and distilled water to complete a volume of 80 ml. The substrates were immersed in the solution at 80 °C for 3-5 h. Later, the substrates were annealed at 300 °C for 1-3 h to promote their crystallization and formation of the SnSb2S4 compound. XRD analysis confirmed that pristine thin films contain the SnS and Sb2S3 binary phases, and the SnSb2S4 phase resembles after annealing, having a crystallite size of 7 nm. The SnSb2S4 thin films showed a compact and homogeneous morphology, an α of 1x105 cm^{-1}, and Eg of 1.50 eV for direct-forbidden transitions. These results indicate that it is possible to obtain SnSb2S4 thin films by CBD and exhibit adequate properties for their use as an absorber in TFSCs.

→ *Return to the schedule*

Deploying Interfacial Engineering to Maximize Efficiency in a Biomass Combuster

Sami Khan

Simon Fraser University

Abstract:

Wood-burning stoves are widely used to heat houses, offices, and other spaces, with over 18 million wood stoves worldwide. They create a warm, comfortable ambiance and can be used in remote and off-grid communities. In addition, wood has the potential to be a renewable energy source since, when burned, it releases approximately the same amount of carbon dioxide the tree absorbed as it grew, making it roughly carbon neutral. However, soot accumulation on the stoves' walls significantly reduces the heat flux and efficiency. From our calculations, we find that a 0.1mm layer of soot reduces the heat flux by 30%.

Herein, we develop a novel method to oxidize soot accumulated on combuster surfaces using microtextures developed by sandblasting. Analyzing the changes in the soot areas before and after heating, we find that the soot oxidation rate is increased on microtextured stainless steel (SS) 430 and glass when compared to smooth samples at fixed temperatures and durations. For example, the percentages of soot oxidation on smooth and rough SS 430 samples after heating to 510°C for 10 minutes are 10.7% and 95.7%, respectively. Moreover, analyzing smooth and rough samples covered with soot after heating to 530°C for 45 minutes using X-ray Photoelectron Spectroscopy (XPS), we find high percentages of iron and chromium on the rough sample, indicating that the soot layer was fully oxidized.

Furthermore, we demonstrate how systematic microtextures can control the wetting and crystallization of phase-change materials that are used to harness and store the heat from biomass combusters. We investigate the effect of the surface roughness parameters on the nucleation rate by testing the reversibility of molten salts on various rough silicon substrates. The substrate with the highest pillar density shows the fastest nucleation rate. Application of these microtextures to the phase change materials is expected to give efficiency benefits to energy storage from biomass combusters.

→ *Return to the schedule*

Bioleaching of Silca-Sulfide Gold Ore Deposits, Tigray-Ethiopia

Goitom Gebreyohannes Berhe, Desta Berhe Sbhatu, Samuel Estifanoc Gebre, Kiros Hagos Abay, Genet Gebryohannes Mihretu, Gebrekidan Mebrahtu Tesfamariam, Sumuel Alemayo, Mulugeta Sisay Cheru, Afewerk Gebre

Mekelle University, College of Natural and Computational Sciences

Abstract:

Oxidative leaching an alternative and low-cost compare to use cyanide chemical extraction methods of gold from low-grade gold sulfide. The oxidation of finely ground sulfide containing gold of May-Hibey deposited by Acidithiobacillus ferrooxidans was evaluated in in cell density, pH, and extraction efficiency of Fe and Au in shake flasks experiments. The compositional and elemental analysis of the beneficiated ore was analyzed using XRD and EDXRF spectroscopy. The major elements of the ore are silicon, iron, and sulfur 62.456, 15.441, 7.912 wt% and grade of the gold 4.356 mg/L, respectively. The XRD spectra, dominant phases of the gold sulfide ore concentrated indicated that the major compositions of the ore are quartz, syn (major, SiO2), silconsulfide (SiS2), pyrite (FeS2) and polymetallic elements such as; silderenrite, gismandine, siderenikite, hematite, syn. The result of both experiments, with and without blank bacteria was evaluated. The pH of the blank was almost constant and the pH of the bioleached was lowered from time to time. A. ferrooxidans bacturium always grew better and better during the whole bioleaching process, For the A. ferrooxidans, the density of cells was the maximum reached 90.00 × 107 cells/mL at 11 weeks and decreased 87.00 × 107 cells/mL from 12 weeks. This inhibition was may be due to the presence of polymetallic elements resulting in decreasing metal tolerant of the A. ferrooxidans. Then, bacterial had a better effect on the solubilization of total iron and total gold than that of the without bacteria. For leaching by the bacteria, the extraction of total iron and gold maximum reached 92.16% (14.23 mg/L) and 99.97% (4.355 ppm), respectively, after 11 weeks. While, leaching without bacteria the extraction of total iron and gold change at 11 weeks. At the later stage of bioleaching, the extraction of total iron and sulfide had a decrease trend, which might be due to the formation of secondary minerals.

→ *Return to the schedule*

Use of Carbonized Rice Bran for Adsorption of Lead (ii) Ions in Aqueous Solution

Sandeep Kaur Gill, Rajiv Arora, Bohar Singh

G. N. Constructions, Shaheed Bhagat Singh State University

Abstract:

Heavy metals are harmful to live beings even though they are present in small amounts. This study was performed by utilizing carbonized rice bran adsorbent for the adsorption of Lead (II) ions in an aqueous solution. The charcoal was characterized using XRD and SEM-EDX. The batch experiments were performed to optimize the parameters for the maximum adsorption of the lead ions, and the parameters involved were – pH, initial ion concentration, amount of adsorbent, contact time, and temperature of the lead solution. A dose of 6 g L-1 of biosorbents in solutions with an initial pH of 8.5, an initial Pb(II) concentration of 10 mg L-1, and a contact time of 60 min resulted in the maximum Pb(II) removal efficiency. Carbonized rice bran is an inexpensive adsorbent to remove lead ions from aqueous solutions because of its high metal uptake capacity as indicated by results.

→ *Return to the schedule*

Assessing the Feasibility of a 2-Step Method for Leaching Synthetic Scheelite in H2SO4 and H2O2 Solution

Idil Mutlu Tuncer, Jing Liu

University of Alberta

Abstract:

Canada's Critical Minerals Strategy for 2021 emphasizes the significance of tungsten, a rare element. Today, tungsten production relies on scheelite, which is known as a secondary resource with a lower-grade and complex ore structure, Due to the exploitation and reduction of high-grade wolframite resources. Synthetic scheelite has become an increasingly important source due to its low impurity content and accessibility, particularly in ongoing laboratory-scale leaching studies. The most recent laboratory-scale study succeeded in a feasible and clean process for leaching synthetic scheelite minerals using a solution formed by mixing H2SO4 and H2O2. This leaching process takes place at normal pressures and low temperatures (50-60 °C) without the need for high temperature and high pressure, providing an advantage in terms of low energy consumption. Furthermore, the low volatilization of H2SO4 makes the process eco-friendly and does not create an environmental threat or waste. Although this method is considered an efficient way to leach synthetic scheelite, there are some disadvantages of the process, such as the low thermal stability and short shelf life of H2O2, which is more expensive than the stable H2SO4. H2O2 also tends to decompose naturally upon contact with water and/or air, which may reduce its effectiveness during leaching.

In this work, to prevent H2O2 loss, a 2-step method is proposed and applied by adding H2O2 to complete the leaching process for the shortest possible time, thus preventing its degradation and achieving economic benefits by reducing its concentration. This study found that the recommended temperature and leach times could be decreased, and the recommended feed amount could be increased. It is confirmed that the proposed 2-step method using H2SO4 and H2O2 can effectively extract tungsten from synthetic scheelite, and can increase the profitability by reducing the H2O2 amount by preventing its decomposition.

→ *Return to the schedule*

Built to Last: How NMR Spectroscopy is Improving Materials for Nuclear Waste Disposal

Scott Kroeker

University of Manitoba

Abstract:

Nuclear power contributes significantly to our global energy portfolio and remains an alternative to fossil-fuel combustion. However, spent nuclear fuel is highly radioactive and contains long-lived radioisotopes which must be immobilized for hundreds of thousands of years to safeguard human and environmental health. The extreme time-scale and health risks associated with this problem place exacting demands on the materials used to sequester high-level radioactive waste. This presentation will show how nuclear magnetic resonance (NMR) spectroscopy is being used to improve the materials and processes involved in nuclear waste vitrification. New glass compositions are being developed to increase the retention of radioactive species in the glassy phase and prevent their separation into water-soluble crystalline phases. The molecular-level structural basis of chemical durability is being studied to enhance resistance to glass dissolution in aqueous underground environments. Surface alteration layers are analysed to better understand their formation and protective properties. Multinuclear magnetic resonance can offer key information about each of these critical aspects of radioactive waste immobilization to help ensure that glassy wasteforms are reliable and safe for millennia to come.

→ *Return to the schedule*

The Investigation of Usability of High Carbon Ferrochrome Slag as a Slag Conditioner at Iron&Steel Industry

Gökhan Başman, Tuğçe ERGÜL, Hande Ardıçoğlu, Tuğçe Özcan

Eti krom INC.

Abstract:

Ferrochrome is an alloy containing 50% - 70% chromium and 50% - 30% iron. Ferrochrome produced by reducing chromite ores enriched by extracting from mineral deposits in electric arc-resistance furnaces using coke. High carbon Ferrochrome slag is produced as a waste in the production of high carbon ferrochrome. High carbon ferrochrome slag is mainly composed of MgO, Al203, and SiO2. In this study, the use of high carbon ferrochrome slag as a slag modifier in the iron and steel industry was investigated. High carbon ferrochrome slag was sent to different iron and steel producers for testing and chemical analyzes of iron and steel slag were made after the high carbon ferrochrome slag was used. According to the theoretical and practical results obtained, it has been observed that high carbon ferrochrome slag can be used as a slag conditioner in the iron and steel industry.

→ *Return to the schedule*

Work Function-tailored Nitrogenase-like Fe Double-atom Catalysts on Transition Metal Dichalcogenides for Nitrogen Fixation

Xue Yao, Zhiwen Chen, Chandra Veer Singh

University of Toronto

Abstract:

The work function-activity relationship provides a new strategy to design catalysts by tailoring the work function. A lower work function (ϕ) is widely believed to be in favor of better catalytic activity due to the easier electron transfer from the catalyst surface to reactants and/or intermediates. In this work, the ϕ values of nitrogenase-like Fe double-atom catalysts (Fe2/MX2, MX2: transition metal dichalcogenides) were tailored by altering the MX2 supports for nitrogen (N2) fixation. By density functional theory calculations, it is found that a lower ϕ caused by the increasing period number of transition metal or chalcogen of MX2 impairs the catalytic activity. This abnormal ϕ-activity relationship is mainly due to the over-strong N2 adsorption on Fe2/MX2. Based on our strategy, Fe2/VS2, Fe2/CrS2, Fe2/MoS2, and Fe2/WS2 having relatively large ϕ values (4.44 ~ 5.81 eV) show excellent activity toward N2 fixation with the overpotential values of 0.21 ~ 0.25 V.

→ *Return to the schedule*

Basal Plane Activation via Grain Boundaries in Monolayer MoS2 for Carbon Dioxide Reduction

Ying Zhao, Jun Song

McGill University

Abstract:

The electrochemical carbon dioxide reduction reaction (CO2RR) has been shown to be a promising route to reducing atmospheric carbon dioxide (CO2) to facilitate our transition to a carbon-free economy. Transition metal dichalcogenides (TMDCs) have recently emerged as potential catalyst materials for high-efficiency CO2RR. However, pristine TMDCs are bottlenecked by the insufficiency of active sites in the basal plane. In this study, focusing on polycrystalline 2H MoS2, we perform systematic first-principles calculations to investigate the role of grain boundaries (GBs) on the catalytic performance of MoS2 for CO2RR. Our results show that most GBs contribute to lowering the reaction energy of the potential-limiting step in CO2RR. This effect can be further amplified with the introduction of S vacancies. In addition, introducing GBs with vacancies is shown to act as an effective method to break the scaling relations between reaction intermediates, which is crucial in improving catalytic efficiencies. Our study demonstrates that defect engineering is a promising approach to activate the basal plane of TMDCs for CO2RR and provides valuable insights for the design of high-performance CO2RR electrocatalysts.

→ *Return to the schedule*

GS17

Nano-materials for Waste Heat Conversion into Electrical Energy Thermoelectric generator

Wiqar Hussain Shah

International Islamic University

Abstract:

The electrical and thermal properties of the doped Tellurium Telluride (Tl10Te6) chalcogenide nano-particles are mainly characterized by a competition between metallic (hole doped concentration) and semi-conducting state. We have studied the effects of Sn doping on the electrical and thermoelectric properties of Tl10-xSnxTe6 (1.00 ⩽x⩽ 2.00), nano-particles, prepared by solid state reactions in sealed silica tubes and ball milling method. Structurally, all these compounds were found to be phase pure as confirmed by the x-rays diffractometery (XRD) and energy dispersive X-ray spectroscopy (EDS) analysis. Additionally crystal structure data were used to model the data and support the findings. The particles size was calculated from the XRD data by Scherrer's formula. The EDS was used for an elemental analysis of the sample and declares the percentage of elements present in the system. The thermo-power or Seebeck co-efficient (S) was measured for all these compounds which show that S increases with increasing temperature from 295 to 550 K. The Seebeck coefficient is positive for the whole temperature range, showing p-type semiconductor characteristics. The electrical conductivity was investigated by four probe resistivity techniques revealed that the electrical conductivity decreases with increasing temperature, and also simultaneously with increasing Sn concentration. While for Seebeck coefficient the trend is opposite which is increases with increasing temperature. These increasing behavior of Seebeck coefficient leads to high power factor which are increases with increasing temperature and Sn concentration except For Tl8Sn2Te6 because of lowest electrical conductivity but its power factor increases well with increasing temperature.

→ *Return to the schedule*

Green Corrosion Inhibitors for Drilling Operation: New Derivatives of Fatty Acid-based Inhibitors in Drilling Fluids for 1018 Carbon Steel in CO2-saturated KCl Environments

Mohammad Palimi, Y. Tang, V. Alvarez, E. Kuru, D.Y. Li

University of Alberta

Abstract:

Improving corrosion resistance of oilfield drilling equipment is crucial to the drilling effectiveness, environmental contamination, and operation safety. In this study, inhibition effects of three eco-friendly fatty acid-based inhibitors, Polyethylene glycol-2 oleamide (PEG-2 oleamide), Glycerol myristate (GM) and Glycerol linoleate (GL), in emulsion-based fluids against CO2 corrosion of carbon steel were investigated at room temperature. The corrosion inhibitors were characterized by Fourier transform infrared (FT-IR) spectroscopy and CHNS-O analysis. The corrosion resistance of steels was studied by electrochemical tests including open circuit potential (OCP), electrochemical impedance spectroscopy (EIS) and potentiodynamic polarization. Scanning electron microscopy (SEM), energy dispersive spectroscopy (EDS) and X-ray photoelectron spectrophotometer (XPS) were employed to study surface morphology and the chemical composition of layer adsorbed on the metal surface. The study demonstrates remarkable performance of the three green inhibitors especially PEG-2 oleamide, which shows an inhibition efficiency of 99.7 %. The high inhibition efficiencies were consequence of blocking effect of corrosive ions to reach metal surface by forming a corrosion-protective layer. First-principles calculations and molecular dynamics simulation reveal chemical bonding between the inhibitors and iron surface, and stronger intermolecular attraction in the adsorbed film resulting from PEG-2 oleamide, which renders the PEG-2 oleamide–induced film particularly durable.

→ *Return to the schedule*

Investigating the Localized Deformation Induced by Hydride Precipitation in Zirconium

Masoud Taherijam, Saiedeh Marashi, Hamidreza Abdolvand

Western University

Abstract:

One of the main reasons for the degradation of the zirconium alloys used in nuclear reactors is hydride formation. However, the impact of this process on the development of localized deformation zones is not well-understood. In this study, high spatial resolution electron backscatter diffraction (EBSD) measurement were coupled with a crystal plasticity finite element model to quantify the effects of hydride formation. A zirconium specimen was hydrided without external mechanical loads, then the rotation fields around the precipitated hydrides were measured using EBSD. The experimental and numerical results revealed that hydride precipitation induces large lattice rotations within the zirconium matrix, with the maximum rotation observed at hydride tips. The crystallographic orientations and shapes of hydrides affect the magnitude of rotation fields. Both modeling and experimental results showed the development of parallel geometrically necessary dislocation fields.

→ *Return to the schedule*

Crack Nucleation and Propagation in Dual Phase HCP-BCC Zirconium

Saiedeh Sadat Marashi, Hamidreza Abdolvand

Western University

Abstract:

The alloy Zr-2.5Nb is used for manufacturing the pressure tubes installed in the core of Canada Deuterium Uranium (CANDU) nuclear reactors. This alloy consists of α-zirconium with hexagonal close-packed (HCP) crystals and a minor β-zirconium phase with body centered cubic (BCC) crystals that are mainly located in between the α-grains. This work aims to study the nucleation and propagation of microcracks in dual phase zirconium using a crystal plasticity finite element (CPFE) model. Specifically, the effects of the BCC phase on the redistribution of stress and formation of microcracks in the vicinity of notched specimens are studied in detail. Simulation results show that while microcracks lie on the prism slip system in the single phase HCP zirconium, microcracks may lie on either the basal or prismatic traces, depending on the crystal orientation of the α-grain and the adjacent β-phase features, such as its thickness or distance from the notch. Moreover, a numerical parametric study was conducted which revealed that the β-phase retards crack propagation regardless of its geometrical features or its orientation.

→ *Return to the schedule*

Aluminum Hydride Formed on Aluminum Base Substrates by Hydrogen Plasma Irradiation

Goroh Itoh, Tomoharu Ouchi, Naoyuki Sato, Shigeru Kuramoto and Junya Kobayashi

Ibaraki University

Abstract:

Metal hydrides have attracted attention as hydrogen storage materials, among which aluminum hydride has extremely high hydrogen densities in terms of both mass and volume and also has practically favorable hydrogen release temperature. However, currently, hydrogen gas atmosphere at high temperature and high pressure is required for aluminum hydride formation. So far, we have attempted to synthesize aluminum hydrides from Al-Ti alloy and pure aluminum using hydrogen plasma, which has the potential to generate non-equilibrium reactions at relatively low temperatures and pressures. In the present paper, we will report the results of the characterization on the products that have been obtained by hydrogen plasma irradiation onto Al-Ti alloy and pure aluminum substrates by means of X-ray diffraction, scanning and transmission electron microscopies, as a function of irradiation conditions.

→ *Return to the schedule*

PON1 Enzyme Mutation and Organ Pesticide Usage

Ali Göksu, Tuana Glass Mould

University of Manitoba

Abstract:

Through the research with Farmers and Gastro Intestinal patients analyzed the author brings out a discussion on the potential mutation of the PON1 Enzyme in relation to Organo Pesticide Usage by farmers. The secondary analysis was used to provide a generalized understanding in regards to the quantitive and qualitative data and in order to make research repeatable.

The Organic Pesticide Usage and Worldwide Concerns

Some of the etymologists conducted research on the target audience the male population in regards to Organophosphates related to the male Organophosphate also known as OPs mostly used for insecticides. Unknown OP check is considered to be a very dangerous domain(Boedeker et al., 2020)

Organic Pesticide Cancer and Gastrointestinal Disease

Hepatocellular Carcinoma also known as HCC9 is the fifth most common cancer worldwide and the third leading cause of cancer death(Samant, 2022)Organo-pesticide usage broke its peak around the later 20th century most of the pesticides went unchecked due to the fact that farmers not nearly educated on the usage. The main worry regarding the situation covered is the lack of education about pesticides. It was stated that farmers are not educated well in regard to chemical pesticide usage. It has been reported that most of the farmers are not aware of identifying overdose.

PON1 and Organo Pesticides Relationship

Another domain of oxidative stress correlated with the reduced PON1 activity is the active usage of Organo Pesticides(Hofmann et al., 2009)PON 1 has a direct effect against Organo Pesticide elements. The Agricultural practice around the globe is relatively unknown. The usage of Organo pesticide chemicals between 1990 is unknown. Interestingly the timeline for record increase in PON1 mutation among chronic disease patients is on the rise. (Gün, 2008)

The author brings a worthy discussion point of the statistical relationship between PON1 mutation and its relation to OP overdose.

→ *Return to the schedule*

The Effect of Adding Green Pea Pod Lignin and Industrial Hemp Fiber to Polyester Resin

Hassan Alshahrani

Najran University

Abstract:

The effect of adding green pea pod lignin and industrial hemp fiber to polyester resin was investigated in this study to develop the light weight composite materials. This study also focused on characterization of this composite when material is silane surface treated. The composites were prepared by hand layup process and tested in accordance with respective ASTM standards. The detailed outcomes from this analysis shows that pure resin exhibits much lower values than any other composite designations. The inclusion of 2.0 vol.% of lignin addition for the composite designation PHL3 resulted in the maximum increase in mechanical properties noted up to the 128 MPa, 4.24 GPa, 161 MPa, 5.92 GPa, and 21.8 MPa for tensile strength, tensile modulus, flexural strength, and modulus, respectively.

→ *Return to the schedule*

Strain Rate Induced Mechanical Changes in NASICON Solid Electrolyte Materials

Zachary Carroll, Yu Zou

University of Toronto

Abstract:

Solid-state batteries have come to the forefront of battery research with the potential of providing higher energy density and less flammability compared to traditional lithium-ion batteries. However, solid-state battery technology has run into issues with longevity due to the degradation of battery components over successive charge and discharge cycles. During the charging of a solid-state battery, lithium ions migrate to the anode through the electrolyte and are deposited at the interface between the anode and the solid electrolyte. Over time, the accumulation of lithium can create stresses that drive crack growth through the solid electrolyte, thus causing a loss in battery capacity. As such, understanding how mechanical properties are influenced by the electrochemistry of the battery is crucial. To date, we have completed preliminary work to mechanically characterize a NASICON type material by determining the elastic modulus, hardness, and fracture toughness. Using constant strain rate indentation methods, we were able to determine that the sample possesses an average hardness and elastic modulus of 9.938 GPa and 120.75 GPa respectively. Additionally, fracture toughness was calculated from SEM images of indents to be approximately 1.09 MPa m^0.5 which matches well with results reported in the literature. It was also found that the NASICON sample exhibited strain rate sensitivity in its mechanical properties with hardness increasing under indentation at higher strain rates. However, this same trend does not present itself in the elastic modulus data. These results may provide insight into how the rate of lithium deposition at the anode affects the mechanical response of the solid electrolyte material during the charging of solid state batteries.

→ *Return to the schedule*

Vitrification of Zeolites and Geopolymers for Long-term Immobilization of Cesium and Strontium

Thulasi Elumalai

University of Manitoba

Abstract:

The safe trapping of radioactive waste such as 135/137Cs and 90Sr has become a critical issue with the continuing use of nuclear fission as a carbon-neutral power source. The bioaccumulation of Cs and Sr from contaminated groundwater or food sources can have dire consequences on health due to radioactive decay. Naturally occurring zeolites such as clinoptilolite (CPT), can selectively adsorb Cs and Sr ions from aqueous environments, however its low ion-retention capability hinders its use in long-term disposal. Geopolymers (GP) have been proposed as an encapsulation matrix for Cs- and Sr-loaded CPT, however the poor chemical durability of these materials is exacerbated by the inhomogeneous incorporation of CPT into the GP network, resulting in a material that is neither entirely amorphous nor highly durable. Our approach improves on these partial solutions by adapting the highly durable borosilicate glasses used in immobilizing liquid waste. Waste-loaded zeolites and geopolymers are combined with glass-forming components and melted to form a homogeneous "geoglass". The aim of this study is to understand the incorporation of waste ions into the network structure of these vitrified wasteforms with the help of solid-state NMR spectroscopy, and to optimize compositions to maximize waste loading and chemical durability, leading to safe, high-volume radioactive wasteforms. The development of a glass composition and vitrification process utilizing Cs- and Sr-loaded zeolites and geopolymers as precursors could produce a more efficient, cost-effective, and durable "geoglass" to address the long-term storage of nuclear waste.

→ *Return to the schedule*

GS26

The Effects of Polypyrrole:Carboxymethyl Cellulose Composite Morphology on Capacitance and Conductivity: An Alternative Battery Binder Material

Gamaliel Azariah, Christian Kuss

University of Manitoba

Abstract:

Binder materials are essential components in rechargeable Li-ion batteries, providing electrode stability, cohesion, and many other benefits. Overall battery performance is influenced by factors such as capacitance and electrical conductivity of binders. These properties dictate the energy-storing capability and charge-discharge rates of batteries.

Doping of polypyrrole (PPy) with carboxymethyl cellulose (CMC) produces the composite polypyrrole:carboxymethyl cellulose (PPy:CMC), a promising binder material due to its environmentally benign fabrication, structural cohesion, and innate electrical conductivity. Basic oxidative polymerization of PPy yields nanospherical morphologies, while the use of organic dye additives produces nanofibrillar morphologies. Changes in capacitive and conductive properties have been observed to correlate with these morphological changes of PPy, however, the same trend has not been explored under its utilization in PPy:CMC binders.

Within the present work, nanofibrillar and nanospherical PPy were synthesized in situ with CMC to produce PPy:CMC composites. Characterizations were made using X-ray photoelectron spectroscopy (XPS) and scanning electron microscopy (SEM). Conductivity was measured using the four-point probe method, while capacitance and additional characterization were evaluated through cyclic voltammetry of symmetric cells containing binder-only electrodes as well as lithium-containing half cells.

→ *Return to the schedule*

A Novel Approach to Mineral Carbonation from Ultramafic Tailings

Sara Gardideh, Mansoor Barati

University of Toronto

Abstract:

Mineral carbonation approach for reducing global warming has garnered interest on a worldwide scale. Due to the benefits of permanent storage and abundant mineral resources, mineral carbonation (MC) is one of the most effective strategies for sequestering CO2. The combination of mineral processing for primary metal recovery and mineral carbonation for carbon sequestration is an emerging field of study with the potential to minimize capital costs.

A detailed study of low-pressure gas–solid carbonation of ultramafic tailings in a dry environment has been accomplished. In order to track the changing structure of serpentine minerals and their reactivity as a function of temperature (300-900 oC), CO2 partial pressure (25-90 mol %), and thermal preconditioning, thermogravimetry has been utilized. The incongruent CO2 van der Waals molecular diameters with the octahedral-tetrahedral lattice constants of serpentine were used to explain the mild carbonation reactivity. Serpentine requires additional thermal-treatment to remove hydroxyl groups, resulting in the chemical transformation to pseudo-forsterite, which is a mineral composed of isolated SiO4 tetrahedra linked by octahedrally coordinated magnesium ions. The heating treatment above 850 oC is adequate to remove chemically bound water from the lattice. Particles with a diameter < 34 (µm) are desirable, and thermally treated serpentine at 850 oC for 2.30 hours reached 65% CO2 storage capacity. The decrease in particle size, increase in temperature, and magnetic separation can dramatically enhance carbonation.

→ *Return to the schedule*

GS28

The Role of Atomic-scale Defects in Single-Atom Catalysis

Shiva Mohajernia

University of Alberta

Abstract:

Single-atom (SA) research has opened up new avenues in heterogeneous catalysis, reduced reliance on expensive metals, and provided unprecedented control over atomistic effects. This has led to the creation of superior active sites and allowed for the development of metal-support interfaces with precise chemical and structural control. The remaining challenge in this field is obtaining high SA loading while avoiding nanoparticle formation.

Herein, the atomic-scale defect engineering approach is shown to be an effective strategy to act as traps for SA sites as co-catalyst for catalytic H2 generation. Defect generation, their type, and density are monitored by electron paramagnetic resonance spectroscopy (EPR) as the most precise method to study atomic-scale defects. Defect engineering is performed by conventional thermal reduction and novel room-temperature techniques. We show that an optimized SA-Pt decorated substrate greatly enhances the normalized catalytic H2 generation activity compared to a conventional nanoparticle-decorated TiO2 surface. HAADF-STEM, XPS, and EPR investigation jointly confirm the atomic nature of the decorated Pt on TiO2 support. Our results show that the defect engineering and SA decoration strategy can be successfully applied to scalable morphologies, namely nanosheet powders and well-aligned, hierarchical, high surface area nanostructures such as nanotubes for electrodics applications. Notably, the density of the relevant surface exposed defect centers—thus, the density of SA sites, which play a key role in catalytic activity—can be controlled.

→ *Return to the schedule*

GS29

Visible Light Driven Nd2O3/Mo(S,O)3-x·0.34H2O Heterojunction for Enhanced Photocatalytic Degradation of Organic pollutants

Sleshi Fentie Tadesse, Dong-Hau Kuo, Worku Lakew Kebede, Girma Sisay Wolde

Ming Chi University of Technology, National Taiwan University of Science and Technology

Abstract:

Developing low-cost and visible-light-driven metal oxide and sulfide-based photocatalysts for the degradation of organic dyes has been a major area of research to mitigate environmental pollution. In this study, a low-cost and facile precipitation method at a low temperature of 95◦C was used to synthesize visible-light-driven Nd2O3/Mo(S,O)3-x · 0.34H2O heterojunctions. The crystal structure, elemental composition, optical, and electrical properties of as-prepared materials were investigated using various analytical techniques. Organic dyes of methyl orange (MO), Rhodamine B (RhB), and Methylene blue (MB) were selected as model organic pollutants to evaluate the photocatalytic efficiency of as-synthesized materials under visible light irradiation. 20 mol% NdMoOS nanocomposite showed excellent degradation efficiency, and it decomposed 98.8%, 99.9%, and 99.8% of MO, RhB, and MB after 120 min, 90 min, and 90 min visible light irradiation, respectively. HPLC-MS analysis further confirms the complete removal of dyes. The formation of heterojunction, high charge separation, and low recombination rate of photoinduced e--h+ pairs can contribute to the enhanced photocatalytic activity. Superoxide radicals (O2–•), hydroxyl radicals (HO•), and holes (h+) were identified as major oxidative species involved in the photocatalytic degradation mechanisms of MO, RhB, and MB dyes.

→ *Return to the schedule*

Development of an Adaptive Periodic Magnetorheological based Metamaterial to Attenuate Wide-Band Low-Frequency Noise and Vibration

Hamid Jafari, Ramin Sedaghati

Concordia University

Abstract:

An adaptive periodic low-frequency wave filter utilizing smart magnetorheological elastomers (MREs) has been developed to control the wave filtering frequencies. MREs are smart multi-functional materials capable of altering their mechanical properties and configurations in response to an applied magnetic field stimulus This property makes them attractive for various applications, particularly the development of novel adaptive low-frequency wave filters with adaptable bandgap areas.

In this study, MREs are modelled as hyperelastic materials, and their dynamic response is analyzed through Bloch's theorem and periodic boundary conditions. The results reveal that the proposed adaptive wave filter can significantly outperform traditional filters and can adapt to changes in the frequency of the input elastic/acoustic waves. The ability to adapt to these changes is vital for low-frequency wave filtering, as the frequency and amplitude of the input signal can vary significantly in practical settings.

Furthermore, the study demonstrates that using MREs in this application enhances the performance of low-frequency wave filters in a range of practical settings. This is because MREs have a high damping ratio and can be controlled easily with an applied magnetic field. This allows the filter to have a dynamic response tailored to the input sound and vibration requirements, leading to improved performance. The results of this study highlight the significance of this work in the field of low-frequency wave filtering and suggest that MREs have the potential to play an important role in the development of advanced filtering systems. Further research is needed to fully realize the potential of MRE in tunable wave filtering design.

→ *Return to the schedule*

Loading Variable Effects on Fatigue Behavior of Wood Flour HDPE Composites

Babak Mokhtarnia, Mohammad Layeghi

University of Tehran

Abstract:

This work investigated the flexural fatigue properties of wood flour HDPE composites. Composites with polymer matrix were fabricated and subjected to 3-point bending fatigue tests. Cyclic loads were performed at different loading ratios (0.1 and 0.3) and frequencies (0.9 and 5.2 Hz) to determine the effect of these parameters on the fatigue behavior of composite samples. Cyclic stress amplitude versus number of cycles to failure (S-N) curves of experiments were plotted and compared. For safe fatigue design and material reliability index, a 95% confidence interval band of fatigue lives were plotted. Stiffness reduction approach was used to evaluate and monitor damage evolution. An experiment like this provides insight into fatigue properties of Wood-fiber plastic composites (WPCs) to improve the life of parts under cyclic loading.

→ *Return to the schedule*

Synthesis, Characterization and Molecular Simulation of Polymers Enhanced with Halloysite Nanotubes

Ron Miller, Rafaela Aguiar, Oren Petel

Carleton University, University of Toronto

Abstract:

Nanocomposites and nanostructures often behave in ways that are counterintuitive to our expectations from macroscopic analogues, and we are interested in exploring these behaviours and exploiting them for improved material performance. In particular, we have been interested in improving the high-strain-rate response of polyurethanes (PUs), using Halloysite nanotubes (HNTs) in their synthesis. We have synthesized PU-HNT composites with less than 1 wt% HNT, and demonstrated that these materials show a 21% increase in fracture toughness and 35% increase in spall strength. More importantly, our characterization and modeling work elucidates the underlying mechanisms of these improvements, and shows that the HNTs are not behaving as a traditional toughening phase in a composite. Rather, they act to favourably modify the microstructure in the surrounding polymer matrix during synthesis.

→ *Return to the schedule*

Optimizing Extrusion and Fabrication of Phosphate Glass-Based Microstructured Optical Fibers for Biomedical Applications

Seyed Hossein Mussavi Rizi, Davide Luca Janner, Nadia Boetti, Diego Pugliese

Politecnico di Torino

Abstract:

Bioresorbability, tailorable mechanical properties, and a wide transparency window of 300–2600 nm make bioresorbable phosphate glasses excellent alternatives to conventional silicate-based glasses in biomedical applications. However, fabricating bioresorbable phosphate glass fibers by extrusion is yet to be duly explored, primarily because of recrystallization onset at lower temperatures than those of silicate glass counterparts. To fill this gap, we investigated the fabrication of microstructured bioresorbable optical fibers by extrusion and stack-and-draw techniques. Extrusion parameters such as die design, time, force, temperature, and speed were optimized to achieve preforms with various inner and outer diameters. Several extrudates were fabricated with 10.50 and 10.15 mm outer diameters and 5.25 and 7.40 mm inner diameters. The preforms were subsequently stretched, stacked, and drawn to fibers with diameters ranging from 120 to 250 µm. The resulting fibers were capable of guiding light and functioning as microfluidic channels. The microfluidic channel (25 µm diameter, 20 cm long) was tested for liquid delivery, and the corresponding images show that light was well confined into the core with low attenuation loss. This optimized extrusion process promises significant energy savings and reduced waste glass, offering a sustainable method for fabricating bioresorbable phosphate glass optical fibers with a vast potential as theranostic devices employed in specific areas inside the body without requiring a removal procedure.

→ *Return to the schedule*

A Scanning Fabry-Perot Cavity for the Study of THz Frequency Magnon Polaritons

Christina Balanduk

University of Manitoba

Abstract:

Study of hybrid quasiparticles, such as the cavity magnon polariton, is of strong interest towards the improvement of sensors and the development of modern memory storage devices. Through this work, we present the initial findings of a custom-built scanning Fabry-Perot cavity within a time-domain THz spectrometer. The cavity is designed to study the coupling between THz photons and a samples magnon modes. The cavity applies custom fabricated silicone Bragg reflectors to achieve a THz cavity with low transmission and a high quality factor. Preliminary results are presented of multiferroic, antiferromagnetic bismuth orthoferrite (BFO). BFO has known electromagnon modes at 0.530 and 0.555 THz [1]. By tuning the cavity frequency, we investigate the splitting of BFO's resonant frequency modes, and thus the coupling between THz photons with BFO's magnons.

[1] A. Braconnier, "A scanning Fabry Perot cavity for the study of terahertz frequency polaritons," Master's thesis, 2022.

→ *Return to the schedule*

N-halamine-based Antimicrobial Fabric Finish for Frontline Workers – Application Techniques and Performance Evaluation

Anita Amir Labonno, René Arredondo, Paulina de la Mata, Jane Batcheller, James Harynuk, Patricia I. Dolez

University of Alberta

Abstract:

Textile materials have a larger surface area, which creates a suitable platform for microbes to flourish. As a result, they can act as a vector for transmission to humans. Therefore, antimicrobial functionality in textile materials is highly desirable to protect the wearer and minimize cross-contamination. In this study, a biocidal finish for front liners' protective clothing - military personnel and healthcare workers – was prepared using N-halamine as the antimicrobial agent. The advantage of N-halamine is that upon depletion of the active element, the nitrogen-halogen bond can be regenerated with a source of free halogens. The optimal halogen was selected based on the loading ratio, impact on colour, and ease of application on the fabric. Since the nitrogen-halogen bonds in N-halamine compounds are sensitive to UV radiation, UV absorber nanoparticles were added to the finish to improve the durability of the biocidal functionality. Two methods of application of the finish on the fabrics were explored: the wet and dry routes. The wet route involves dissolving the N-halamine polymer in a solvent and applying the solution to the fabric as a finish. For the dry route, the nanoparticle/N-halamine composite is made into a powder that is sprinkled on the fabric and melted using a hot press. The performance of the treated fabric was assessed in terms of strength, colour, flammability, stiffness, air and water vapor permeability, and compatibility with a water-repellent finish if originally present on the fabric. The durability of the finish was also evaluated using simulated service conditions: abrasion, perspiration, light, laundering, and storage for several months. Finally, the antibacterial efficacy of the finish was measured: 99.999% bacteria kill was observed with halogen concentration on the fabric as low as 0.03%. This shows that N-halamine polymers offer an interesting potential for developing biocidal fabric finishes and reducing cross-contamination by microbes.

→ *Return to the schedule*

Mechanistic Study of Pathogen Inactivation on Salt-coated Filters

Sumin Han

University of Alberta

Abstract:

Conventional masks have limitations in counteracting the spread of pathogens due to the absence of antimicrobial effects. The biocontaminated mask surface can be a source of contact transmission, raising safety concerns. Besides, the single use of conventional masks can lead to a supply shortage during pandemics/epidemics and the use of handmade cloth masks with limited filtration efficiency. To address this issue, we have created salt-coated spunbond polypropylene fabrics, which can effectively inactivate pathogens within a short period of time. Previous research performed with salt-coated filters has proven the efficacy of salt-coated filters (i.e., strain non-specific inactivation, reusability, rapid inactivation, fabric-independent inactivation, etc.); however, its mechanistic study has not been conducted. For mechanistic understanding of the bacterial/viral inactivation, time-dependent viability of the pathogen (influenza virus A/Puerto Rico/8/34 and Klebsiella pneumoniae) were characterized at various conditions of salt (i.e., NaCl/KCl/K2SO4 salts in the form of powders, saline solutions, and salt-coated filters). Then, their inactivation kinetics were compared with time-dependent XRD data post exposure to 2.5–4 μm aerosols. Interestingly, salt powders and salt-coated filters achieved a similar level of inactivation efficiency/behavior, which matched the salt-recrystallization process. This study indicates that the major pathogen viability loss is attributed to drying-induced salt crystallization whose antimicrobial effect does not rely on the strain specificity. Therefore, we believe that our research can contribute to the development of highly effective antimicrobial face masks based on salt-coated filters.

→ *Return to the schedule*

Polypyrrole:Caboxymethyl Cellulose as Electrode Binder Material: Comparative Study Between Nanoscale Morphologies

Gamaliel Azariah

University of Manitoba

Abstract:

With the increasing demand for advanced consumer electronics, comes the constant need to improve energy storage systems. For decades, rechargeable lithium-ion batteries (LIBs) have been used extensively in portable electronics such as laptops, mobile phones, etc. A crucial component of any LIB system, the electrodes, rely on polymeric binder material to provide a mechanical binding between electrode components and overall stability. Therefore, improving the effectiveness of binders will contribute to enhancement in battery performance. The polymer composite polypyrrole:carboxymethyl cellulose (PPy:CMC) has shown great promise as an alternative binder material due to its environmentally benign fabrication process and advantages in cohesion and conductivity compared with common binder composites.

PPy:CMC is a polymer composite consisting of a highly tunable conducting polymer polypyrrole (PPy) doped with water-processable binder carboxymethyl cellulose (CMC). As a highly tunable polymer, polypyrrole has been shown to exist in a multitude of nanostructure morphologies when polymerized under certain conditions. The use of organic dyes as an additive during the polymerization gives rise to nanofibrillar PPy, exhibiting not only a spiky morphology but also unique electrochemical properties.

This research focuses on the utilization of nanofibrillar PPy as a component in PPy:CMC binder for LIBs. Synthesized nanofibrillar PPy (with the use of methyl orange dye) was compared with nanospherical PPy (synthesized without the use of dyes) in a PPy:CMC composite scenario. Characterizations were made using x-ray photoelectron spectroscopy (XPS) and scanning electron microscopy (SEM). Comparisons in electrical conductivities were performed using the four-point probe method. The specific capacitance of these materials was evaluated through a symmetric cell system utilizing cyclic voltammetry.

→ *Return to the schedule*

Fluorinated Omniphobic Coatings for Low-Surface-Tension Liquids

Shashwata Moitra, Constantine M Megaridis

University of Illinois at Chicago

Abstract:

There has been extensive research on capillary-driven transport of high surface tension liquids (e.g., water, glycerol etc.), but only limited attention has been given to contact-line confined transport of liquids with low surface tension (e.g., oils, alcohols, etc.). When the fluid surface tension drops below 40 mN/m, repellency becomes extremely difficult. This situation is encountered in many engineering applications and thus is of high technological importance. In this work, we use a fluorinated nanocomposite coating deposited on a surface textured by laser etching, a scalable technique that requires no lithography implementation. The approach results in the repellency of liquid hydrocarbons with surface tensions as low as 21mN/m. The repellency of several liquids with surface tensions in the range 21-72mN/m is experimentally investigated. Comparisons are performed between the velocities acquired by fluids transported pumplessly on a wedge-shaped wettability-patterned track, due to confinement imposed by the superomniphobic background surrounding the wettable track. Finally, travel distance and velocities of low-surface tension liquids transported on inclined ramps against gravity on similar wedge-shaped wettability-patterned tracks are compared.

→ *Return to the schedule*

4-Alkoxycinnamic Acid Derived Calamitic Liquid Crystals (LCs) as Potential Low Molecular Mass LC Alignment Materials

Jehangir Khan

Paris Lodron University of Salzburg

Abstract:

Calamitic liquid crystals (LCs) have gained the interest of researchers due to their nematic and smectic phases. The anisotropic properties of these LCs make them important for display technologies. They have also found applications in thermography, drug delivery and most excitingly in permanent optical storage devices. In calamitic LCs, mesophase stability is due to rigid core and terminal chain length.

A series of 4-alkoxycinnamates with two flexible alkoxy and alkoxycarbonyl chains were synthesized to study their liquid crystalline behavior. Single crystal X-ray analysis revealed the crystalline structure and a dimer packing was indicated due to H-bonding interactions between two molecules when packed anti-parallel in a crystal structure. Most of the compounds within series show SmA phase only during cooling scan. Only the compound with short terminal chains exhibited nematic along with SmA phase. A monotropic SmC phase was observed for compounds with octyloxy terminal chain. However, X-ray diffraction studies also demonstrated that the SmA to SmC phase transition is not accompanied by a significant interlayer space reduction, which may be attributed to strong intermolecular interactions within the layers. In all the compounds, the mesophase was supercooled prior to crystallization.

→ *Return to the schedule*

TTB-based Ba2K2Gd3Fe5O15 Electroceramic with Sodium (Na) as a Dopant for Capacitors: Electrical and Magnetic Properties

Sameed Khan, Fayaz Hussain

NED University of Engineering and Technology

Abstract:

Dielectric capacitors are drawing a lot of interest for better-pulsed power due to their quick charge and discharge rates and high-power density. Energy density does have a limit, and efficiency and thermal stability are also not ideal. This has long been a barrier to the creation of appealing dielectric materials. In general, instead of lead-based piezoelectric ceramics, which are toxic and not environmentally friendly, capacitors are now made of polymers and ceramics because they provide the best combination of capacitance, dielectric loss, breakdown strength (BDS), and thermal stability. At room temperature, polymer dielectric capacitors have a high power/energy density, but at temperatures beyond 100 °C, they are unreliable and prone to dielectric failure. As a result, dielectric ceramics are the sole viable solution for high-temperature applications. In this research paper, solid-state synthesis was used to create Ba2K2Gd3Fe5O15 and Ba2K(1-x)NaxGd3Fe5O15 Tetragonal Tungsten Bronze (TTB) based lead-free high-density ceramics with Sodium (Na) as a dopant in varying fractions (x = 0.25, 0.5, 0.75, and 1.0). The stoichiometric powder was first dried in a furnace, mixed with ethanol, and ground for 1 hour in a ball mill. Followed by calcination at 800 °C for 2 hours. The mixture was milled again and particle size analysis was performed. The powder was then compacted and next the ceramic tablets were sintered at 1050 °C for 2 hours, followed by polishing to the required thickness, and surfaces were covered with silver paste before being fired, and electric and magnetic properties were studied. The capacitance was found to be high, but with higher dielectric losses, and as the dopant percentage increased, the dielectric losses began to decrease. The conductivity test revealed that the material can behave similarly to a semiconductor due to high conductance if the parameters are controlled.

→ *Return to the schedule*

Curved-based Auxetic Metamaterials for Energy Absorption, Vibration Isolation, and Electricity Generation Applications

Ramin Hamzehei, Nan Wu

University of Manitoba

Abstract:

Architected lattice structures, so-called mechanical metamaterials, are artificially designed structures exhibiting extraordinary mechanical properties mostly due to their specific geometrical designs compared to the parent materials from which they are made. In this regard, this study introduces novel additively manufactured (3D printed) curved-based auxetic metamaterials for multiple engineering applications, including energy absorption, vibration isolation, and electricity generation (energy harvesting). Straight struts and connections in traditional auxetic metamaterials are changed to diverse curved beams, whose shape and arrangement are tuned to study their design effects on the mechanical behaviors of the metamaterial, like stiffness at different strains, elastic-plastic deformations, and inner stress distributions, for different applications.

→ *Return to the schedule*

Innovative Piezo Materials /Technologies

Lala Agamirov-Nost

Single Crystals Innovative Sensors Inc.

Abstract:

The urgent transition to Clean Energy with more efficient renewables, technologies must be conducted based on smarter, structural materials development and implementation. I am presenting first time in Canada most advanced Piezo Hard and Soft materials. Advanced Piezo materials are gaining more and more attention with advanced manufacturing, & are extremely beneficial for worldwide applications, including most emerging ones. A) Hard piezo crystals -as main sensing system for worldwide applications/ industries - for variety of sensors, actuators, transducers, which, are in use in Canada only with 3.2% of required warranty, with incorrect monitoring and very old manufacturing. B) Soft unique designed, multilayered piezo benders/ Array/PEHs - analog to PV Panels. C)Piezo materials - are non-flammable, high energy density, long lasting (25-30 years), without any chemistries involvement, controllable- introduce clean, sustainable Renewable Sources of Energy. Innovative piezo technologies are enabled to solve crucially important climate changing problems. We can't afford to lose any source of clean sustainable energy, especially piezo with many advanced properties for smart integration with different energy sources/and applications (Batteries, clean buildings, to compensate many Hydrogen energy losses, to make nuclear reaction happen with clean renewables, etc.). Every kind of batteries introduce different problems (different chemistries, energy density, flammability, charge-recharge cycles, etc.) with sharp rise in raw materials, CAMs prices, and battery pack prices have increased as much as 47% since 2021. Any kind of batteries, will need supportive integrated technology. Piezo Array imbedded into vehicles' tires produce clean electricity just driving the vehicle with much less amount of batteries to decrease huge impact on mining industry, for real ZEV (website), without any needs of charging stations infrastructure to charge batteries for 8 hours.

→ *Return to the schedule*

Analysis of Nonlinear Piezoelectric Energy Generator under Friction-induced Vibration

Yu Xiao, Nan Wu

University of Manitoba

Abstract:

Research on piezoelectric energy transducer, which has higher energy density compared to electrostatic and electromagnetic transducers, have been conducted on transverse and longitudinal mode energy generation to collect energy from ambient vibrations and possibly become an efficient solution for power supply of wireless devices. In this work, nonlinear magnet-engaged shear mode (d_15) piezoelectric energy generator, which utilizes the friction-induced vibration (FIV) and high shear mode piezoelectric coefficient to improve the energy output, is studied. A piezoelectric coupled friction-induced vibration mathematical model including magnetic nonlinear spring is developed to accurately calculate the dynamic vibration response and voltage output of the systems, and the Stribeck friction model is applied to properly describe the stick-slip motion. Considering the emergence of limit cycle due to the stick-slip phenomenon to be the boundary of the unstable and stable region of the system, a critical sliding velocity v_0 exists and splits the region. The influences of the normal force F_N, material static friction coefficient μ_static, dynamic friction coefficient μ_k, and decay factor β on the critical velocity are investigated, and the results indicate that the increase of μ_k and β can reduce the unstable region and generation of FIV, whereas, the increase of F_N and μ_static can promote the occurrence of FIV. The energy generation process is assessed by transient charging simulation of a storage capacitor, which was experimentally validated in the literature. Parameter studies are conducted to investigate the influences of the material friction parameters on the energy generation regarding the operation velocity range (OVR) and sum of RMS power (SRCP) to guide the generator design with higher output.

→ *Return to the schedule*

Aptasensors Based on 2D Asymmetric Geometry MoS2 Diodes for Label-Free and Ultrasensitive Detection of Cytokine Biomarkers

Mirette Fawzy, Thushani De Silva, Michael M. Adachi, Karen L. Kavanagh

Simon Fraser University

Abstract:

Cytokines are small immune-system signaling proteins found in body fluids such as blood, saliva, and sweat, that are considered as biomarkers for numerous health conditions and diseases. An abnormal variation in cytokine concentrations is an indicator of uncontrolled inflammatory reactions that has been associated with diseases such as cancer, diabetes, and Alzheimer's. Most diseases, particularly cancers, can often be cured if they are detected at an early stage. Thus, the ability to monitor and detect a slight change in cytokine levels is of great significance for early clinical diagnosis.

In our recent work, we reported the development of aptasensors based on 2D MoS2 diodes with geometrically asymmetric contacts for rapid, label-free, highly sensitive and specific detection of tumor nercosis factor-α (TNF-α), a representative inflammatory cytokine biomarker.

Our biosensors employ mechanically exfoliated multilayer MoS2 flakes with asymmetric geometry as the sensing channel, and aptamers (short single-stranded nucleic segments) as the bioreceptors. The sensing area is passivated with a thin aluminum oxide layer (around 5 nm) using atomic layer deposition technique (ALD) to provide available sites for facile functionalization with bioreceptors. Interactions between the immobilized aptamers and TNF-α at the sensor surface induce a change in surface energy that alters the current-voltage rectification behavior of the MoS2 diode, which can be read out using a two-electrode configuration.

The experimental results demonstrate that our sensor can rapidly and specifically respond to the change in TNF-α concentration with a limit of detection as low as 10 fM. The key advantages of this diode sensor are the simple fabrication process and electrical readout, and therefore, the potential to be applied in a rapid and easy-to-use, point-of-care, diagnostic tool.

→ *Return to the schedule*

Optimized Lithography-Free Fabrication of Sub-100 nm Nb2O5 Nanotube Films as Negative Supercapacitor Electrodes: Tuned Oxygen Vacancies and Cationic Intercalation

Doha Mohammed, Kholoud E. Salem, Nageh K. Allam

Cairo University, The American University in Cairo

Abstract:

The direct growth of sub-100 nm thin film metal oxides has witnessed a sustained interest as a superlative approach for the fabrication of smart energy storage platforms. Herein, sub-100 nm Zr-doped orthorhombic Nb2O5 nanotube films have been synthesized directly on Nb-Zr substrate and tested as negative supercapacitor electrode materials. To boost the pseudocapacitive performance of the fabricated films, supplement Nb4+ active sites (defects) have been subtly induced into the metal oxide lattice, resulting in 13% improvement in the diffusion current at 100 m V/s over that of the defect-free counterpart. The defective sub-100 nm film (H-NbZr) exhibits areal and volumetric capacitances of 6.8 mF/cm2 and 758.3 F/cm3, respectively. The presence of oxygen deficient states enhances the intrinsic conductivity of the thin film, resulting in a reduction in the bandgap energy from 3.25 to 2.5 eV. The assembled supercapacitor device made of nitrogen-doped activated carbon (N-AC) and H-NbZr (N-AC//H-NbZr) can keep 93, 83, 78, and 66 % of its first cycle capacitance after 1000, 2000, 3000, and 4500 successive charge/discharge cycles, respectively. An eminent energy record of approximately 0.77 µWh/cm2 at a power of 0.9 mW/cm2 is achieved at 1 mA/cm2 with superb capability.

→ *Return to the schedule*

Nickel-doped Cobalt Oxyhydroxide Nanowires Coupled Polyaniline Functionalized Carbon Cloths as Multifunctional Electrocatalysts for Hydrogen/Oxygen Evolution Reactions at All pH Levels

Niranjanmurthi Lingappan, Wonoh Lee

Chonnam National University

Abstract:

Hydrogen represents a carbon-free and sustainable energy carrier. Electrochemical water splitting via hydrogen evolution reaction (HER) and oxygen evolution reaction (OER) is a green approach for the hydrogen production. Nevertheless, unfavorable thermodynamics and sluggish kinetics limit the water splitting efficiency. While the benchmark catalysts such as Pt@C and RuO2/C catalysts display remarkable catalytic activity, the inferior durability remains a major concern. Further, scarcity and high demand result in sharp rise in cost, hindering their large-scale commercialization. Herein we rationally design the synthesis of nickel-doped cobalt oxyhydroxide nanowires grown on PANi functionalized CF (Ni@CoOOH@PANi-CF) as multi-functional electrocatalyst for HER and OER. In this design, the interfacial PANi layers substantially improve the surface functionality of the CF substrate and thereby facilitates strong coupling interaction with the Ni@CoOOH catalyst, which influences the charge transport kinetics across the catalyst/substrate interface and also maintains the structural integrity of the overall catalyst throughout the cyclic and long-term durability tests. Furthermore, the Ni@CoOOH provide abundant active sites for the dissociation of water, while the PANi-CF facilitates the adsorption of H+ ions from the intermediates and promotes its convention to hydrogen molecules, which accelerates the HER effectively. Due to these intriguing features, the Ni@CoOOH@PANi-CF manifested remarkable HER efficiency with low overpotential (35, 30, and 100 mV mV at 10 mA cm-2) in acidic, alkaline, and neutral electrolytes. Besides, the Ni@CoOOH@PANi-CF demonstrated batter durability even in acidic electrolyte. As a key functionality, PANi layers protected the carbon surface from corrosive reactions and suppressed the active catalyst dissolution, resulting in high tolerance for both HER and OER at all pH conditions.

→ *Return to the schedule*